Garwood, Gerri

From: Bradley, Kevin <kbradley@rti.org>
Sent: Thursday, March 12, 2015 2:23 PM
To: Garwood, Gerri
Subject: FW: IFC Flare data cited in public comments on proposed AP-42 EFs
Attachments: IFC Flare Test Facility Results Jan 2010.pdf

Gerri,

Below is Jim Seebold's response, and attached is a report from the IFC. I'm not sure that it's the same one referenced by API in their letter (number 56), but the numbers in the attachment match the values stated in the comment letter. I'm asking him to clarify/confirm the reports. This report is just that—there's no raw data in it.

Also, I looked through the presentation that he links to at the end, and it, like his response, is focused on wind effects on flare combustion efficiency.

Let me know what you think.

Kevin

From: Jim Seebold [mailto:jim.seebold@earthlink.net]
Sent: Thursday, March 12, 2015 12:11 PM
To: Bradley, Kevin
Subject: Re: IFC Flare data cited in public comments on proposed AP-42 EFs

Well, Kevin, I'm hesitant because while we thought at the time that IFC was making an important contribution, we have since learned that there was a serious flaw in the IFC (and other) work.

Subsequent full-scale PFTIR field testing has revealed the stark reality that small soda-straw-like "flares" operating in a toy bench-top "wind tunnel" hardly give a realistic picture of wind-induced combustion efficiency degradation in real industrial flares in the field. It's simple aerodynamics and I think most unbiased observers with any experience at all would simply respond ***"Duh!"*** to that revelation.

Regrettably, that's also true for the 1-6"D "flares" we tested by extractive sampling in the IFC wind tunnel. At the time we were pretty impressed with the contribution that we thought we were making but now I wonder about that especially in the case of so-called wind-induced combustion efficiency degradation.

But maybe I'm too hard on us and I've decided to attach the IFC results ...

In any event, if you or any of your commenters want to know the ***real*** story about the performance of real industrial flares in the field you should have a look at the plethora of papers that have been published since the IFC wound-up its work such as:

Combustion Efficiency of Real Industrial Flares in the Field -
No Evidence Whatsoever of Wind-Induced CE Degradation
Scott Evans and James G. Seebold
http://content.lib.utah.edu/cdm/compoundobject/collection/AFRC/id/14337/rec/17

Click on the link. You'll have to click on the "Download" button that appears on the screen. I didn't attach it because it's 16MB ...

Cheers, Jim

From: Bradley, Kevin
Sent: Wednesday, March 11, 2015 1:19 PM
To: jim.seebold@earthlink.net
Subject: IFC Flare data cited in public comments on proposed AP-42 EFs

Mr. Seebold,

I am Kevin Bradley with RTI International in North Carolina, and I am working with Gerri Garwood of the EPA's Office of Air Quality & Planning Standards on the Proposed AP-42 Emission Factors.

Multiple commenters on the proposed flare emissions factors cited 2010 flare test data from the International Flare Consortium and suggested that the EPA review and include these flare data. I wanted to follow up with you about getting copies of these flare data, if it can be shared. If you can share any flare data, it would be helpful to know what industries and sources the data covers and what measurement methods were used (PFTIR, extractive sampling, etc.).

Thank you in advance for any help you can offer,

Kevin Bradley
RTI International
(919) 541 8803

3/12/2015

Natural Resources Canada | Ressources naturelles Canada

CanmetENERGY

Leadership in ecoInnovation

Flare Test Facility – Results

P. Gogolek, A. Caverly, C. Balderson

CanmetENERGY - Ottawa

J. Pohl

Energy International

R. Schwartz

John Zink

J. Seebold

Consultant

Prepared for the International Flaring Consortium

January 2010

Funding provided by members of the International Flaring Consortium

Canada

DISCLAIMER

This report was prepared by CanmetENERGY as an account of work funded by the International Flaring Consortium. CanmetENERGY has made all reasonable efforts to ensure the exactness of the information provided in this report and the opinions expressed herein are those of CanmetENERGY solely. However, neither CanmetENERGY, the International Flaring Consortium, nor any person acting on behalf of them;

a. Makes any warranty or representation, expressed or implied with respect to the accuracy, completeness, or usefulness of the information contained in this report, or that the use of any information, apparatus, method, or process disclosed in this report may not infringe privately-owned rights, or

b. Assumes any liability with respect to the use of, or for damages resulting from the use of, any information, apparatus, method, or process disclosed in this report.

Reference to specific commercial products in this report does not represent or constitute an endorsement, recommendation, or favoring by CanmetENERGY, the International Flaring Consortium, nor any person acting on behalf of them, of the specific manufacturer or commercial product. The involvement by CanmetENERGY in this project is not to be used for promotional purposes beyond being identified as an independent third party evaluator.

TABLE OF CONTENTS

1.0 Introduction 1

2.0 Baseline, Scale-Up and Regime Transition Tests 4

2.1 Introduction 4

2.2 Test Plan 5

2.2.1 Scaling Tests 5

2.2.2 FRR Tests 6

2.2.3 Fuel Modification Tests 7

2.2.4 Transition Testing 7

2.3 Results and Discussion 8

2.3.1 Scale-up Tests 8

2.3.2 Fuel Modification Tests 18

2.3.3 Transition Testing 20

2.4 Conclusion 23

3.0 Simple Fuel Gas Tests 25

3.1 Introduction 25

3.2 Test Plan 25

3.3 Results 26

3.4 Discussion 28

3.5 Conclusion 29

4.0 Steam-assist Tests 31

4.1 Introduction 31

4.2 Test Plan 31

4.3 Results 32

4.4 Discussion 37

4.5 Conclusion 50

5.0 Dilution testing 52

5.1 Introduction 52

5.2 Test Plan 52

5.3 Results and Discussion 53

5.4 Conclusion 57

6.0 Trace emissions 59

6.1 Introduction 59

6.2 Carbon Monoxide 60

6.3 Nitrogen Oxides 62

6.4 Hydrocarbons 64

6.5 Conclusion 69

7.0 Conclusion 71

7.1 Experimental studies of the flare efficiency in the transition between jetting and wake-stabilized regimes. 71

7.2 Experimental studies of the effect of wind on steam-assisted flares. 72

7.3 Experimental studies on the limiting hydrogen concentration for steam-assisted flares and wind blown flares. 73

7.4 Experimental measurements of HRVOC and NO_x measurements for flares with and without steam-assist. 73

7.5 Correlation of fuel properties to correlate the flare efficiency with flare gas composition, particularly accounting for the special case of hydrogen, and the inert gases nitrogen and carbon dioxide. 74

7.6 Correlation of flare efficiency with steam-assist rate that includes the flare gas composition, perhaps unifying steam with the handling of nitrogen and carbon dioxide dilution. 74

7.7 Gaps Remaining or Identified 75

8.0 References 76

9.0 Appendix 77

LIST OF FIGURES

Figure 1 - Baseline testing results for 1" basic pipe firing natural gas. 9

Figure 2 - Baseline testing results for 2" basic pipe firing natural gas. 9

Figure 3 - Baseline testing results for 3" basic pipe firing natural gas. 10

Figure 4 - Baseline testing results for 4" basic pipe firing natural gas. 10

Figure 5 - Baseline testing results for 6" basic pipe firing natural gas. 11

Figure 6 - Results of all baseline tests firing natural gas. 11

Figure 7 - Results for all pipe sizes, with results reported by the University of Alberta, correlated with the Power Factor. The solid line is equation (2-2) fit to the results for 3", 4" and 6" pipes. 13

Figure 8 - Replotting Figure 7 as a semi-log plot, to better display the spread of the data. 14

Figure 9 - Replotting Figure 7 with only the results for pipes 3" or larger. 14

Figure 10 - Replotting Figure 9 as a semi-log plot to better display the spread of the data. 15

Figure 11 - Fraction of inefficiency due to the emission of methane correlated with the Power Factor. 16

Figure 12 - Destruction efficiency for methane for the tests with natural gas and the basic pipe. 16

Figure 13 - Conversion inefficiency for 3" and 6" pipes fitted with FRR, plotted against the Power Factor. The solid line is the fit to the basic pipes 3" and larger, equation (2-2). 17

Figure 14 - Destruction efficiency for 3" and 6" pipes fitted with FRR, plotted against the Power Factor. The solid line is the fit to the basic pipes 3" and larger, equation (2-3). 18

Figure 15 - Results for tests with 3" and 6" basic pipes firing a mixture of 85%-v natural gas with 15%-v propane. The blue line is the fit to the natural gas results, the solid black line is equation (2-4). 19

Figure 16 - Results for 3" basic pipe firing a mixture of 40%-v natural gas with 60%-v nitrogen. The solid line is the fit to the natural gas data. 20

Figure 17 - Results for 3" pipe for transition testing versus fuel Reynolds number. Changing the fuel rate has a very small effect. 21

Figure 18 - Results for 3" pipe for transition testing versus wind speed. The change in fuel rate at 1.1 m/s has much smaller effect than the increase of wind speed. 22

Figure 19 - Results for transition testing of 3" pipe correlated with the Power Factor. 22

Figure 20 - Transition test results with 3" pipes versus wind speed. 23

Figure 21 - Conversion inefficiency for unassisted flaring of ethylene and propylene in 3" FRR tip. 26

Figure 22 - Destruction efficiency for unassisted flaring of ethylene and propylene in 3" FRR tip. 27

Figure 23 - Solid carbon emission as a percentage of the total carbon for unassisted flaring of ethylene and propylene in 3" FRR flare tip. 28

Figure 24- Comparison of destruction efficiency of unassisted flaring of ethylene and propylene with that of natural gas in a 3" FRR flare tip. The solid line is equation 2-3, the DE curve for natural gas flared with 3", 4" or 6" basic pipe. 29

Figure 25 - Conversion inefficiency versus steam-to-fuel mass ratio for steam-assisted flaring of natural gas, indexed on nominal wind speed. The zero SFR points did have steam flowing, but the correction of the flow rate produced a negative value. 33

Figure 26 - Destruction efficiency versus steam-to-fuel mass ratio for steam-assisted flaring of natural gas, indexed on nominal wind speed in m/s. The zero SFR points

did have steam flowing, but the correction of the flow rate produced a negative value. 33

Figure 27 - Conversion inefficiency versus steam-to-fuel mass ratio for steam-assisted flaring of ethylene, indexed on nominal wind speed. The circled point appears to be anomalous. 34

Figure 28 - Destruction efficiency versus steam-to-fuel mass ratio for steam-assisted flaring of ethylene, indexed on nominal wind speed. The circled point appears to be anomalous. 35

Figure 29 - Conversion inefficiency versus steam-to-fuel mass ratio for steam-assisted flaring of propylene, indexed on wind speed in m/s. 36

Figure 30 - Destruction efficiency versus steam-to-fuel mass ratio for steam-assisted flaring of propylene, indexed on wind speed. 36

Figure 31 - Conversion inefficiency for steam-assisted flaring of natural gas versus Power Factor, for SFR < 1. 37

Figure 32 - Destruction efficiency versus Power Factor for steam-assisted flaring of natural gas, for SFR < 1. 38

Figure 33 - Conversion inefficiency versus Power Factor for steam-assisted flaring of ethylene, indexed on wind speed. All steam levels included. 39

Figure 34 – Destruction efficiency versus Power Factor for steam-assisted flaring of ethylene, indexed on wind speed. All steam levels included. 39

Figure 35 - Conversion inefficiency versus Power Factor for steam-assisted flaring of ethylene, indexed on wind speed, SFR < 1. 40

Figure 36 - Destruction efficiency versus Power Factor for steam-assisted flaring of ethylene, indexed on wind speed, SFR < 1. 40

Figure 37 - Destruction efficiency versus Power Factor for unassisted and steam-assisted flaring of ethylene, with Steam-to-Fuel Ratio up to 2. 41

Figure 38 - Conversion inefficiency versus Power Factor for steam-assisted flaring of propylene, indexed on wind speed. All steam levels included. 42

Figure 39 - Destruction efficiency versus Power Factor for steam-assisted flaring of propylene, indexed on wind speed. All steam levels included. 42

Figure 40 - Conversion inefficiency versus Power Factor for steam-assisted flaring of propylene, indexed on wind speed, SFR < 1. 43

Figure 41 - Destruction efficiency versus Power Factor for steam-assisted flaring of propylene, indexed on wind speed, SFR < 1. 43

Figure 42 - Destruction efficiency results for flaring propylene, both steam-assisted and unassisted. The CMA data for steam-assisted flaring with SFR < 1 is included. 44

Figure 43 - Destruction efficiency for steam-assisted flaring versus the reduced steam volume fraction. The possibly anomalous data are circled. Recommended maximum is RSVF = 0.8. 46

Figure 44 - Destruction efficiency versus Power Factor for steam-assisted trials with RSVF < 0.8. 46

Figure 45 - Destruction Efficiency results for steam-assisted flaring of natural gas, ethylene and propylene, including the CMA data. All data are restricted to RSVF < 0.8. The Fuel Factor is given in equation 4-4. 48

Figure 46 - Destruction Efficiency results for steam-assisted flaring of ethylene and propylene, including the CMA data. All data are restricted to RSVF < 0.8. The Fuel Factor is given in equation 4-4. 49

Figure 47 - Conversion inefficiency versus heat content of flare gas. 54

Figure 48 - Destruction efficiency versus heat content, volume basis. 55

Figure 49 - Destruction efficiency versus heat content, mass basis. 56

Figure 50 - Destruction efficiency for diluted flare gases versus Reduced Volume Fraction of inert. 57

Figure 51- Conversion of fuel-carbon to carbon monoxide for all tests. 61

Figure 52 - Log-log plot of the conversion to CO against the conversion inefficiency. The solid line indicates 25% of the inefficiency is due to carbon monoxide. 62

Figure 53 - Emission factor for NO_x plotted against conversion inefficiency for all tests. 63

Figure 54 - Emission factor for NO_x for steam-assisted trials. 64

Figure 55 - Emission factors for ethylene plotted against Power Factor for tests with natural gas and propylene. 65

Figure 56 - Emission factors for ethylene plotted against SFR for steam-assisted flaring of natural gas and propylene. 66

Figure 57 - Emission factor for ethylene for tests wtih dilution of natural gas, propane and propylene with carbon dixoide. 67

Figure 58 - Emission factor for 1-butene against SFR for steam-assisted flaring of propylene. 68

Figure 59 - Emission factor for 1-butene plotted against the emission factor for ethylene for the steam-assisted flaring of propylene. The solid square symbols are the emission factors at the detection limit for these trials. 69

Figure 60 - Minimum exit velocities for steam-assisted flaring of ethylene and propylene based on RSVF<0.8 and maximum Power Factor of 2 for propylene and 3 for ethylene. 73

Figure 61 - Baseline testing results for 1" basic pipe firing natural gas. 77

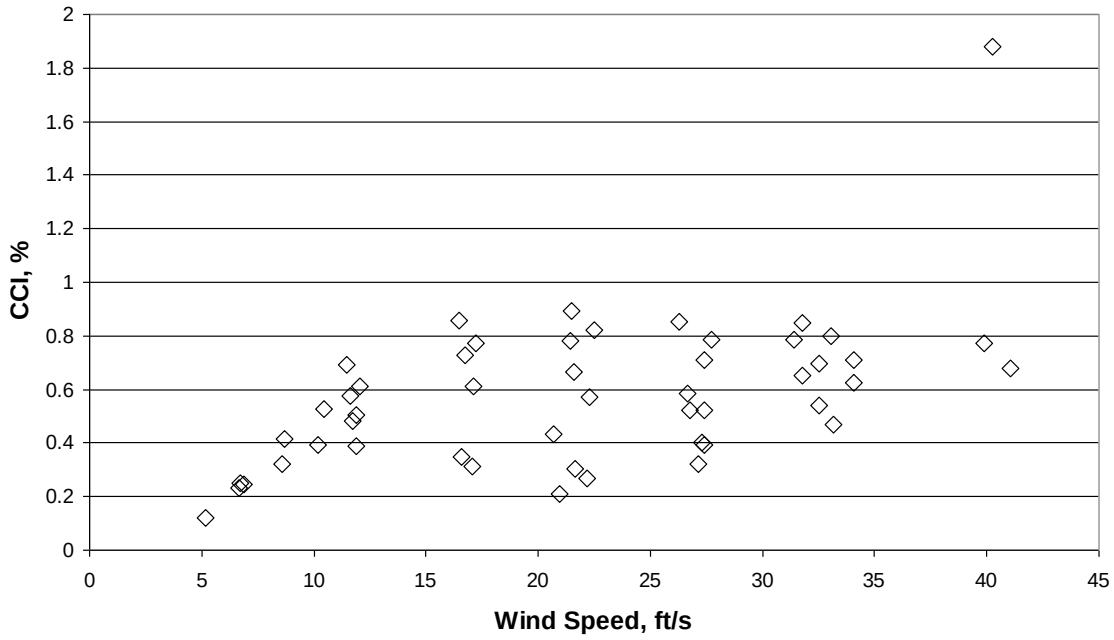

Figure 62 - Baseline testing results for 2" basic pipe firing natural gas. 78

Figure 63 - Baseline testing results for 3" basic pipe firing natural gas. 78

Figure 64 - Baseline testing results for 4" basic pipe firing natural gas. 79

Figure 65 - Baseline testing results for 6" basic pipe firing natural gas. 79

Figure 66 - Results of all baseline tests firing natural gas. 80

Figure 67 - Results for 3" pipe for transition testing versus wind speed. The change in fuel rate at 4 km/h has much smaller effect than the increase of wind speed. 81

Figure 68 - All transition test results versus wind speed. 81

Figure 69 - Conversion inefficiency for unassisted flaring of ethylene and propylene in 3" FRR tip. 82

Figure 70 - Destruction efficiency for unassisted flaring of ethylene and propylene in 3" FRR tip. 82

Figure 71 - Solid carbon emission as a percentage of the total carbon for unassisted flaring of ethylene and propylene in 3" FRR flare tip. 83

LIST OF TABLES

Table 1 - Test matrix for scale-up tests with natural gas. 5

Table 2 - Test matrix for tests with FRR firing natural gas. 6

Table 3 - Test matrix for the fuel modification tests, augmented with propane and diluted with nitrogen. 7

Table 4 - Test matrix for the simple fuel flaring tests. 25

Table 5 - Overall test matrix for the steam-assisted trials. 31

Table 6 - Critical volume fraction (equation 4-2) for fuel gases. 45

Table 7 - Maximum dilution for flammable operation, with energy content and exit velocity. 53

Table 8 - Critical volume fraction for gas mixtures with nitrogen and carbon dioxide. 56

NOMENCLATURE

δ	Destruction efficiency.
ε_{CH_4}	Error in stack methane concentration (ppm).
ε_{CO}	Error in stack carbon monoxide concentration (ppm).
$\varepsilon_{CO_2,in}$	Error in inlet carbon dioxide concentration (ppm).
$\varepsilon_{CO_2,out}$	Error in stack carbon dioxide concentration (ppm).
η	Carbon conversion efficiency.
λ	Stoichiometric air to fuel volume ratio.
ρ_a	Density of air (kg/m^3).
ρ_f	Density of fuel gas (kg/m^3).
σ_c	Reciprocal of increase of carbon in stack gas, summed over all species, ppm^{-1}.
$x^c_{CO_2,f}$	Mole fraction of carbon as carbon dioxide in fuel.
$x^c_{CO_2,out}$	Mole fraction of carbon as carbon dioxide in stack gas.
$\{x_i\}_{allcompounds}$	Composition of gas, the mole fraction of all species.
x_Σ	Volume fraction of species Σ.
X_{st}	Volume fraction of steam in the flare gas/steam mixture.
X^*_{st}	Critical volume fraction of steam, estimated maximum steam dilution for flammable mixture (equation 4-2).
A_p	Open area of flare pipe (m^2).
BMS	Burner Management System.

BTEX	Benzene, toluene, ethylbenzene, and xylenes.
CB	Carbon Balance (%).
CCE	Carbon Conversion Efficiency - the conversion of fuel-bound carbon to carbon dioxide, expressed as a percentage of the mass of carbon as carbon dioxide in the stack gas relative to mass of fuel-bound carbon.
CCI	Carbon Conversion Inefficiency - the failure to convert fuel-bound carbon to carbon dioxide, CCI = 100% - CCE.
DE	Destruction Efficiency - the percentage of a species in the flare gas that is converted into any other species. DE = 100% - FS.
D_p	Diameter of flare pipe (m).
EF_Σ	Emission factor for species Σ.
FRR	Flame Retention Ring.
FS	Fuel Slip, percentage of mass of carbon as fuel species in stack gas relative to the mass of fuel-bound carbon (%) $FS = 100\% - DE$
HRVOC	Highly reactive volatile organic compounds (eg. ethylene, propylene, 1-butene, cis/trans-2-butene, 1,3-butadiene).
I^*	Apex flammability curve when plotted as fuel % against inert %.
LHV_m	Lower Heating Value, mass basis (MJ/kg).
M_a	Molecular mass of air.
$\dot{m}_{air}$	Mass flow of air (kg/h).
$\dot{m}_{bucket}$	Mass flow of steam measured by the bucket (kg/h).
$\Delta\dot{m}^c{}_{CO}$	Net mass flow of carbon as carbon monoxide (kg/h).
$\Delta\dot{m}^c{}_{CO_2}$	Net mass flow of carbon as carbon dioxide (kg/h).
M_f	Molecular weight of flare gas.
$\dot{m}_f$	Mass flow of fuel (kg/h).
$\Delta\dot{m}^c{}_{HC}$	Net mass flow of carbon as hydrocarbon (kg/h).

$\dot{m}_{meter}$	Mass flow as measured by the steam flow meter (kg/h).
M_{Σ}	Molecular mass of species Σ.
P	Pressure (kPa).
PF	Power Factor (dimensionless).
RH	% Relative Humidity.
RSVF	Reduced Steam Volume Fraction.
RVFI	Reduced Volume Fraction Inert.
SDE	Specific Destruction Efficiency (%).
SFR	Steam to Fuel Mass Ratio, the mass ratio of steam-assist to flare gas (kg/kg).
T	Temperature (ºC).
U_f	Exit speed of fuel gas (m/s).
U_w	Mean crosswind speed, (m/s).
$y_{CO_2,in}$	Mole fraction of carbon dioxide in the inlet air (ppm).
$y_{CO_2,out}$	Mole fraction of carbon dioxide in the stack gas (ppm).

1.0 INTRODUCTION

Flares are the primary technology for the safe and economical disposal of combustible gases at production sites and refineries. The performance of, and emissions from, flares are a current issue in some jurisdictions. This is partly because of genuine gaps between the flare research literature and how flares operate in the field, as identified in "Survey of the Literature" (Gogolek et al., 2009a). There is also some confusion about the applicability of some research results to operating flares. We attempted to provide some structure and clarity to the literature in our review. Firstly, we distinguished the jetting and wake-stabilized regimes as distinct limiting modes of operation for flares. The research results from one regime may not be applicable to flares operating in different regimes. For example, the continuous decrease of efficiency, with increasing cross-wind speed, which is well-established for wake-stabilized production flares, may not apply to jetting refinery flares. Secondly, there is a minimum flare pipe size, around 7.5 cm (3 inches), below which the results in the jetting regime are not scalable to full-scale flares. This means some results in the literature are not representative of flares operating at full-scale in refineries or chemical plants.

The International Flaring Consortium (IFC) was formed to address crucial gaps in the science of flares. The first objective of the IFC is to produce a method of predicting flare efficiency from operating variables: flare gas composition and flow rate, steam-assist rate, and wind speed. This method is to include original experimental work as well as the data in the literature. The second objective is to measure the emissions of NO_x, the most important HRVOCs (ethylene, propylene, 1-3 butadiene, and the butenes), and BTEX (benzene, toluene, ethylbenzene and xylenes), and to attempt to develop emission factors for these species based on the same set of operating variables. The third objective is to identify optimal operating conditions and operating envelope for flares.

Referring to the literature review, the following six areas of the flare performance needed to be addressed:

1. Experimental studies of the flare efficiency in the transition between jetting and wake-stabilized regimes.

2. Experimental studies of the effect of wind on steam-assisted flares.
3. Experimental studies on the limiting hydrogen concentration for steam-assisted flares and wind blown flares.
4. Experimental measurements of HRVOC and NO_x measurements for flares with and without steam-assist.
5. Correlation of fuel properties to correlate the flare efficiency with flare gas composition, particularly accounting for the special case of hydrogen, and the inert gases nitrogen and carbon dioxide.
6. Correlation of flare efficiency with steam-assist rate that includes the flare gas composition, perhaps unifying steam with the handling of nitrogen and carbon dioxide dilution.

These are particular areas of study that form the general objectives of the IFC.

The technical background of the IFC experimental programs can be found in separate reports (Gogolek et al. 2009b, Caravaggio and Caverly 2008). Therein we described the equipment, procedures, quality analysis and control, and uncertainty of the derived measures. Herein we report the results of the experiments and analyze the data to obtain predictive expressions for performance and emission factors based on the operating conditions. Over 400 tests were run.

The report is organized as follows. The baseline tests with natural gas, scale-up testing with natural gas, the effect of the flame retention ring, and the transition from jetting to wake-stabilized operation are all in Chapter 2. Chapter 3 has the tests for unassisted flaring of ethylene and propylene. Chapter 4 has the tests for steam-assisted flaring of natural gas, ethylene and propylene. Chapter 5 covers the flaring limits for dilution with nitrogen or carbon dioxide. The trace emissions, NO_x, CO, HRVOCs and BTEX, for all the tests are reported in Chapter 6.

Note on terminology: We use the following definitions of performance measures.

- **Carbon Conversion Efficiency (CCE)**:= the conversion of fuel-bound carbon to carbon dioxide, expressed as a percentage of the mass of carbon as carbon dioxide in the stack gas relative to mass of fuel-bound carbon.

- **Carbon Conversion Inefficiency (CCI)**:= the failure to convert fuel-bound carbon to carbon dioxide, CCI = 100% - CCE.
- **Fuel Slip (FS)**:= percentage of mass of carbon as original fuel species in stack gas relative to the mass of fuel-bound carbon.
- **Destruction Efficiency (DE)**:= the destruction of a particular combustible species, expressed as percentage of 100% minus the mass of carbon of the combustible species in the stack gas relative to the mass of fuel-bound carbon of that combustible species. For a single hydrocarbon species, DE = 100% - FS.

2.0 BASELINE, SCALE-UP AND REGIME TRANSITION TESTS

2.1 Introduction

These tests are preliminary to the main objectives of the IFC. The primary objective of these tests was to test the suitability of the 7.5 cm (3 inch) pipe, with respect to scale-up of results, and to see if smaller pipes can be used. While the "Three Inch Rule" is well established for the jetting regime [see Gogolek et al., 2009a and references therein], it was not clear that such a size limit applied in the strong wind situation that produces the wake-stabilized regime. Pipes with nominal diameters of 1", 2", 3", 4" and 6" were used to test for the lower limit (*Scaling Tests*). While the two larger pipe sizes (4" and 6") can be full-scale for flaring associated gas, industrial flares at refineries, petrochemical and chemical plants are an order of magnitude larger. A dimensionless parameter is developed to correlate the results, which is the prerequisite for successful scale-up of the results.

Natural gas is the baseline fuel for the program because it has several attractive features. Natural gas is easy to handle and low cost because it is provided as a utility and it is directly relevant for purge-and-pilot operation and upstream flaring of associated gas. Additionally, natural gas has been used in other research, notably by the University of Alberta, allowing comparison of the results from the CanmetENERGY Flare Test Facility with other published data (see the Literature Review [Gogolek et al, 2009a]).

The effect of a Flame Retention Ring (FRR) in a cross-wind was tested with 3" and 6" tips (*FRR Tests*). The FRR is a standard appurtenance for industrial flares and provides improved performance with strong jets.

The transition from a vertical jet flame to a wake-stabilized flame was investigated (*Transition Testing*). The question was whether there would be a discontinuous change of performance as the wake-stabilized operation was established. This transition occurs as the wind begins to dominate the jet, either by strengthening of the wind or weakening of the jet. Both transitions were tested and compared.

The momentum flux ratio has been used in the literature for stacks to predict downwash, where the plume is pulled down by the low pressure wake of the stack. The wake-

stabilized flare behaviour is similar, with the flame stabilized in the wake of the flare tip. The utility of this dimensionless parameter is tested both for the transition to wake-stabilized operation and correlating the combustion performance.

Some preliminary testing of flare gas composition effects was done (*Fuel Modification*), to provide guidance on how fuel composition affects performance. One level of dilution of natural gas with nitrogen was tested. One level of enrichment of natural gas with propane, a more reactive fuel, was tested.

2.2 Test Plan

2.2.1 SCALING TESTS

The scaling test matrix is given in Table 1. The flare tips were all basic pipes, Schedule 40 for the nominal size in inches. The flare gas flow, given as fuel mass rate, was at three levels – 10, 20 and 30 kg/h. This gave different exit velocities for the flare gas for the pipes with different diameters. The maximum wind speed was the same for all the pipe sizes. However, the minimum wind speed was not the same. For the smaller pipes, Nominal 1" and 2", the minimum wind speed was determined by the flame rise – the flame would touch the ceiling of the working section of the wind tunnel when the wind speed was lower. For the Nominal 6" pipe, the flame would touch the walls at lower wind speeds. A total of 258 tests were run.

Table 1 - Test matrix for scale-up tests with natural gas.

Pipe Size	Fuel Rate	Exit Velocity	Wind Speed	Number of tests
(Nom. inches)	kg/h	m/s	m/s	
1"	10 - 30	7.3 – 22.2	3.1 - 12	12
2"	10 - 30	1.8 – 5.4	3.1 - 12	50

3”	10 - 30	0.8 – 2.5	2.0 - 12	66
4”	10 - 30	0.5 – 1.4	2.0 - 12	94
6”	10 - 30	0.2 – 0.6	3.5 - 12	36

2.2.2 FRR TESTS

Two flare tips were equipped with FRR. These were provided by John Zink LLC. Both were fabricated using Schedule 80 stainless steel pipe, one 3” Nom and the other 6” Nom. The FRR is composed of S-shaped segments each with 3 holes (see “Equipment & Calculation Report” [Gogolek et al, 2009b] for further details). The segments direct the main portion of the flare gas flow into the centre. The holes and the slots between segments allow a small amount of the flare gas to flow into the relative calm above the segments. This helps to stabilize the flame at high exit velocities. The open area of the 3” FRR tip was equivalent to a 2” open pipe. Similarly the open area of the 6” FRR tip was equivalent to a 4” open pipe. Since the FRR is a standard feature on many flare tips, the FRR was selected as the base tip configuration for this test study. These tests were conducted to characterize the effect of low exit velocity and wind on the performance of the flare tip and how the FRR flare tip results compare to basic pipe flare tips.

Table 2 - Test matrix for tests with FRR firing natural gas.

Pipe Size	Fuel Rate	Exit Velocity	Wind Speed	Number of tests
(Nom. inches)	kg/h	m/s	m/s	
3”	10 - 30	1.9 – 5.5	2.0 - 12	43
6”	10 - 30	0.5 – 1.5	2.0 - 12	43

2.2.3 FUEL MODIFICATION TESTS

These tests were intended to provide guidance on the effect of combustion properties on flare performance. Two mixtures were tested. The first was natural gas with a small amount of propane added to increase reactivity. The mixture was 70%-mass natural gas with 30%-mass propane, which is 85%-vol natural gas and 15%-vol propane. Twenty tests were performed with this mixture flared to a 3" basic pipe; nine tests were performed with a 6" basic pipe. The mass flow rate of the flare gas was at the baseline values of 10, 20 and 30 kg/h.

The second mixture tested was natural gas with substantial nitrogen dilution. The mixture composition was 40%-vol natural gas with 60%-vol nitrogen. The mass flow of natural gas was at the baseline rates of 10, 20 and 30 kg/h, so that the total flow rate of flare gas was much higher, as shown in Table 3. This means the heat input rate, or the power of combustion was kept approximately the same as for the baseline tests with natural gas.

Table 3 - Test matrix for the fuel modification tests, augmented with propane and diluted with nitrogen.

Fuel	Pipe Size	Fuel Rate	Exit Velocity	Wind Speed	Number of tests
	(Nom. Inches)	kg/h	m/s	m/s	
NG/propane	3"	10 - 30	0.6 – 1.8	3.5 – 9.5	20
NG/propane	6"	10, 20	0.15, 0.3	3.5 – 9.5	9
NG/N_2	3"	35 - 105	2 - 6	3.5 – 9.5	24

2.2.4 TRANSITION TESTING

The transition to wake-stabilized operation was addressed. The two questions being tested were:

- Is there a continuous or discontinuous transition for flare performance during the transition to wake-stabilized operation?

- Is the momentum flux ratio useful for correlating the performance during the transition?

Three flare tips were used: 2" basic pipe, 3" basic pipe, and the 3" FRR tip. Natural gas was used in all tests. Each test started at low wind and high fuel rate, producing a vertical flame a minimum of 10 cm above the flare tip. From this initial state, there are two ways of achieving the wake-stabilized mode – by increasing the wind speed and by decreasing the flare gas rate. Each path was followed. Three different flare gas rates (20, 25, and 30 kg/h) were used for the 2" pipe. Only one flare gas rate (30 kg/h) was used for the 3" basic pipe and 3" FRR tip.

2.3 Results and Discussion

To study and evaluate a flare, two main criteria are introduced in this Section (and they are later used in the entire Report): "conversion inefficiency", and "destruction efficiency".

Usually to characterize a process, "efficiency" (and not "inefficiency") is the primary criterion to consider, so use of "conversion inefficiency" should be here somehow justified. Specially, that using "conversion efficiency" would be more consistent with the use of "destruction efficiency" - as both criteria should aim towards as high values as possible (100%) in a well burning flare; they should, likely, have also similar trends as functions of variables such as power factor, wind speed , Reynolds number, or (for steam assisted flares) steam-to-fuel ratios. However, the efficiencies are quite high. It is easier to demonstrate dependence on operating variables the inefficiency.

2.3.1 SCALE-UP TESTS

The inefficiencies for the individual pipe sizes are presented in Figures 1 through 5, plotted against wind speed. In all cases the inefficiency of carbon conversion increases with increasing wind speed. However, the inefficiency for the 2" pipe appears to be almost constant for 5 m/s to 12 m/s. Figure 6 brings all the results together in one chart, showing the large spread.

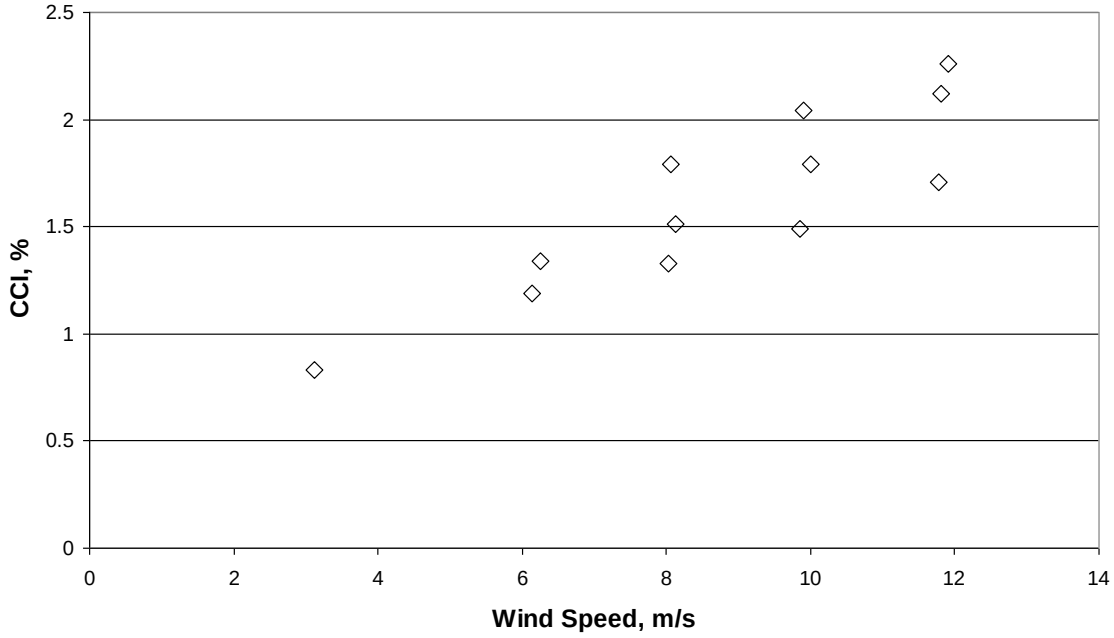

Figure 1 - Baseline testing results for 1" basic pipe firing natural gas.

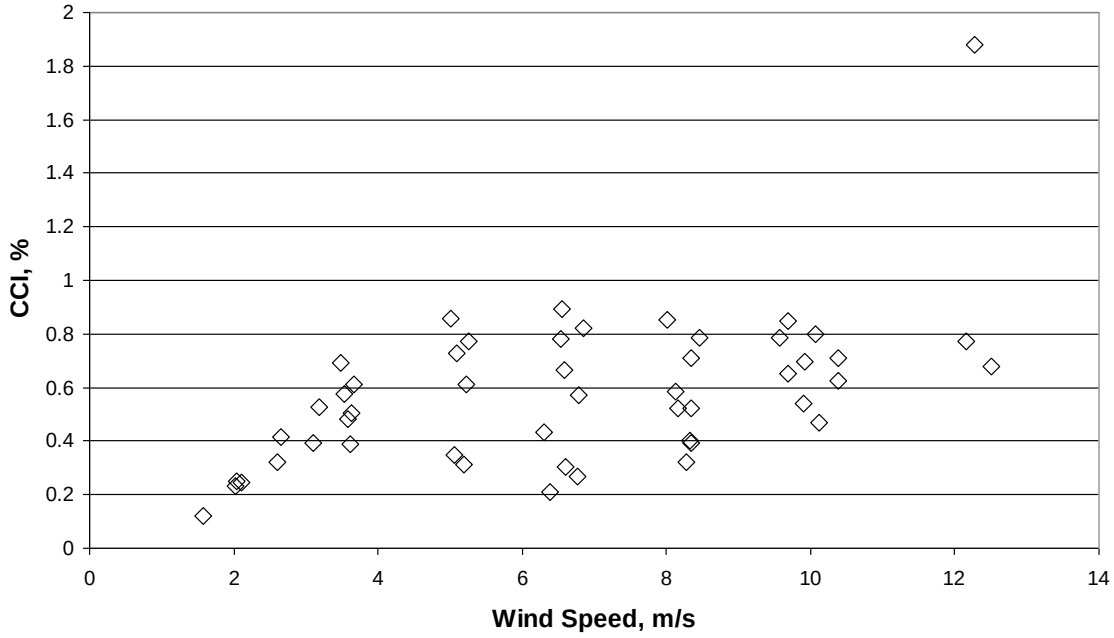

Figure 2 - Baseline testing results for 2" basic pipe firing natural gas.

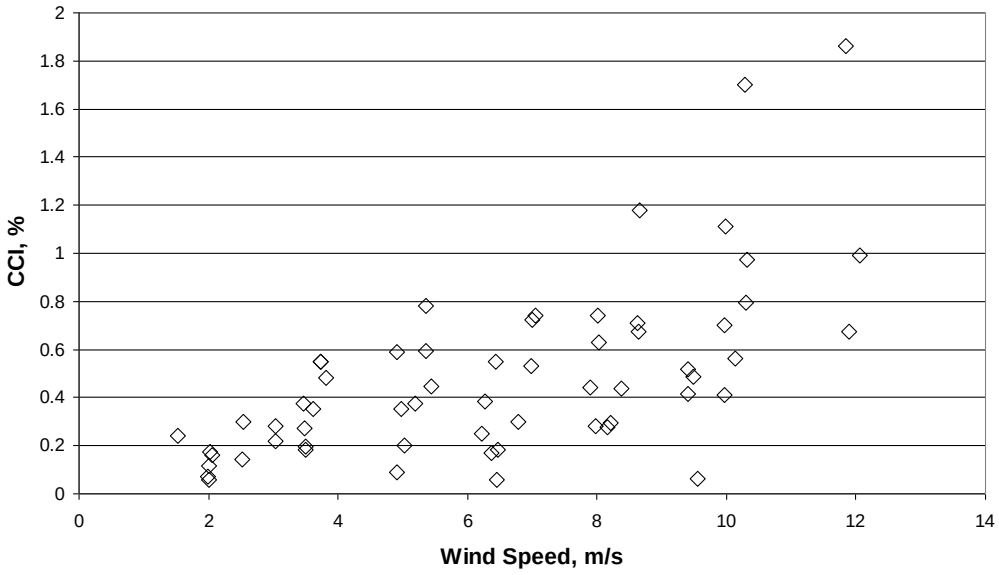

Figure 3 - Baseline testing results for 3" basic pipe firing natural gas.

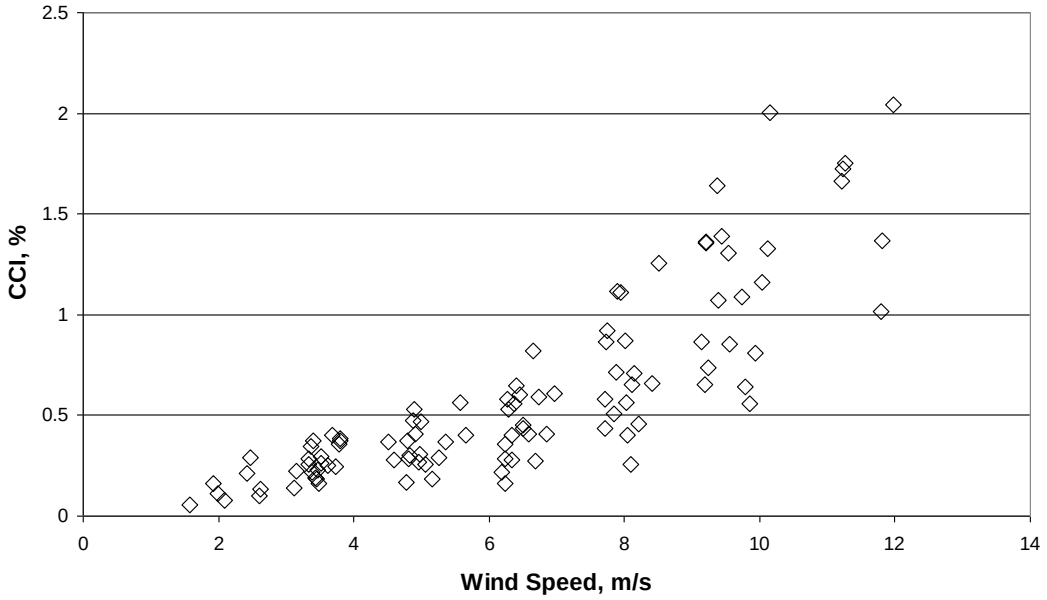

Figure 4 - Baseline testing results for 4" basic pipe firing natural gas.

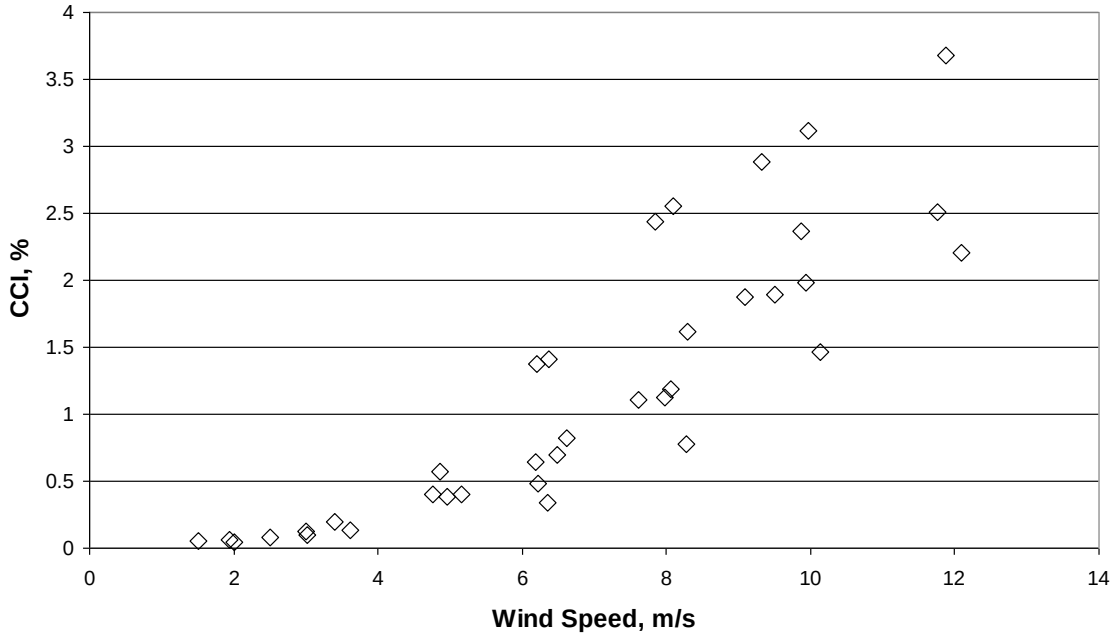

Figure 5 - Baseline testing results for 6" basic pipe firing natural gas.

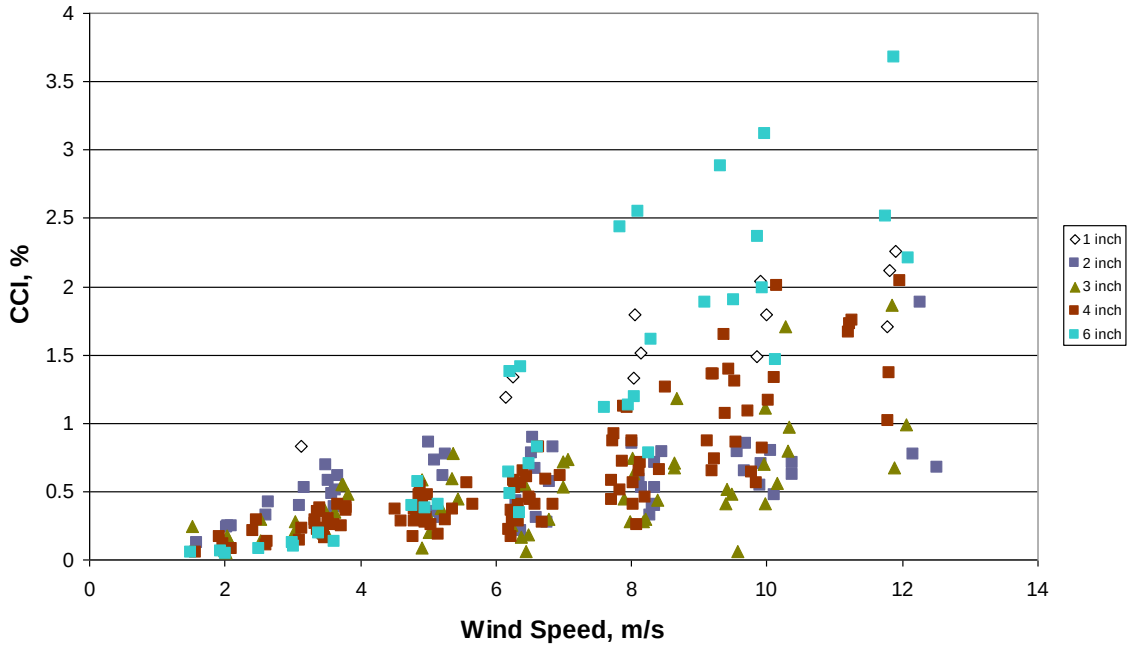

Figure 6 - Results of all baseline tests firing natural gas.

The independent variables for these tests are the wind speed, flare gas rate, and pipe diameter. In our literature review [Gogolek et al., 2009a], we showed that the Buoyant

Plume dimensionless parameter[1] developed by the University of Alberta failed to correlate their data from 1", 2" and 4" pipes. We developed our own dimensionless parameter from the ratio of the cross-wind power to the power of combustion of the flare gas. The cube root of this ratio gives the Power Factor.

$$PF = \left(\frac{\rho_a U_w^3 D_p^2}{\dot{m}_f LHV_m} \right)^{1/3} = \left(\frac{\rho_a U_w^3 D_p^2}{\rho_f A_p U_f LHV_m} \right)^{1/3} \tag{2-1}$$

This factor is linear in the wind speed. If the scaling of the flare operation is according to the exit velocity of the flare gas, the Power Factor is independent of flare tip diameter. Figure 7 has the scale-up data with the data from the University of Alberta plotted against the Power Factor. It is clear that the 1" pipe data diverges significantly from the rest, giving much higher inefficiency at lower values of Power Factor. The dashed line for the "U of A fit" is their correlation calculated for a 6" pipe. Notice how the exponential dependence gives unrealistically high values of inefficiency compared to our experimental values. Figure 8 uses a semi-log plot to display the spread of the data. Here it is easier to see that the inefficiency for the 2" pipes also diverges from the grouping for the larger pipe sizes. The demonstrates that results from pipes smaller than 7.5 cm (3") are not scalable to larger diameter pipes.

Figures 9 and 10 show the results for only the 3", 4" and 6" pipe sizes. There is a good correlation with the Power Factor. The 4" pipe data from the University of Alberta are included. The solid line fit to the data is equation 2-2.

---

[1] Buoyant plume parameter is $BP = \frac{U_w}{\sqrt[3]{g D_p U_f}}$. The "U of A fit" is a simple exponential of the Buoyant Plume parameter. See Gogolek et al. (2009a) for details.

$$CCI = 0.1 + \frac{PF}{1 + \left(\frac{6}{PF}\right)^2} \qquad (2\text{-}2)$$

This form of equation is better suited for extrapolation, since as the Power Factor gets large the predicted inefficiency increases linearly with Power Factor.

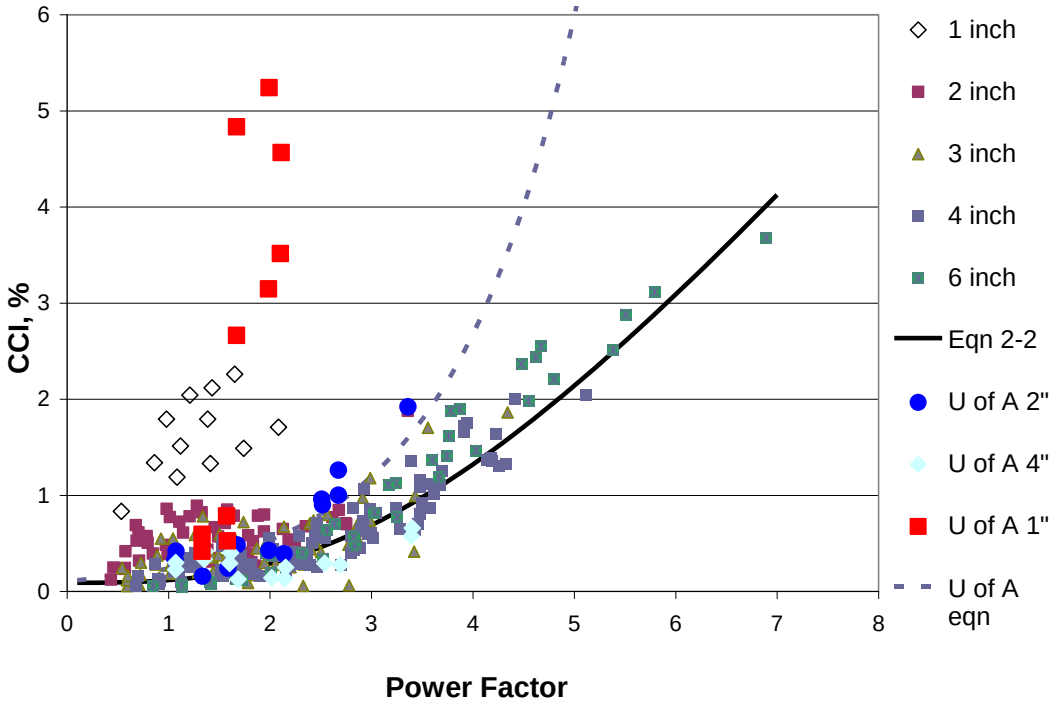

Figure 7 - Results for all pipe sizes, with results reported by the University of Alberta, correlated with the Power Factor. The solid line is equation (2-2) fit to the results for 3", 4" and 6" pipes.

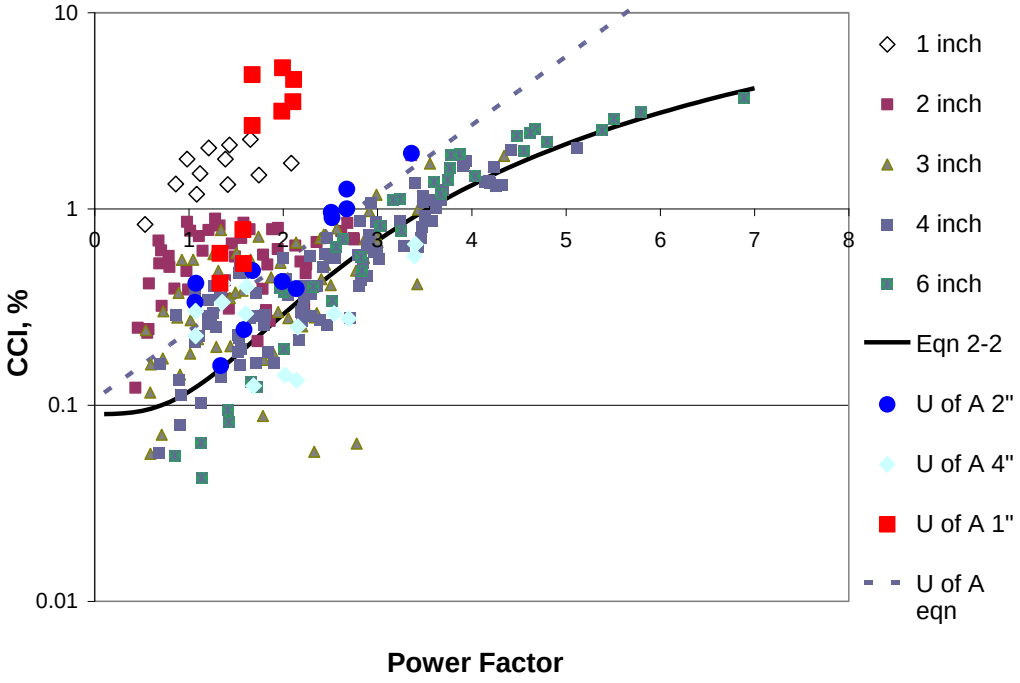

Figure 8 - Replotting Figure 7 as a semi-log plot, to better display the spread of the data.

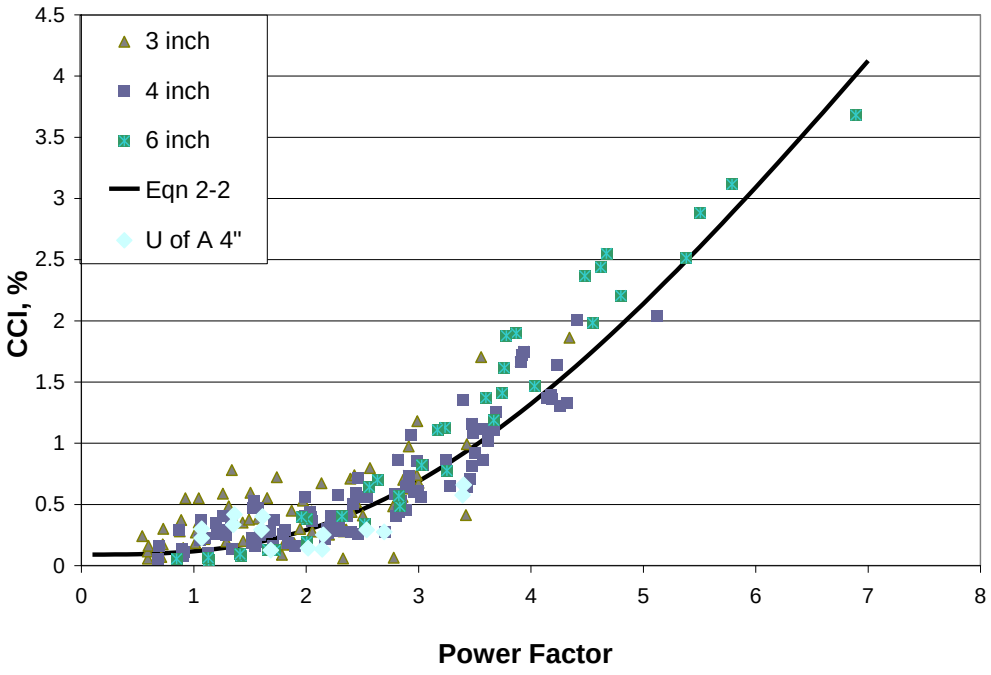

Figure 9 - Replotting Figure 7 with only the results for pipes 3" or larger.

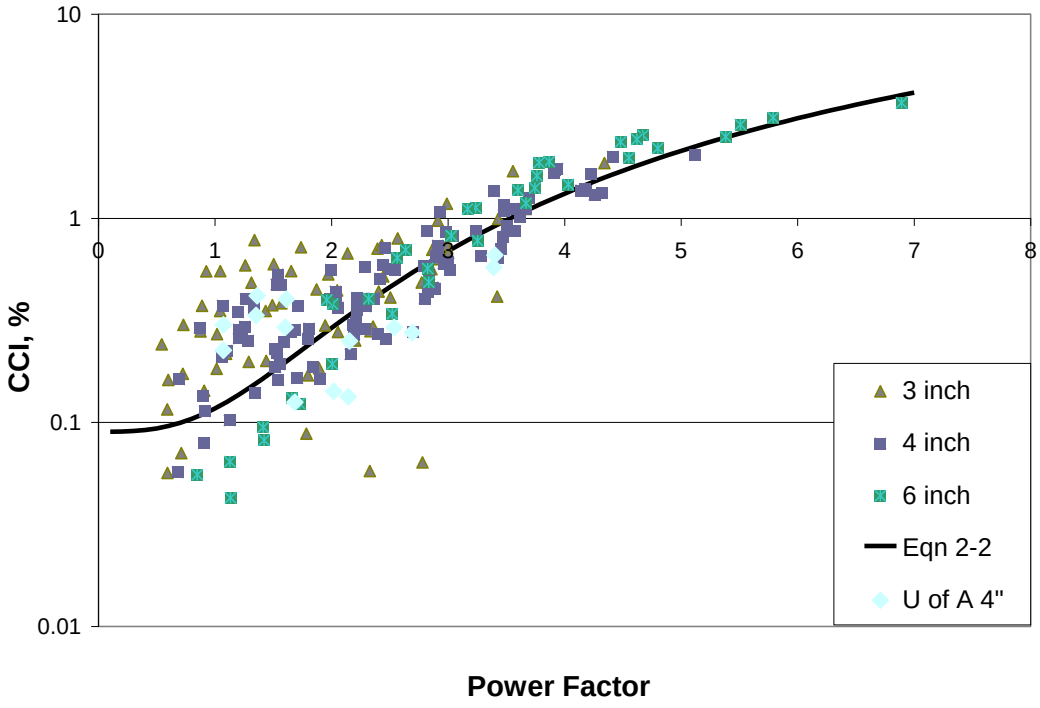

Figure 10 - Replotting Figure 9 as a semi-log plot to better display the spread of the data.

The conversion inefficiency measures the failure of the flare to convert the natural gas to carbon dioxide. The two mechanisms are incomplete combustion, producing carbon monoxide, and fuel stripping, emitting methane. Figure 11 shows the percentage of conversion inefficiency due to fuel stripping, i.e. emitting methane, correlated with the Power Factor. Fuel stripping accounts for 60% to 80% of the inefficiency. The destruction efficiency data for these tests with the basic pipe are plotted against the Power Factor in Figure 12. The DE data have more scatter than the corresponding CCI data. The Power Factor is a useful correlating parameter.

$$DE = 99.9 - \frac{0.4PF}{1+\left(\frac{3.5}{PF}\right)^4} \qquad (2\text{-}3)$$

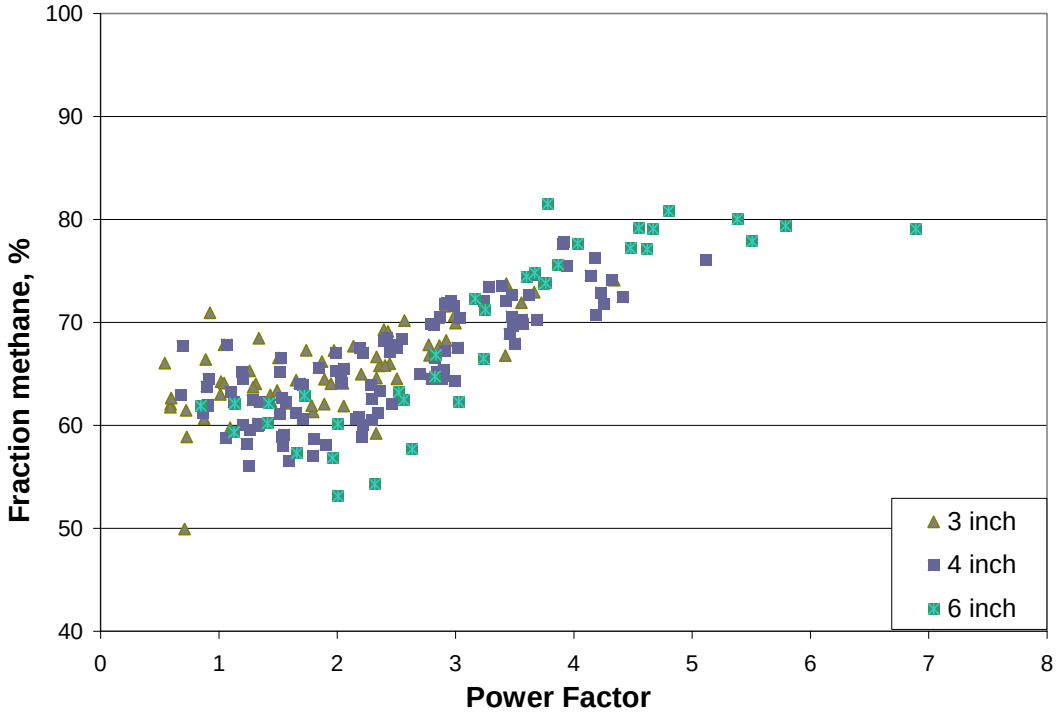

Figure 11 - Fraction of inefficiency due to the emission of methane correlated with the Power Factor.

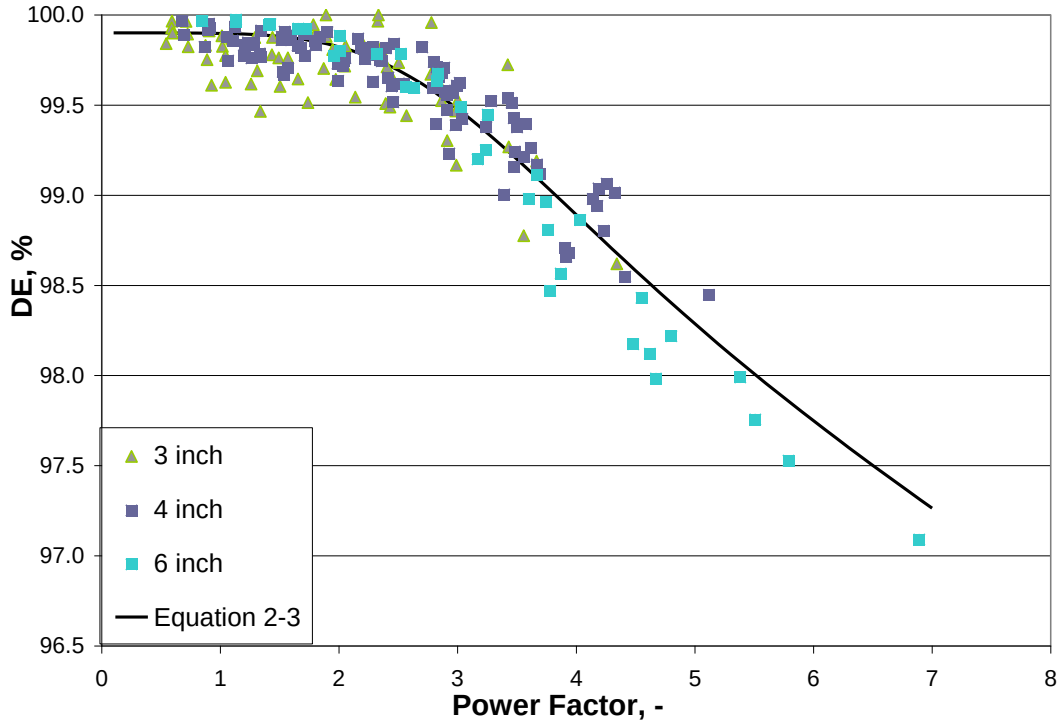

Figure 12 - Destruction efficiency for methane for the tests with natural gas and the basic pipe.

Figure 13 shows the conversion inefficiency for 3" and 6" pipes equipped with the Flame Retention Ring (FRR). The solid line is equation (2-2), the fit to the inefficiency data for basic pipes. While there is a great deal more spread that for the basic pipe data, the FRR data are in moderate agreement. For the rest of the work, it is important to note that the 3" FRR data displays higher inefficiency than the basic pipes and the 6" FRR tip. This means that the results with the 3" FRR over-predict the inefficiency of larger tips.

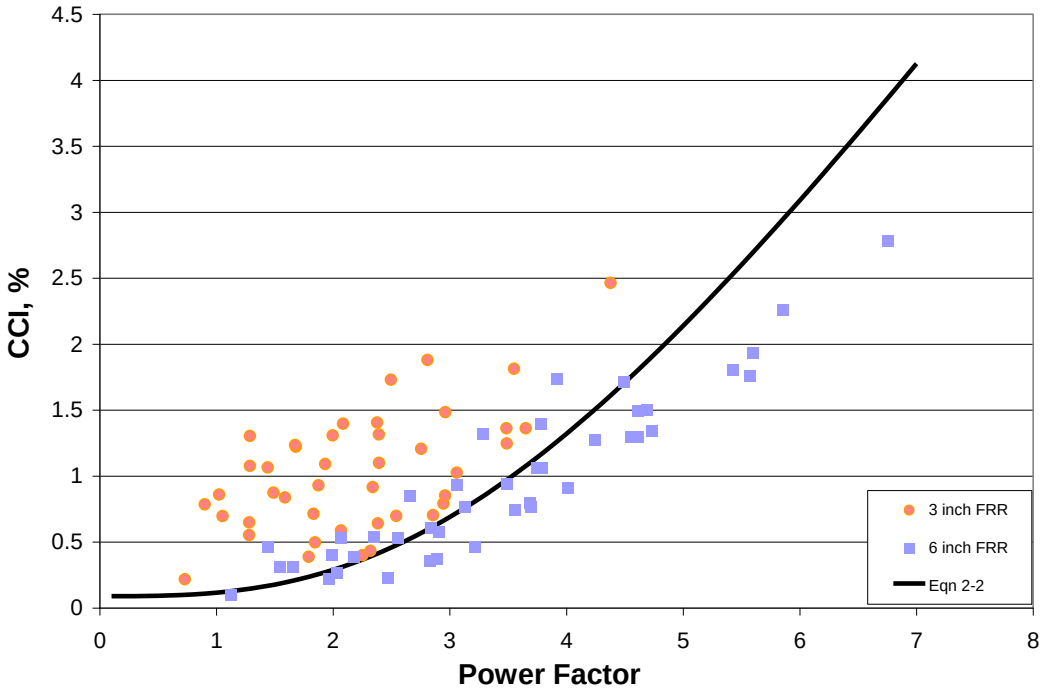

Figure 13 - Conversion inefficiency for 3" and 6" pipes fitted with FRR, plotted against the Power Factor. The solid line is the fit to the basic pipes 3" and larger, equation (2-2).

The DE data for these tests are plotted in Figure 14. Only a couple of points are slightly below the 98% threshold. The equation fit to the data for the basic pipe is plotted here. The DE for the 3" pipe with FRR is lower, and the DE for the 6" pipe with FRR is larger.

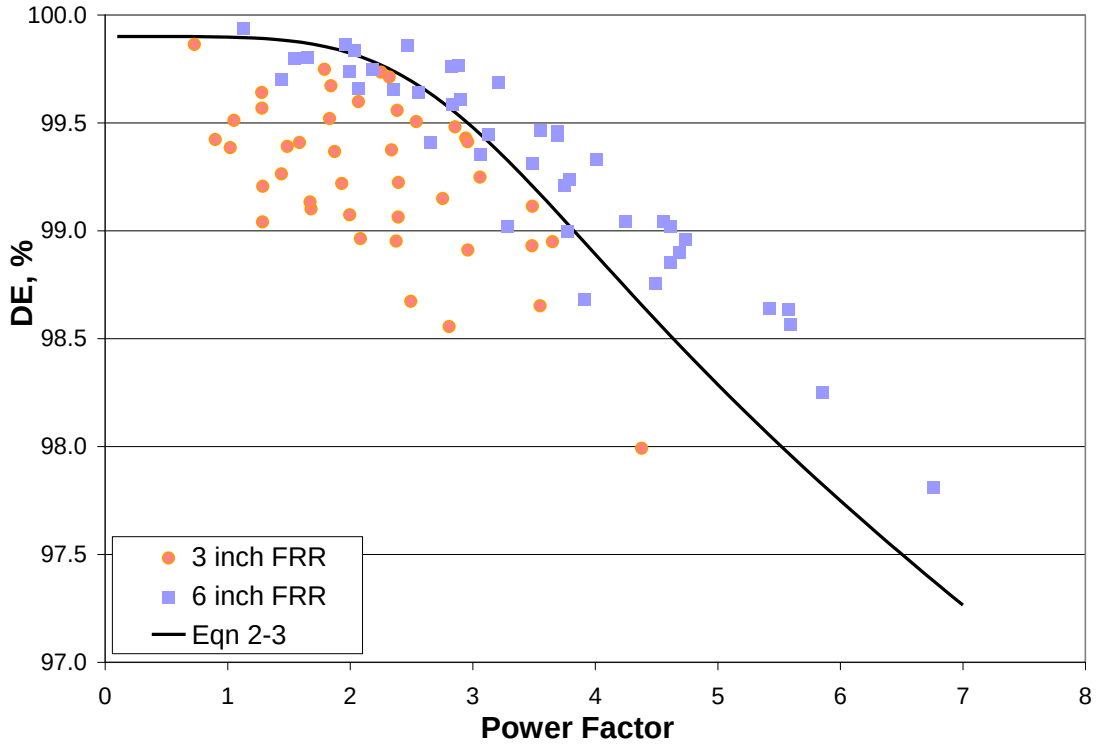

Figure 14 - Destruction efficiency for 3" and 6" pipes fitted with FRR, plotted against the Power Factor. The solid line is the fit to the basic pipes 3" and larger, equation (2-3).

2.3.2 FUEL MODIFICATION TESTS

These tests had a perturbation of the baseline fuel composition, natural gas. It was enriched with 15%-vol propane and diluted with 60%-vol nitrogen. These tests were intended to provide some guidance on modelling the effect of fuel composition in the subsequent tests.

Figure 15 shows the results for the propane-enriched tests. The blue solid line indicates equation 2-2. The data are well correlated with the Power Factor, in the same form as equation 2-2.

$$CCI = 0.1 + \frac{0.5PF}{1 + \left(\frac{6}{PF}\right)^2} \qquad (2\text{-}4)$$

This indicates that for small values of the Power Factor, the effect of fuel composition is small. As the Power Factor gets large, the effect of the enrichment with 15%-vol propane is to half the conversion inefficiency.

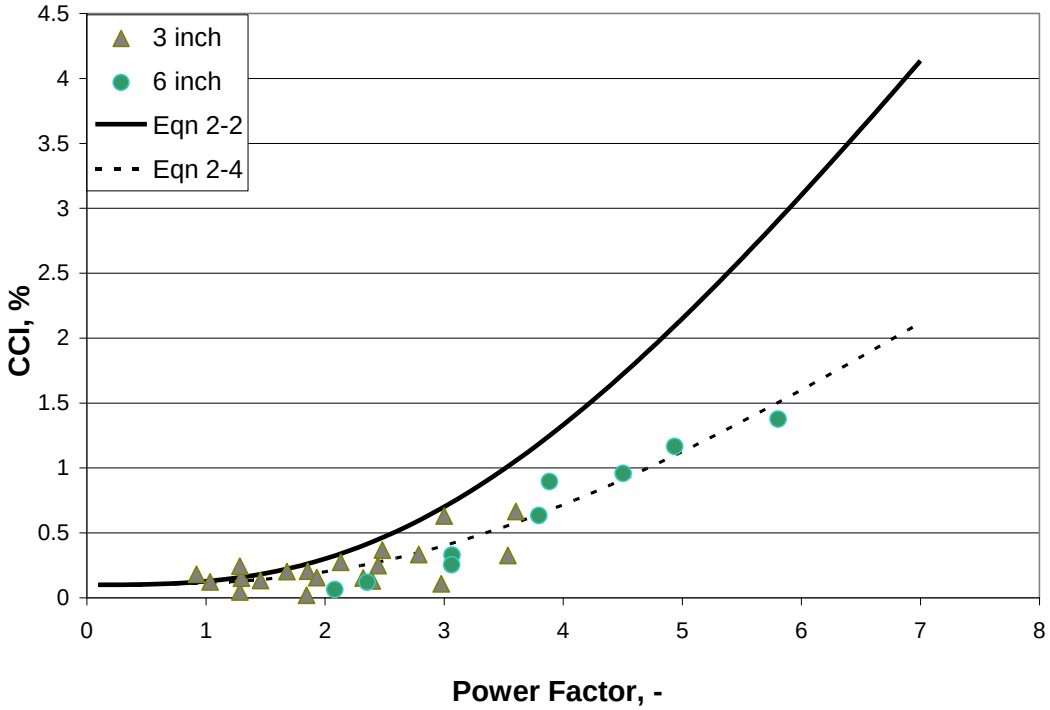

Figure 15 - Results for tests with 3" and 6" basic pipes firing a mixture of 85%-v natural gas with 15%-v propane. The blue line is the fit to the natural gas results, the solid black line is equation (2-4).

Figure 16 shows the conversion inefficiency results with 60%-vol dilution with nitrogen. Comparison with Figure 9 should convince the reader that the nitrogen dilution at this level produced no significant change in conversion efficiency. However, the range of PF covered ($1 < PF < 3$) shows relatively flat response.

These two figures pose a difficult question on modelling the fuel effects. The nitrogen dilution produces a much bigger change in the combustion properties of the mixture (such a laminar burning rate or adiabatic flame temperature) than the enrichment with 15%-vol propane. However, the effect of the propane addition is substantial while dilution has no noticeable effect.

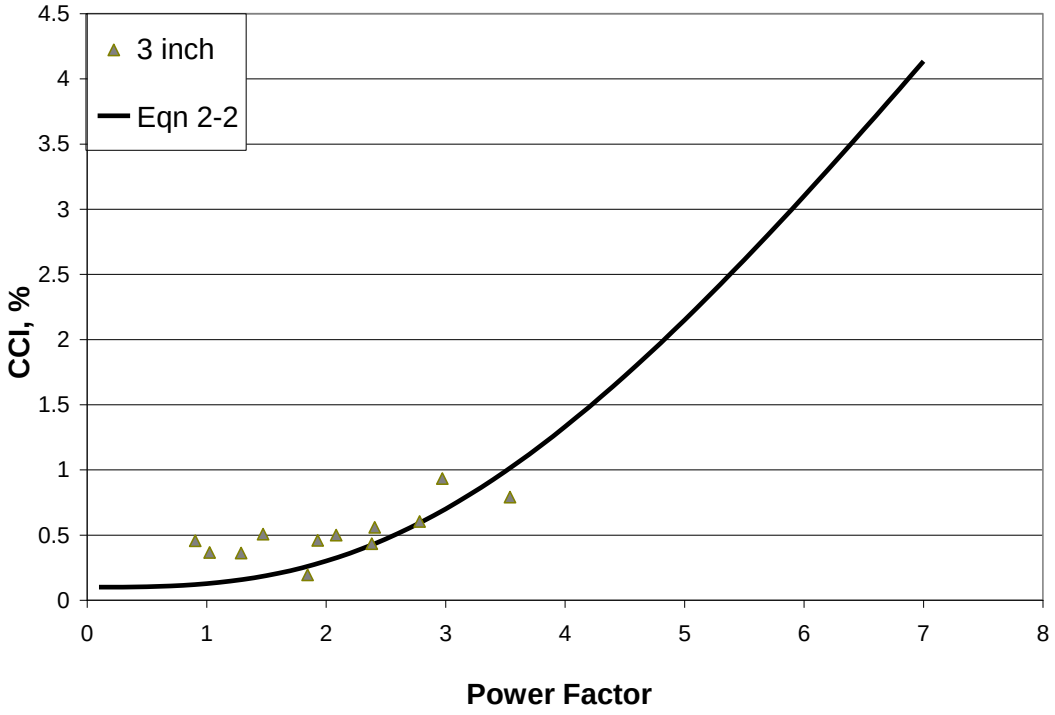

Figure 16 - Results for 3" basic pipe firing a mixture of 40%-v natural gas with 60%-v nitrogen. The solid line is the fit to the natural gas data.

2.3.3 TRANSITION TESTING

The transition to wake-stabilized operation was tested with 2", 3" and 3" FRR flare tips. Since the results for the 2" pipe has been shown not to scale to larger sizes, we will concentrate on the 3" pipe results. Figure 17 shows conversion inefficiency for the 3" pipe in the two paths to wake stabilized operation. The pipe Reynolds number is proportional to the flare gas flow rate. Changing the flare gas flow rate produces very little change in the inefficiency, as indicated by the nearly horizontal line. However, increasing the wind speed produces a marked increase in the inefficiency, the vertical line in Figure 17 and the curved line in Fig 18. Figure 19 plots the inefficiency against the Power Factor. The correlation is reasonable. However, all the transition data are plotted in Figure 20 against the wind speed and display a good correlation with that single operating variable for these transition tests.

That the fuel ramping and wind ramping produce drastically different inefficiency with the same momentum flux ratio indicates that the momentum flux ratio has limits for

correlating the performance of flares. However, the transition to wake-stabilized operation, determined visually, occurred at momentum flux ratio of around 3 for all three pipes. This agrees with the downdraft literature for smoke stacks as we described in the literature review [Gogolek et al., 2009]. Although smoke stacks are non-reacting flows and flares are strongly reacting, this coincidence may be worth further investigation. If the momentum flux ratio is to be useful for understanding flare performance, it would be for marking the regime boundary for wake-stabilized operation.

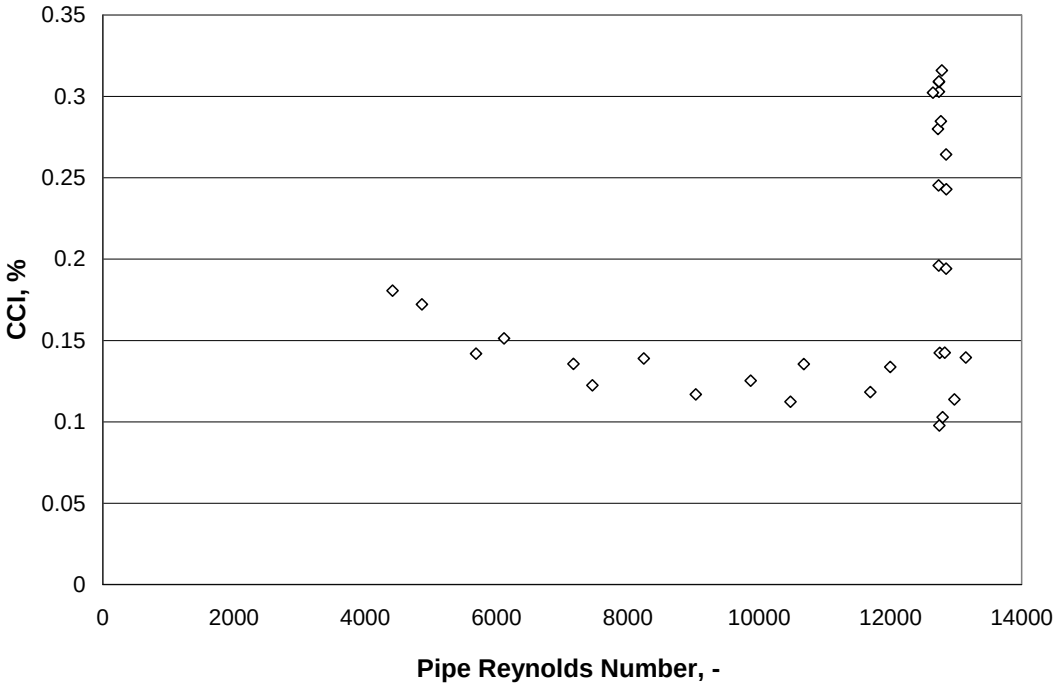

Figure 17 - Results for 3" pipe for transition testing versus fuel Reynolds number. Changing the fuel rate has a very small effect.

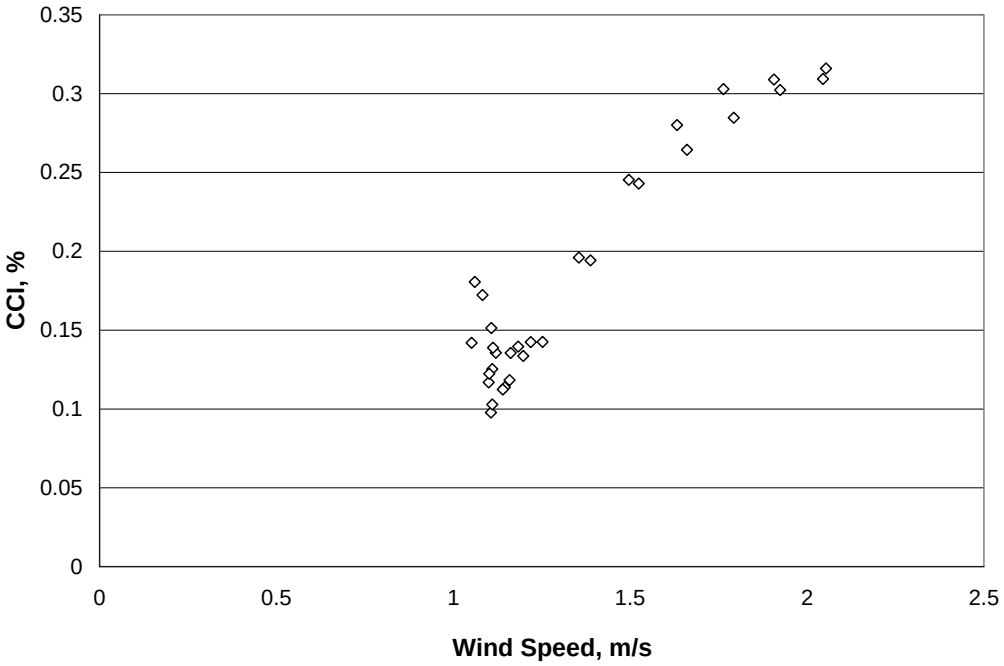

Figure 18 - Results for 3" pipe for transition testing versus wind speed. The change in fuel rate at 1.1 m/s has much smaller effect than the increase of wind speed.

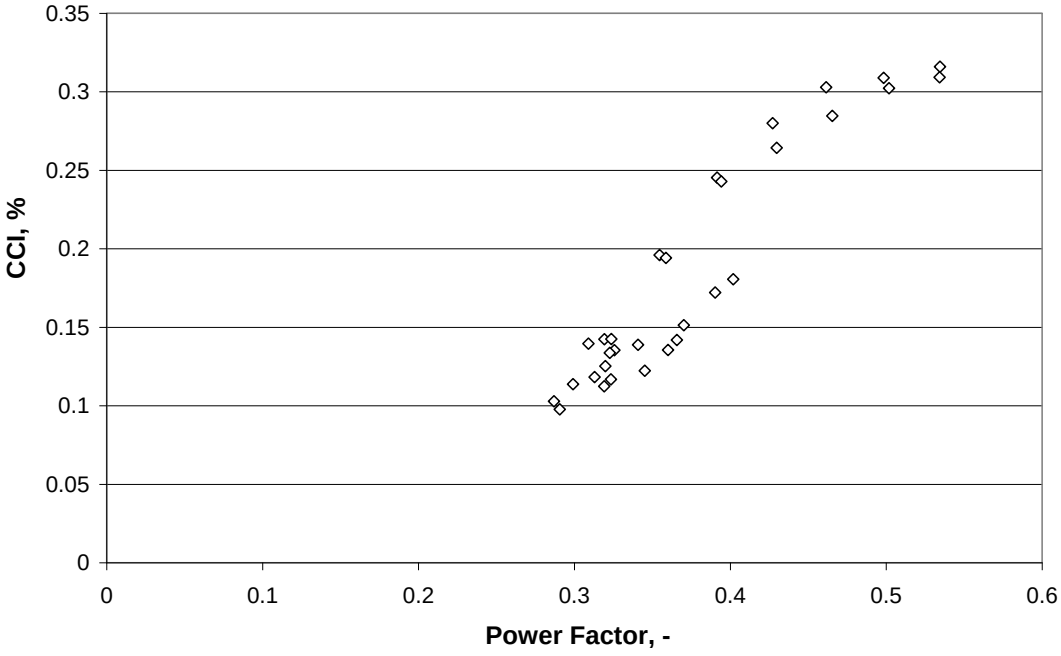

Figure 19 - Results for transition testing of 3" pipe correlated with the Power Factor.

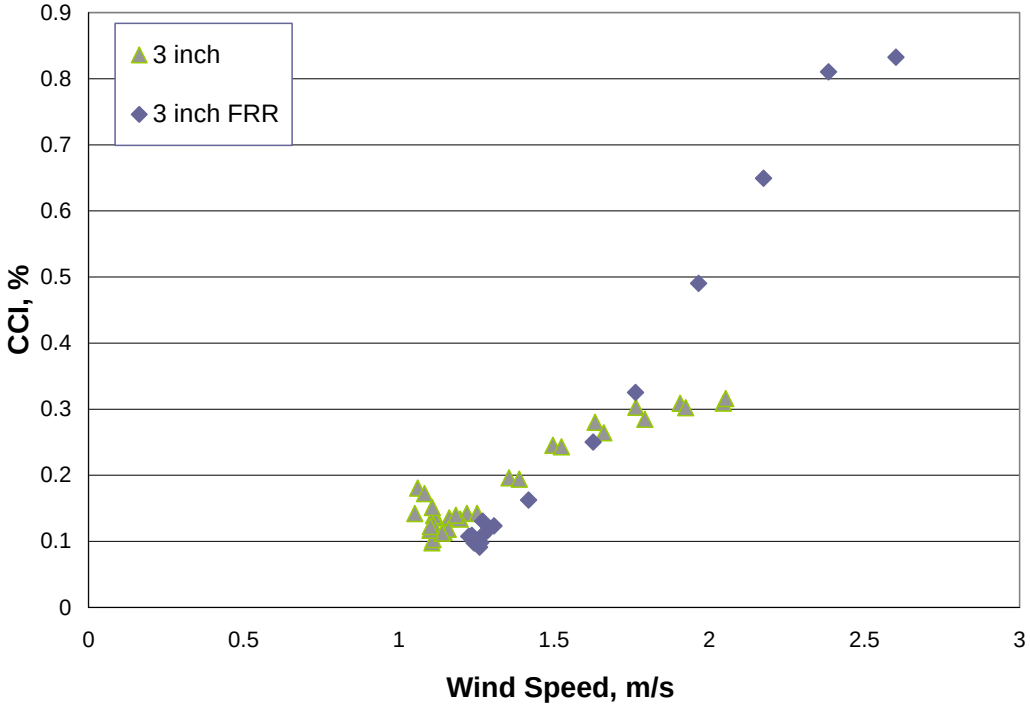

Figure 20 - Transition test results with 3" pipes versus wind speed.

2.4 Conclusion

These baseline tests with natural gas have produced several results useful for the further work on flare performance.

- It is conclusively shown that there is a "Three Inch Rule" for the wake-stabilized operation of flares with wind, as there is for jetting (no wind) operation. This means that results for pipes smaller than 7.5 cm (3 inches) do not scale-up to larger pipes. This is important to keep in mind when small pipe results are used for guiding operating practice.
- The Power Factor (equation 2-1) appears to be a useful dimensionless parameter for correlating flare performance data. It incorporates the effects of wind speed, flare gas rate, and pipe diameter. This indicates the potential for results correlated with the Power Factor to apply to larger diameter flares. However, the PF does

not contain information about the combustion properties of the flare gases. It would have to be augmented to correlate performance of different flare gases and gas mixtures.

- Equation 2-2 is a correlation of the CCI with the Power Factor for results with 3", 4" and 6" pipes flaring natural gas (see Figure 9). This correlation should be useful for solution gas flaring.
- Augmentation of natural gas with 15%-vol propane produced a significant reduction in inefficiency. Equation 2-4 is the correlation of the CCI with the Power Factor for this flare gas (see Figure 15); it is a simple modification of equation 2-2.
- Dilution of natural gas with 60%-vol nitrogen produced no noticeable change in inefficiency (see Figure 16).
- The Flame Retention Ring (FRR) does have an effect on the performance of the flare compared to the basic pipe. It gives slightly worse performance for the 3" pipe and slightly better performance for the 6" pipe (see Figures 13 and 14). Physical change to flare tip configuration affect flare emissions. Results from this test work apply to small pipe flares that have and don't have flare retention rings, such as production flares. Since our further work was done with the 3" FRR tip, the results in subsequent chapters underestimate the efficiency
- Transition testing shows that the there is a continuous change in the performance of the flare as the wake-stabilized regime is established. When the transition is accomplished by reducing the flare gas rate, there is negligible change in the inefficiency. When the transition is accomplished by increasing the wind speed, the inefficiency is increased.

3.0 SIMPLE FUEL GAS TESTS

3.1 Introduction

These tests investigated the effect of wind on the inefficiency and destruction efficiency (DE) for unassisted operation. All the tests were performed using the 3" FRR tip. The two gases flared were ethylene and propylene. Unassisted flaring of these gases produces significant soot, and particulate sampling was performed for all these tests to measure the emission rate. The results of these tests are compared to our baseline results for natural gas from Chapter 2.

3.2 Test Plan

The variables investigated are the fuel rate and wind speed for each fuel. The test matrix is given in Table 4. The mass rate of flare gas was the same for both fuels.

Table 4 - Test matrix for the simple fuel flaring tests.

Fuel	Rate	Exit velocity	Wind Speed
	kg/h	m/s	m/s
Ethylene	10, 30	1.2, 3.4	3.8, 7.0, 10.3
Propylene	10, 30	0.75, 2.2	3.8 – 10.8

The tests with ethylene had three levels of wind speed. The tests with propylene had 5 levels, covering the same range. The ranges of exit velocity of the flare gas do overlap. A total of 17 tests were performed.

3.3 Results

The conversion inefficiency results for all the tests with ethylene and propylene are plotted against wind speed in Figure 21. The results for propylene show high conversion inefficiency and non-monotonic behaviour with wind speed. The inefficiency results for ethylene are lower and basically monotonic with wind speed.

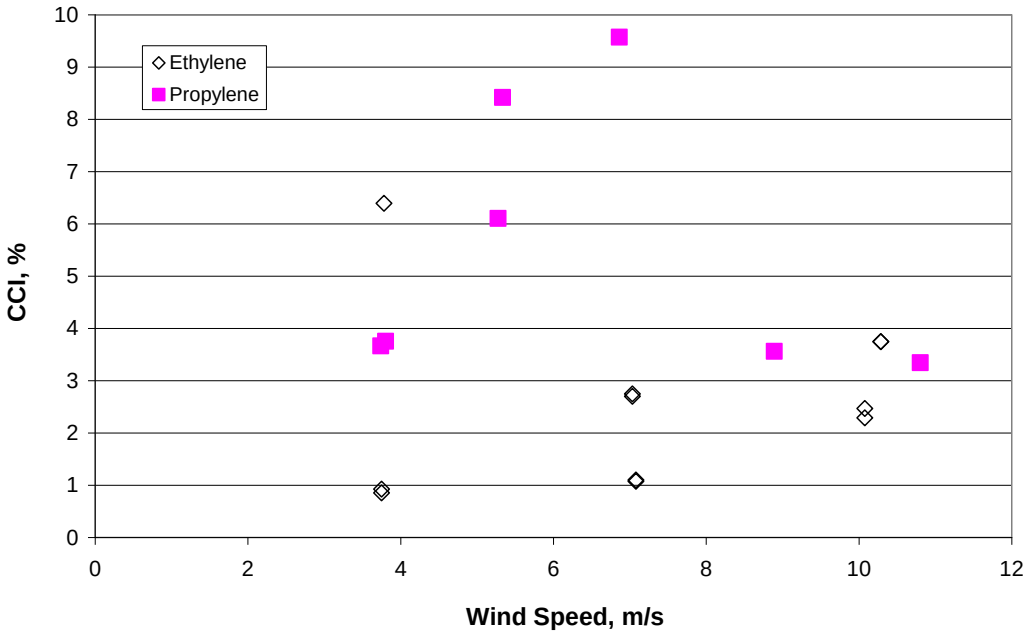

Figure 21 - Conversion inefficiency for unassisted flaring of ethylene and propylene in 3" FRR tip.

The DE results are shown in Figure 22. Better than 98% DE is achieved for all wind speeds for ethylene flaring without assist. The DE for propylene drops below 98% above 8 m/s wind, but remains better than 97%. The difference between the CCI and De is due primarily to the formation and emission of particulate carbon, soot.

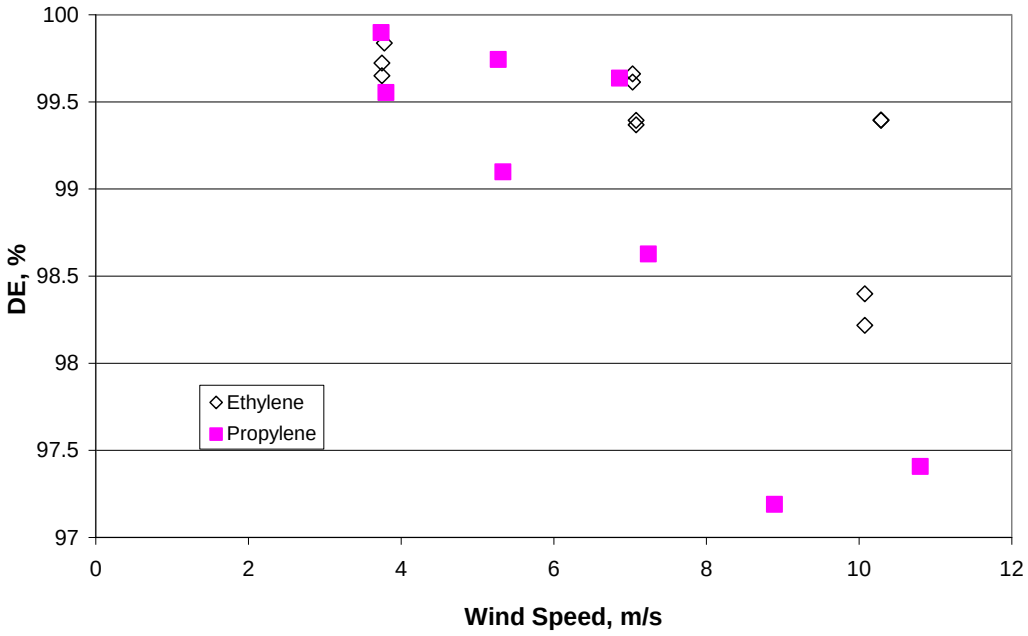

Figure 22 - Destruction efficiency for unassisted flaring of ethylene and propylene in 3" FRR tip.

The soot emission, solid carbon emitted as percent of total carbon flared, is shown in Figure 23. The behaviour of the two fuels is markedly different. Soot emission goes to zero for wind speed above 8 m/s for propylene. The soot emission for ethylene is constant with respect to wind speed.

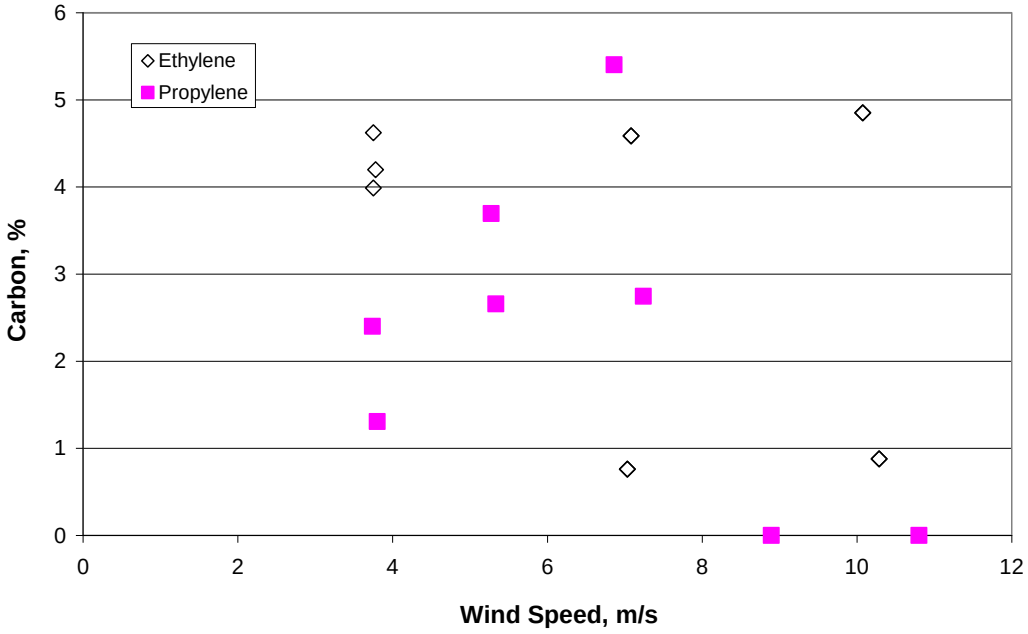

Figure 23 - Solid carbon emission as a percentage of the total carbon for unassisted flaring of ethylene and propylene in 3" FRR flare tip.

3.4 Discussion

The simple fuel results show that high destruction efficiencies are obtained even at very high wind speeds for these two fuels. Figure 24 plots these results against the Power Factor, together with equation (2-2) for natural gas flared in a basic pipe and the data for the natural gas flared with the 3" FRR tip. The basic pipe fit has higher DE. There is a large amount of scatter for the natural gas DE with the 3" FRR tip. This covers the data points for ethylene and propylene. However, it does appear that the Power Factor can correlate the DE results for ethylene and propylene.

Ethylene has higher DE than propylene, which is to be expected from its combustion properties. As seen with the enrichment of natural gas with propane, the differences in fuel properties become evident only at the higher values of Power Factor. When the Power Factor is small all the fuels have high DE.

The correlation using the Power Factor indicates that these results should be scalable to large flare pipes, as shown in the previous chapter.

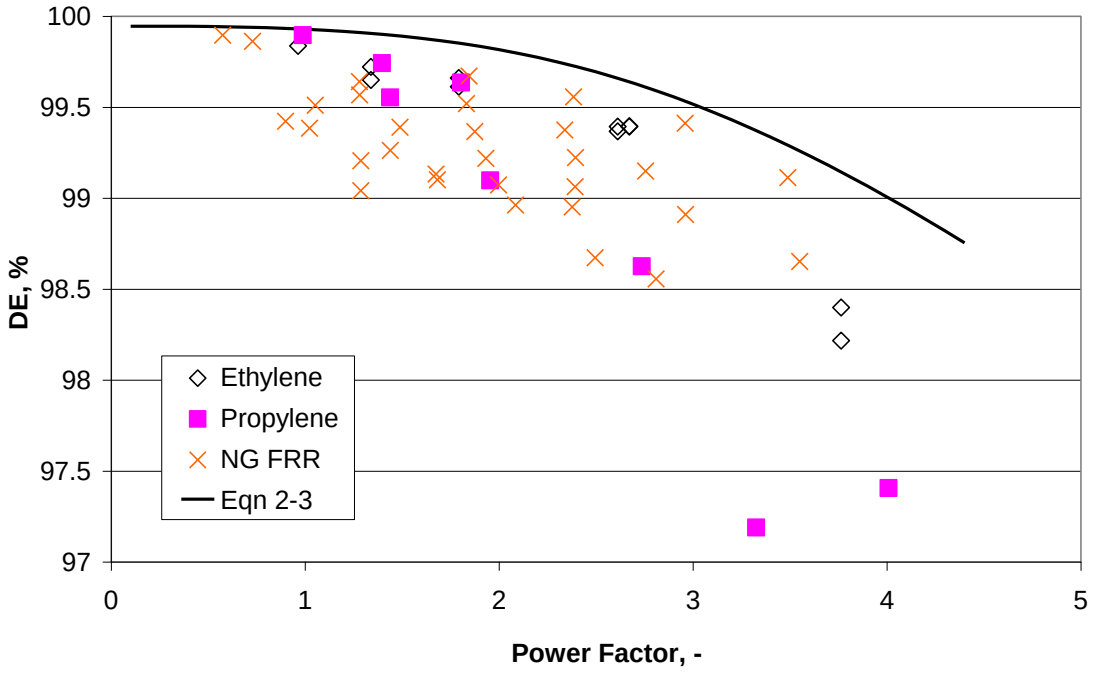

Figure 24- Comparison of destruction efficiency of unassisted flaring of ethylene and propylene with that of natural gas in a 3" FRR flare tip. The solid line is equation 2-3, the DE curve for natural gas flared with 3", 4" or 6" basic pipe.

3.5 Conclusion

Tests of the unassisted flaring of ethylene and propylene established the following:

- Particulate carbon makes a significant contribution to the carbon conversion inefficiency (CCI). It does not affect the Destruction Efficiency. For ethylene, it is around 5% of total carbon, independent of wind speed. For propylene, particulate carbon emissions increase with wind speed to a maximum around 6% at 7 m/s. Carbon emission dropped below the measurement threshold of 0.1% of fuel carbon at higher winds for propylene.
- Destruction Efficiency decreases with wind speed but remains better than 98% for ethylene even at the highest wind speed tested (11 m/s).
- DE for propylene decreases more with wind speed, falling below 98% above 8 m/s. DE is above 97% for all winds for propylene.

- DE for unassisted flaring of ethylene and propylene is correlated with the Power Factor. The scale-up results in the previous chapter indicate that these DE results for ethylene and propylene have the potential to scale-up to large flare tip sizes.

4.0 STEAM-ASSIST TESTS

4.1 Introduction

Here we test the effects of steam-assist on the flaring of natural gas, ethylene and propylene. Flaring natural gas generally does not require steam-assist. However, a steam-assisted flare may have a purge flow of natural gas and the steam nozzles with stand-by flow. Some of the tests with natural gas are therefore with low flow rates for both the flare gas and the steam.

The tests with ethylene and propylene are intended to be more normal operation of the flare, with these model gases. There was no measureable soot for the steam rates used in this study.

These results are presented against the standard measure of level of steam-assist, the steam-to-fuel mass ratio (SFR). The Power Factor is also used to analyse the data, with some success. A new measure of the steam-assist rate, the Reduced Steam Volume Fraction (RSVF), is derived in equation 4-3 to assist the analysis.

The CMA tests (McDaniel, 1983) on the steam-assisted flaring of propylene had little or no wind. Those results are not directly comparable to ours. However, they will be used as a possible extrapolation of our results to the condition of low wind speed.

4.2 Test Plan

All tests used the 3" FRR tip, with the steam-ring provided by John Zink LLC. See the report on the experimental facility for a description of the equipment [Gogolek et al, 2009b]. Three wind speeds were used. The test matrix is given in Table 5.

Table 5 - Overall test matrix for the steam-assisted trials.

Fuel	Fuel Rate	Exit Velocity	Wind Speed	SFR
	kg/h	m/s	m/s	kg/kg
Natural gas	7 - 30	1.2 – 5.8	3.5 – 9.5	<0.3 – 2.2
Ethylene	10, 30	1.1 – 3.3	3.5 – 9.5	0.24 – 3.4

Propylene	10, 20, 30	0.7, 1.4, 2.2	3.5 – 9.5	0.3 – 1.2

There are 6 tests with natural gas that had steam flow but the measurement of the steam flow was faulty. These were low flow tests and hence the steam rate was set to zero.

There was only one test with ethylene at the high flare gas rate of 30 kg/h.

The maximum SFR for propylene was 1.2. The flame was quenched at higher steam rates. Published work, particularly the CMA study [McDaniel, 1983], indicated that propylene can have an SFR up to 3.5 before performance is significantly degraded. The difference in these measurements is addressed in the Discussion section.

4.3 Results

The conversion inefficiency and DE results for steam-assisted flaring of natural gas are presented in Figures 25 and 26, plotted against the SFR and indexed by the wind speed. Wind clearly has a strong negative impact on the performance of the flare. Natural gas test results for destruction efficiency and combustion inefficiency are much degraded compared to the mid-1980's CMA and EPA test results. IFC results do not produce 98-99% destruction efficiency as the CMA and EPA tests did. IFC test results have 90-95% destruction efficiency. IFC test results extend only to Steam-to-fuel ratio of 1.0 before severe degradation of destruction efficiency happens. CMA and EPA test results experienced such degradation when SFR > 3.5.

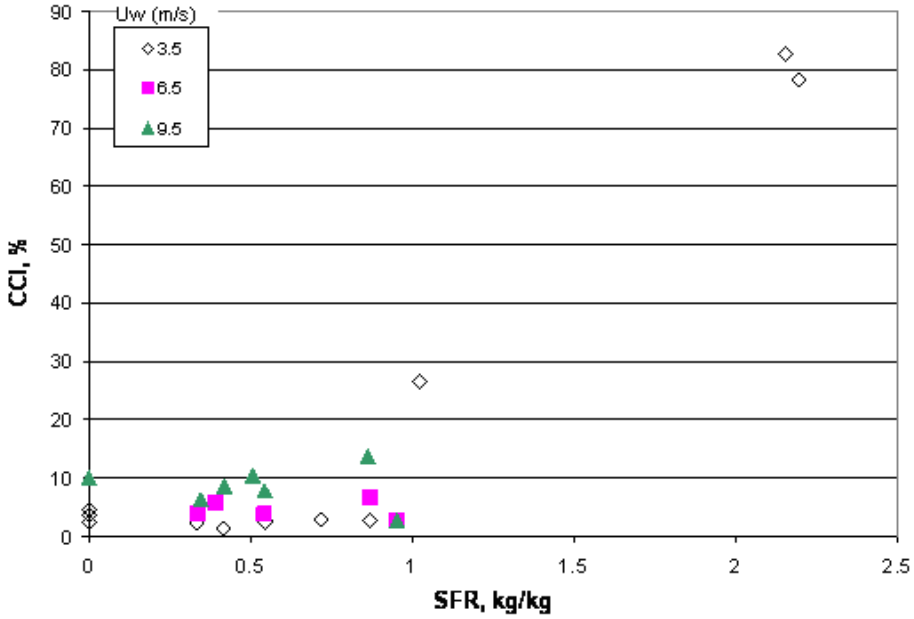

Figure 25 - Conversion inefficiency versus steam-to-fuel mass ratio for steam-assisted flaring of natural gas, indexed on nominal wind speed. The zero SFR points did have steam flowing, but the correction of the flow rate produced a negative value.

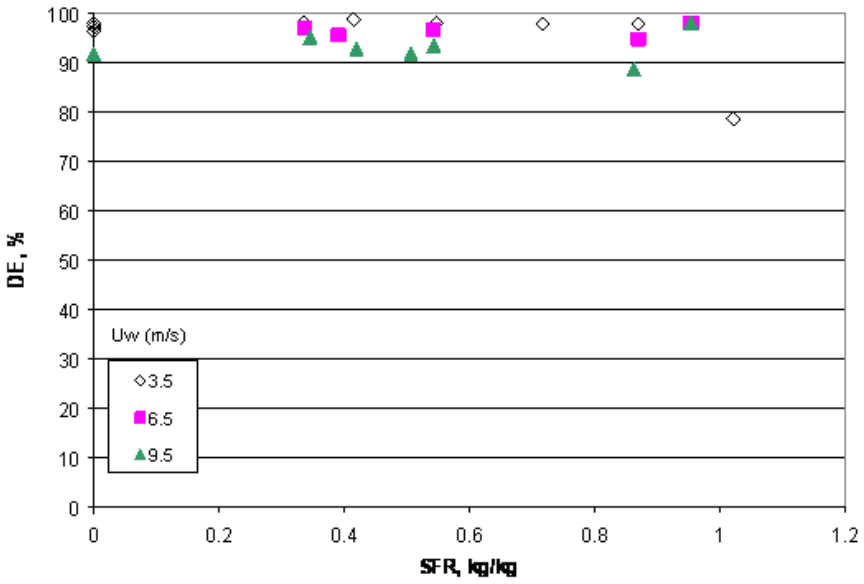

Figure 26 - Destruction efficiency versus steam-to-fuel mass ratio for steam-assisted flaring of natural gas, indexed on nominal wind speed in m/s. The zero SFR points did have steam flowing, but the correction of the flow rate produced a negative value.

The conversion inefficiency and DE for steam-assisted flaring of ethylene are presented in Figures 27 and 28, plotted against SFR and indexed by wind speed. The test with SFR=1.5 appears to be anomalous, giving a very high inefficiency. Ethylene test results for destruction efficiency and combustion inefficiency are degraded compared to the mid-1980's CMA and EPA test results. IFC results do not produce 99.91% destruction efficiency as the CMA tests did in the flare screening facility. IFC test results have 95-99% destruction efficiency. IFC test results extend only to Steam-to-fuel ratio of 0.8 before severe degradation of destruction efficiency happens. CMA and EPA test results experienced such degradation when SFR > 3.5. API RP521 suggests a 0.4 - 0.5 SFR for ethylene.

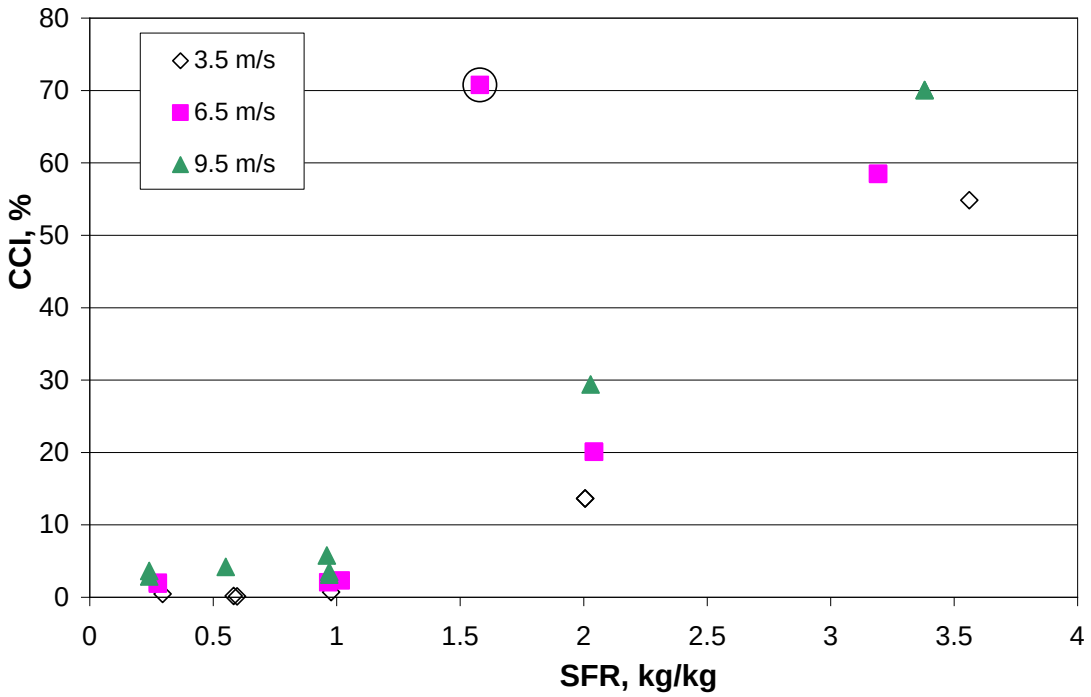

Figure 27 - Conversion inefficiency versus steam-to-fuel mass ratio for steam-assisted flaring of ethylene, indexed on nominal wind speed. The circled point appears to be anomalous.

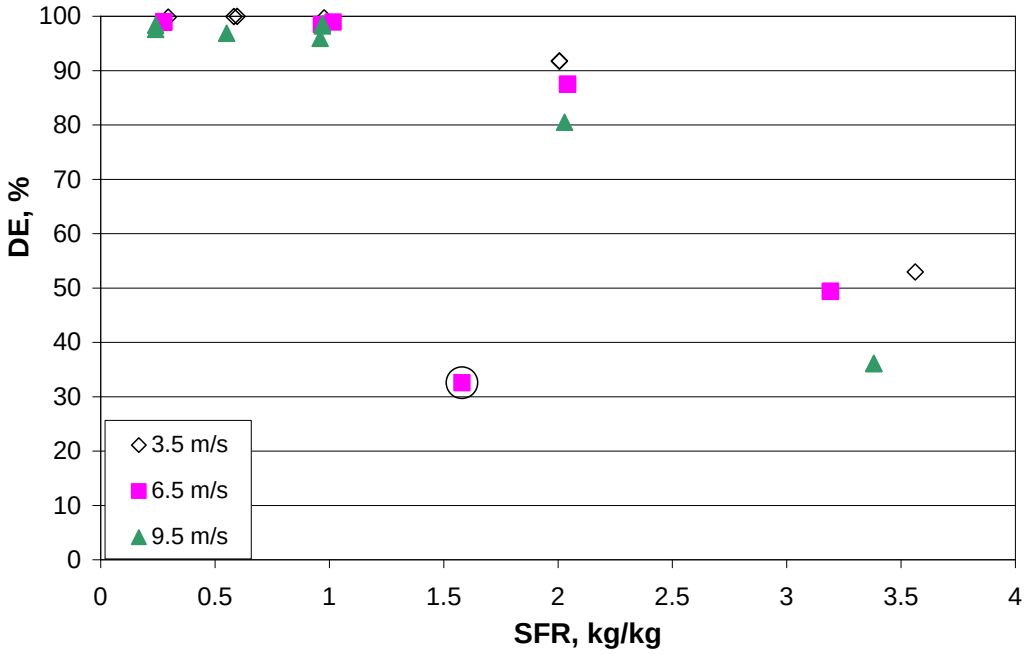

Figure 28 - Destruction efficiency versus steam-to-fuel mass ratio for steam-assisted flaring of ethylene, indexed on nominal wind speed. The circled point appears to be anomalous.

Figures 29 and 30 present the conversion inefficiency and DE for steam-assisted flaring of propylene, plotted against SFR and indexed on wind speed. The test results for AFR = 0.8 appear to be anomalous. Propylene test results for destruction efficiency and combustion inefficiency are degraded compared to the mid-1980's CMA and EPA test results. IFC results do not produce 99.98% destruction efficiency as the CMA tests did in the flare screening facility. IFC test results have 88-98% destruction efficiency. IFC test results for Steam-to-fuel ratio above 0.6 show severe degradation of destruction efficiency. CMA and EPA test results experienced such degradation when SFR > 3.5. API RP521 suggests a 0.5 - 0.6 SFR for propylene.

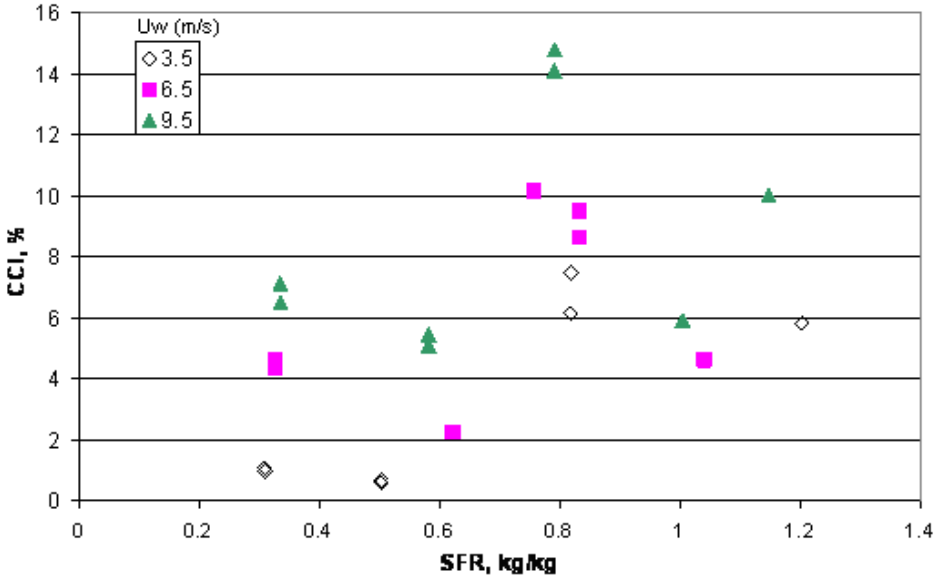

Figure 29 - Conversion inefficiency versus steam-to-fuel mass ratio for steam-assisted flaring of propylene, indexed on wind speed in m/s.

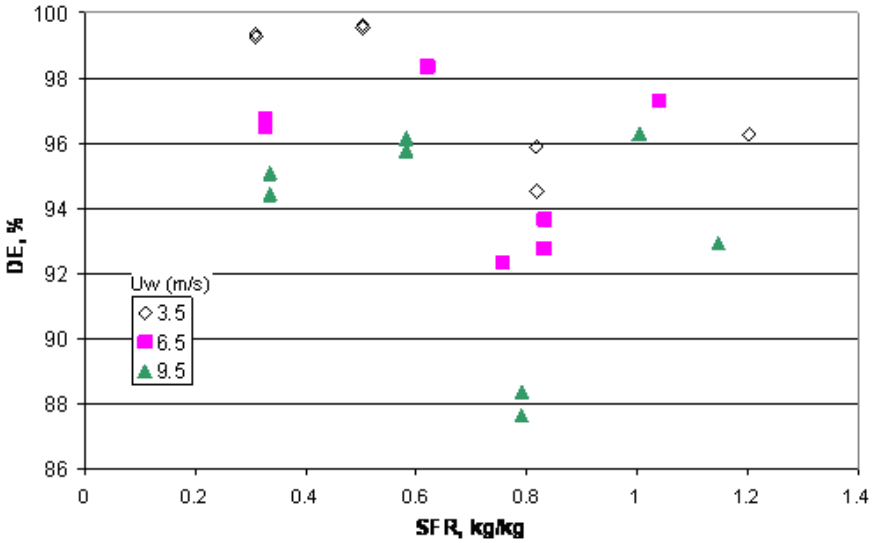

Figure 30 - Destruction efficiency versus steam-to-fuel mass ratio for steam-assisted flaring of propylene, indexed on wind speed.

4.4 Discussion

The first level of analysis is to use the Power Factor to correlate the performance measures. Figures 31 and 32 show the conversion inefficiency and DE for the natural gas tests with SFR < 1 plotted against the Power Factor. These show that a Power Factor less than 1.3 is needed to get DE better than 98%, when flaring natural gas.

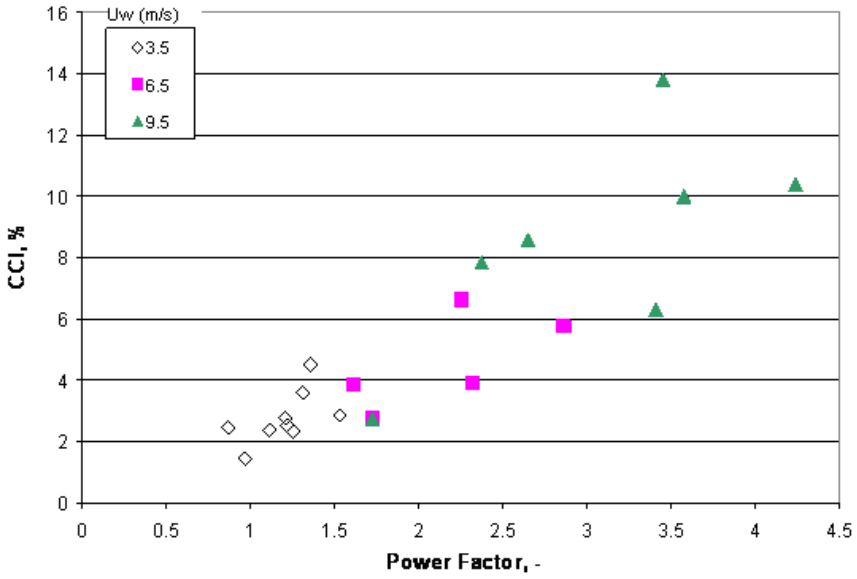

Figure 31 - Conversion inefficiency for steam-assisted flaring of natural gas versus Power Factor, for SFR < 1.

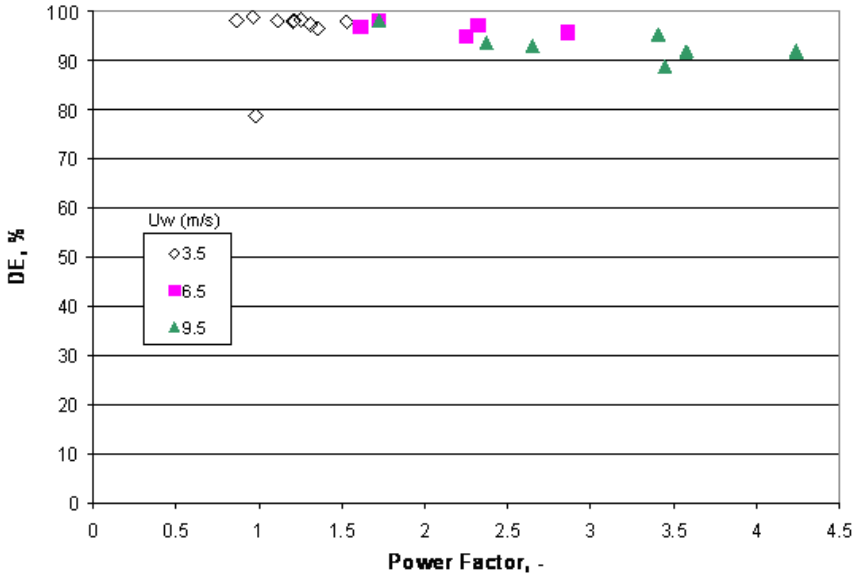

Figure 32 - Destruction efficiency versus Power Factor for steam-assisted flaring of natural gas, for SFR < 1.

Figures 33 and 34 show the conversion inefficiency and DE for ethylene plotted against Power Factor, for all values of SFR. There are clearly three separate divisions between the data, corresponding to the three different values of SFR. One can extrapolate the data separation to the point of zero Power Factor, corresponding to no wind. The middle DE data, with SFR = 2, extrapolates to better than 98% DE with no wind. This shows the sensitivity of the case of low fuel flow to the cross-wind.

Figures 35 and 36 present only the results with SFR < 1. The Power Factor correlates the results and the figure shows that the DE > 98% is obtained when the Power Factor is less than 3. However, these figures show that the wind can have a very strong effect on the performance of steam-assisted flares.

In Figure 37 we have included the DE results for unassisted flaring of ethylene. There is a clear decrease in destruction efficiency as the SFR is increased. The dependence on the Power Factor, which combines the effects of wind speed and flare gas rate, is clear for the different steam-assist rates.

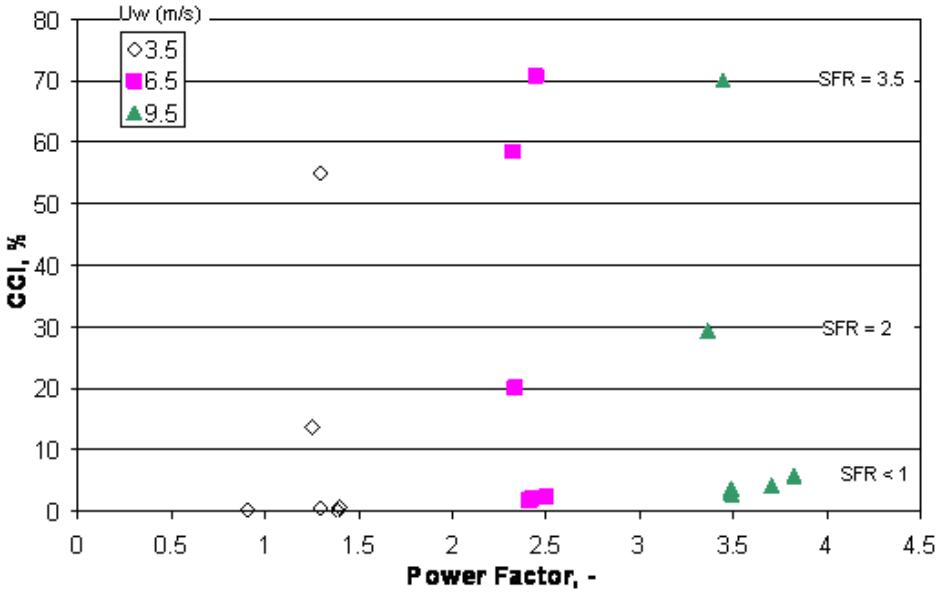

Figure 33 - Conversion inefficiency versus Power Factor for steam-assisted flaring of ethylene, indexed on wind speed. All steam levels included.

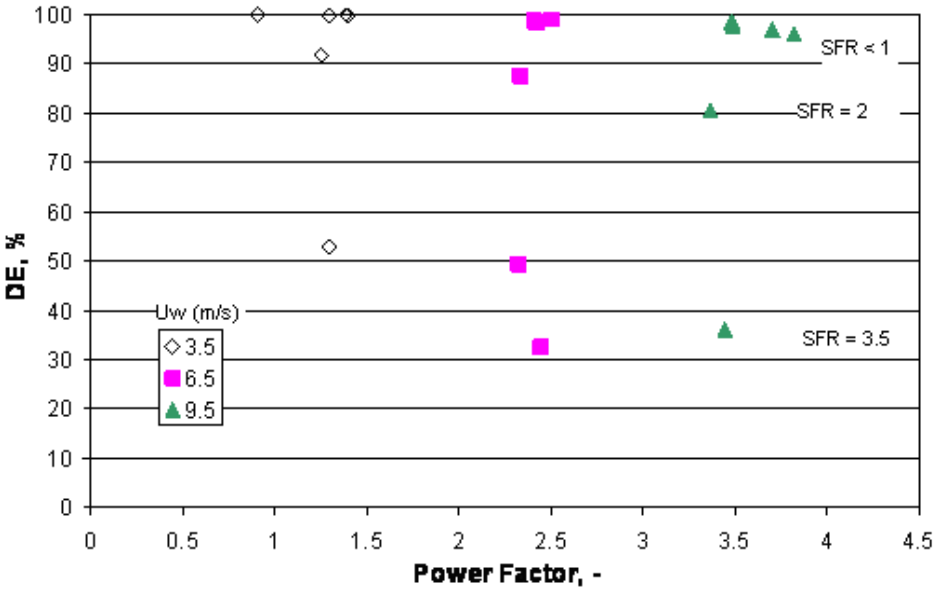

Figure 34 – Destruction efficiency versus Power Factor for steam-assisted flaring of ethylene, indexed on wind speed. All steam levels included.

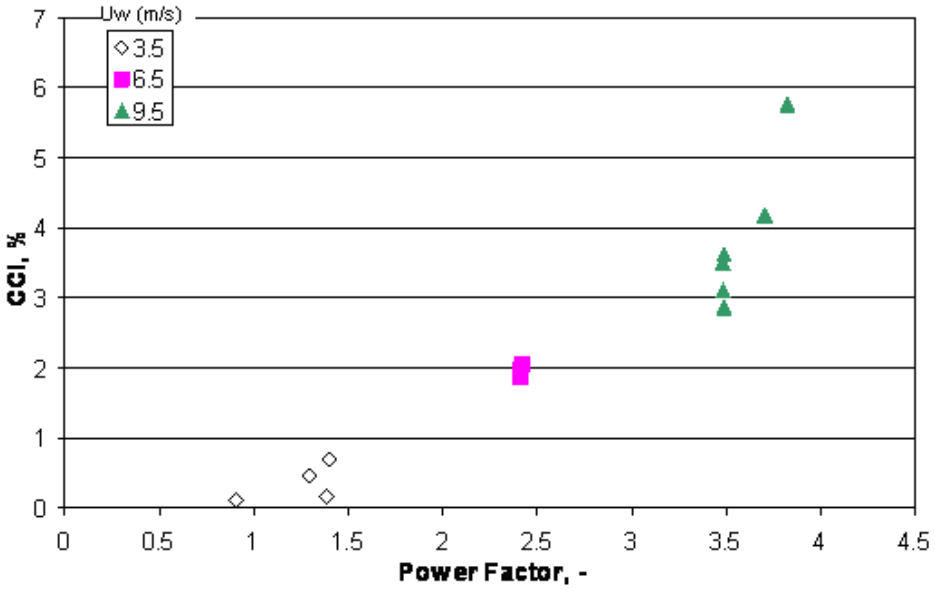

Figure 35 - Conversion inefficiency versus Power Factor for steam-assisted flaring of ethylene, indexed on wind speed, SFR < 1.

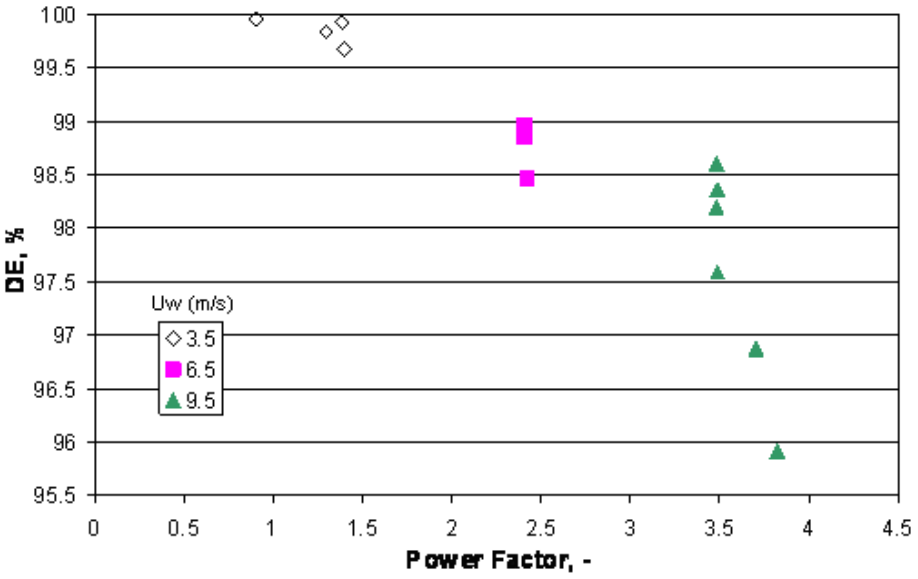

Figure 36 - Destruction efficiency versus Power Factor for steam-assisted flaring of ethylene, indexed on wind speed, SFR < 1.

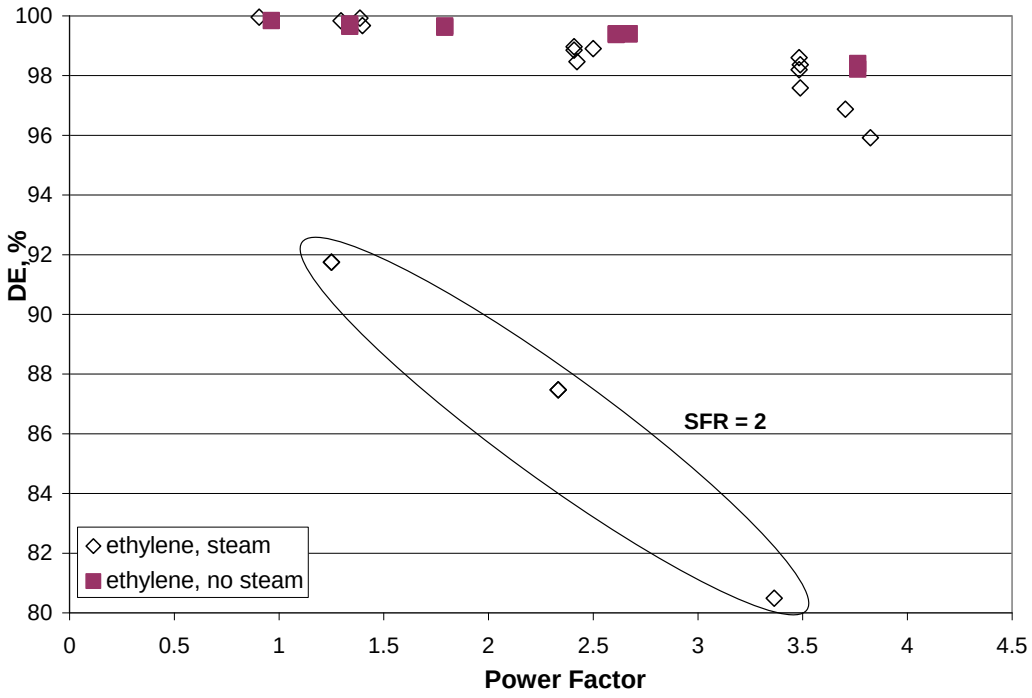

Figure 37 - Destruction efficiency versus Power Factor for unassisted and steam-assisted flaring of ethylene, with Steam-to-Fuel Ratio up to 2.

The conversion inefficiency and DE results for propylene are plotted against the Power Factor in Figures 38 through 42. These display two separate divisions of the data. However, unlike for ethylene, this separation does not correspond to different SFR values. Figures 39 and 40 show that the lower data include points with SFR > 1. The points in the upper data division are from two particular test days, March 19 and March 25, 2008. These are the data for SFR = 0.8 noted above. Close inspection of the run data did not identify any particular problems with those tests, though there is clearly something peculiar about the results. If we neglect those data, the remaining results show that a Power Factor less than 2 is needed to have DE > 98%.

Figure 42 collects the DE results for our steam-assisted and unassisted tests and the steam-assisted DE from the CMA tests. The anomalous data for SFR = 0.8 are circled. The CMA data, which were tests with low wind speed, are the extrapolation to low wind speed of our data.

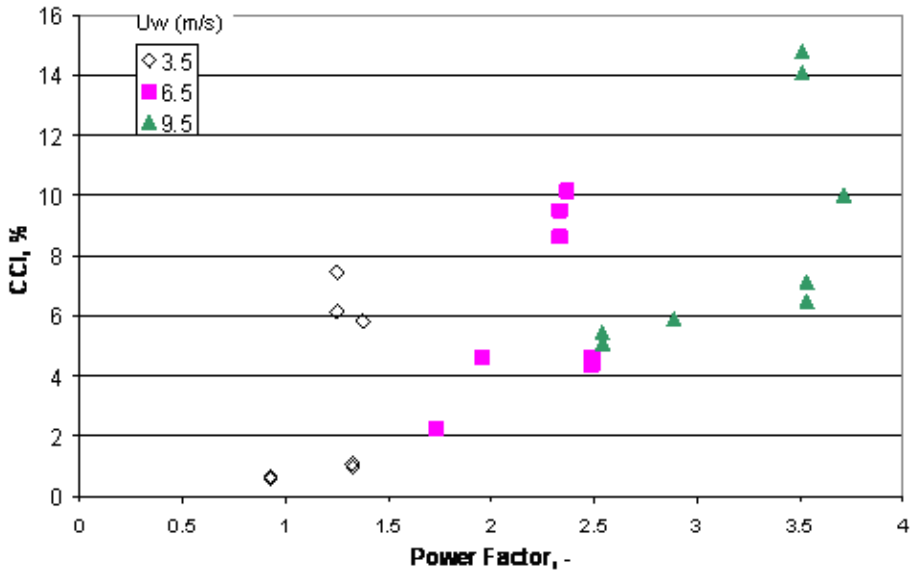

Figure 38 - Conversion inefficiency versus Power Factor for steam-assisted flaring of propylene, indexed on wind speed. All steam levels included.

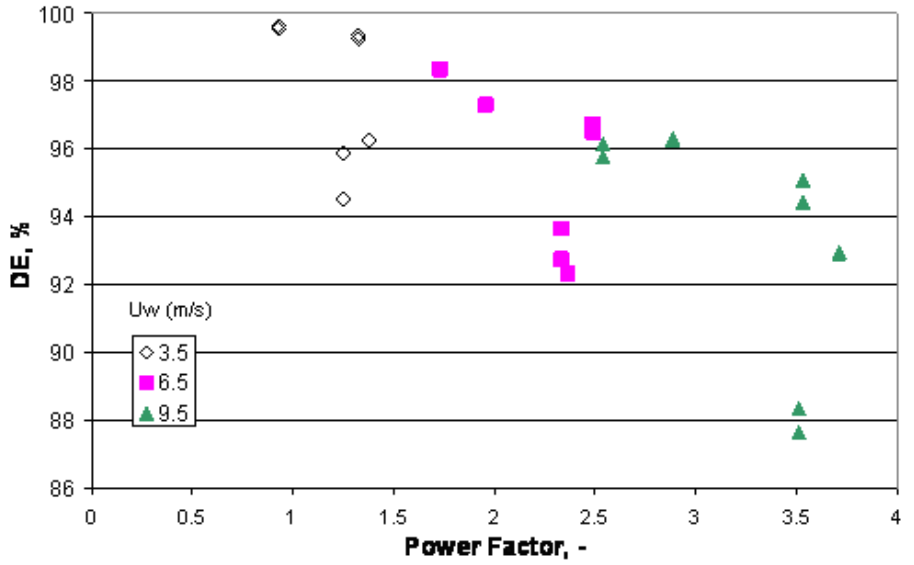

Figure 39 - Destruction efficiency versus Power Factor for steam-assisted flaring of propylene, indexed on wind speed. All steam levels included.

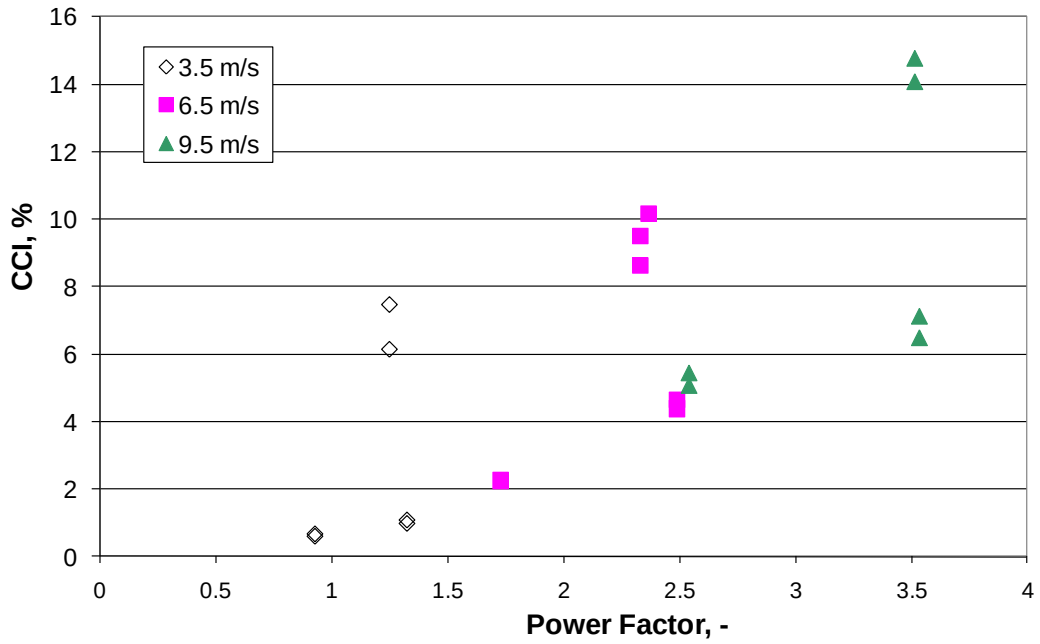

Figure 40 - Conversion inefficiency versus Power Factor for steam-assisted flaring of propylene, indexed on wind speed, SFR < 1.

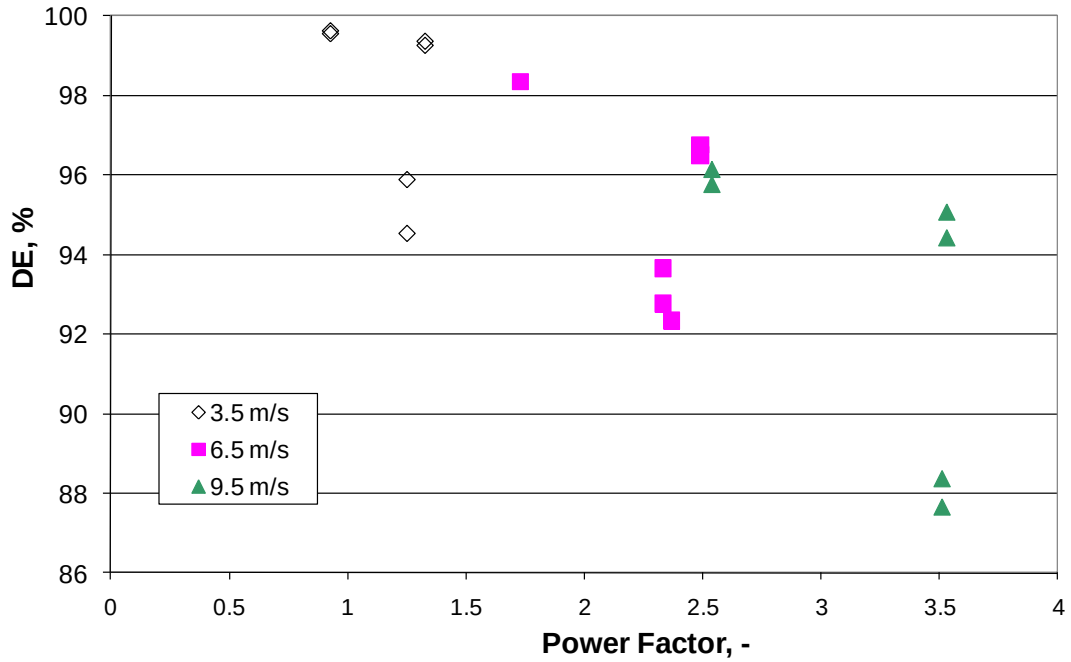

Figure 41 - Destruction efficiency versus Power Factor for steam-assisted flaring of propylene, indexed on wind speed, SFR < 1.

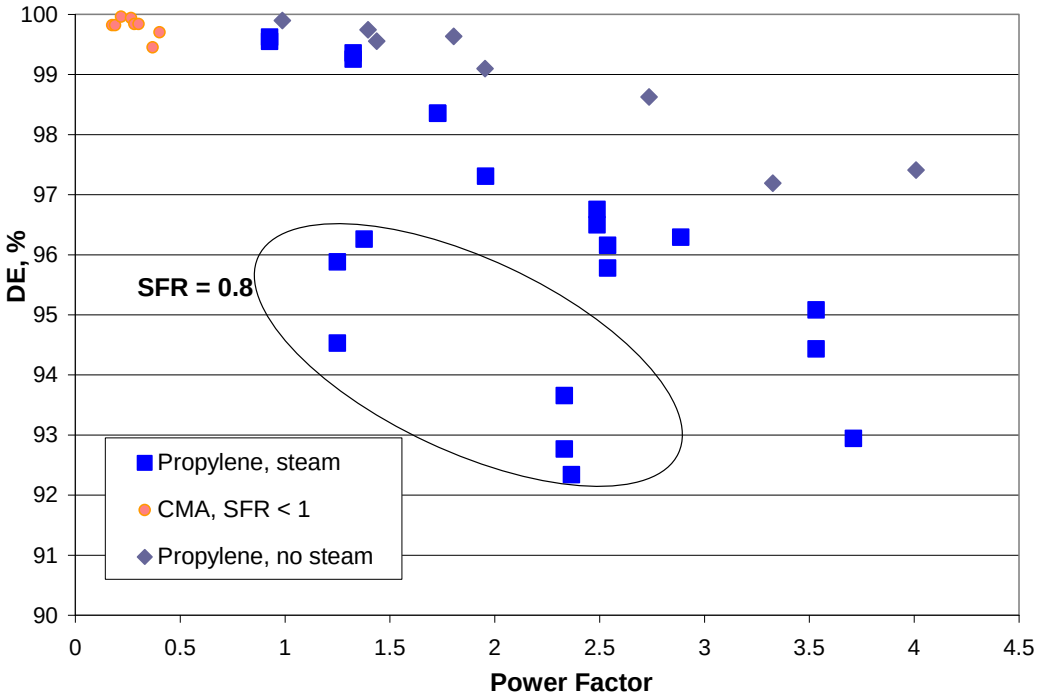

Figure 42 - Destruction efficiency results for flaring propylene, both steam-assisted and unassisted. The CMA data for steam-assisted flaring with SFR < 1 is included.

The results for the different fuels can be brought together by looking at the steam volume fraction. Assume that the flare gas and steam are well-mixed. The volume fraction of the steam in the mixture is given by

$$X_{st} = \frac{SFR}{18/M_f + SFR} \tag{4-1}$$

Here M_f is the molecular weight of the flare gas.

The volume fraction of steam (or any inert compound) has an upper limit determined from the flammability limits (I^*). For the gases used in this work the apex of the flammability diagrams was tabulated in the Literature Review (Table 6) [Gogolek et al, 2009a] for nitrogen and carbon dioxide. The apex for steam was taken to be midway between those two values. Using using this apex value for steam I^* together with the stoichiometric air:fuel volume ratio λ, the critical volume fraction of steam is

$$X^*_{st} = \frac{(1+\lambda)I^*}{\lambda I^* + 1} \tag{4-2}$$

This critical volume fraction is used to normalize the actual volume fraction of steam as calculated by (4-1).

$$RSVF = \frac{X_{st}}{X^*_{st}} \tag{4-3}$$

This gives the Reduced Steam Volume Fraction (RSVF). The critical volume fraction for steam is given in Table 6.

Table 6 - Critical volume fraction (equation 4-2) for fuel gases.

	I*	λ	Critical Volume Fraction Steam
Methane	34	9.55	0.845
Ethylene	42.5	14.32	0.919
Propylene	34	21.48	0.921

Figure 43 presents all the steam-assisted flare results for DE plotted against the RSVF. This collapses the data almost onto a single curve. From this figure, one can conclude that the maximum RSVF should be around 0.8 when flaring ethylene or propylene in the presence of wind. The CMA data for flaring undiluted propylene is included in this figure. In the low wind situation for those tests, we see that the RSVF is slightly above 1 for the 'over-steaming' data (SFR of 5.7 and 6.7)

In Figure 44, we have plotted the DE data with RSVF < 0.8 against the Power Factor, including the CMA data for propylene. There is a good correlation for each of the different fuels used. The CMA data fit as the extrapolation of our propylene data to low Power Factor conditions. It should be possible to further collapse these data onto a single curve through a judicious selection of combustion properties of the fuels.

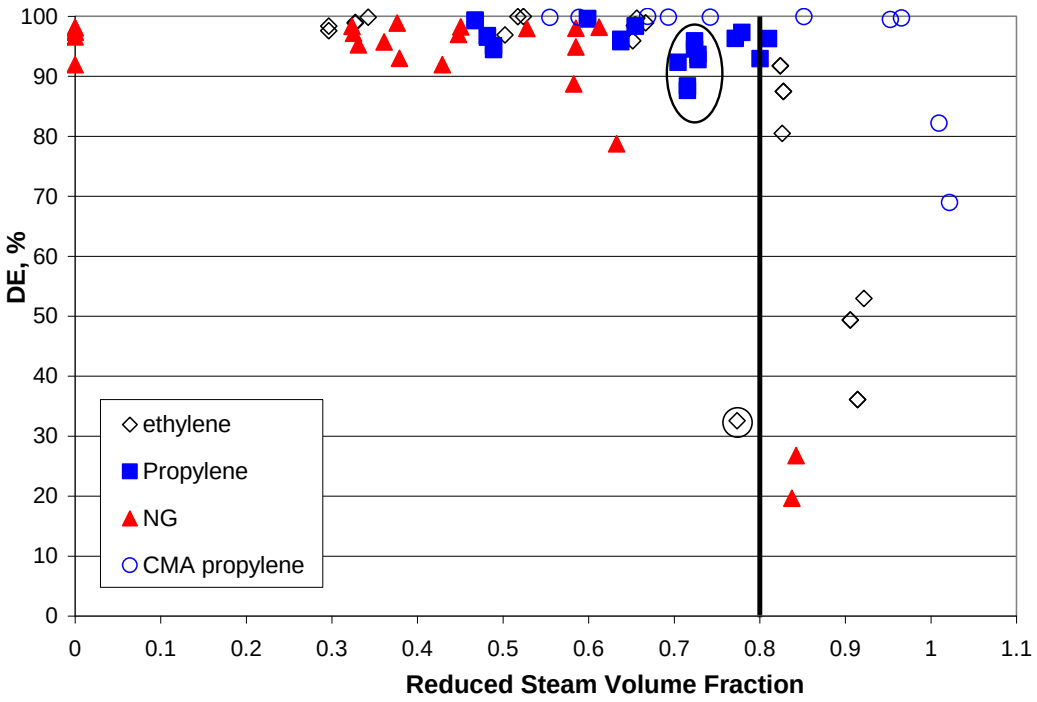

Figure 43 - Destruction efficiency for steam-assisted flaring versus the reduced steam volume fraction. The possibly anomalous data are circled. Recommended maximum is RSVF = 0.8.

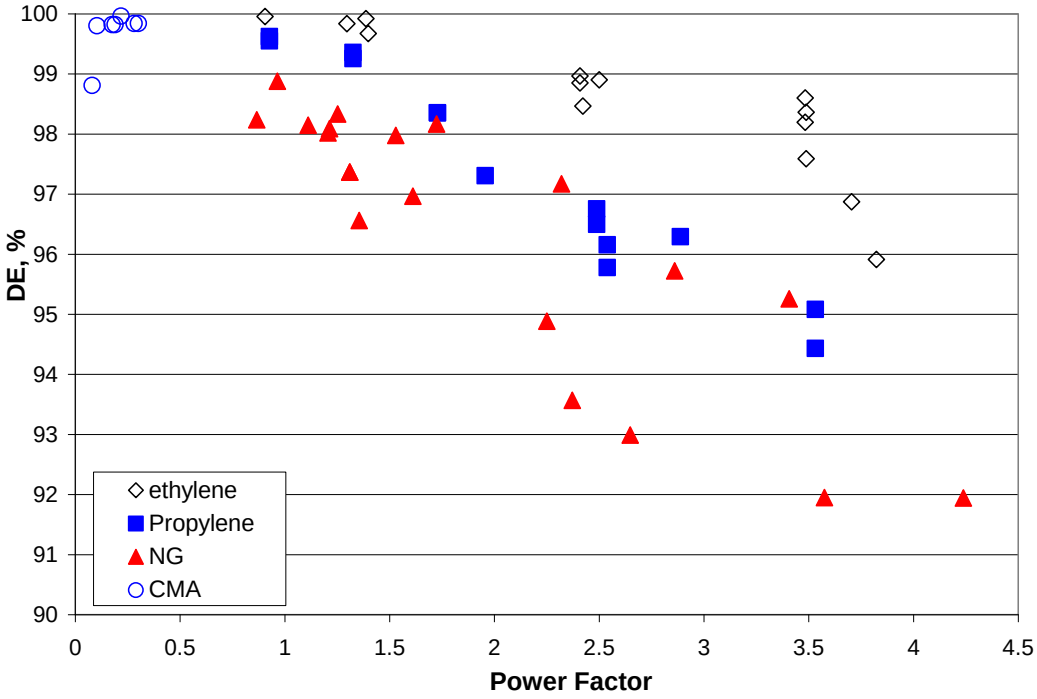

Figure 44 - Destruction efficiency versus Power Factor for steam-assisted trials with RSVF < 0.8.

A first step at a suitable Fuel Factor uses the flammability limits. A simple conceptual model of the mixing of flare gas with air considers the gases as packets that coalesce and divide. A flammable packet has fuel content between the upper and lower flammability limits. A rough measure of the amount of mixing that can be endured by the packets while remaining flammable is the flammability spread divided by the lower flammability limit and this measure is larger for more reactive gases. So our Fuel Factor is the reciprocal of this, so that larger Fuel Factor means a less reactive gas and lower efficiency.

$$\text{Fuel Factor} = \frac{LFL}{UFL - LFL} \tag{4-4}$$

The DE data for RSVF < 0.8 for natural gas, ethylene, propylene and the CMA are plotted against the product of the Fuel Factor and the Power Factor in Figure 45. This fuel factor does not fit the data for natural gas very well. This may be because there are kinetic limitations for natural gas flaring. The data for natural gas are removed in Figure 46.

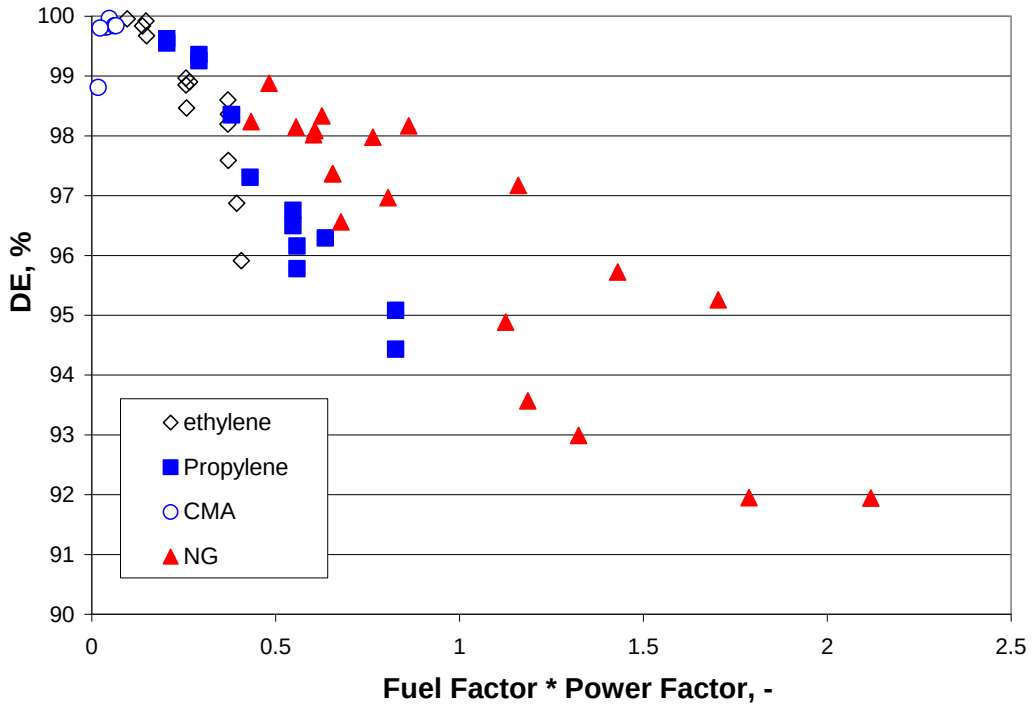

Figure 45 - Destruction Efficiency results for steam-assisted flaring of natural gas, ethylene and propylene, including the CMA data. All data are restricted to RSVF < 0.8. The Fuel Factor is given in equation 4-4.

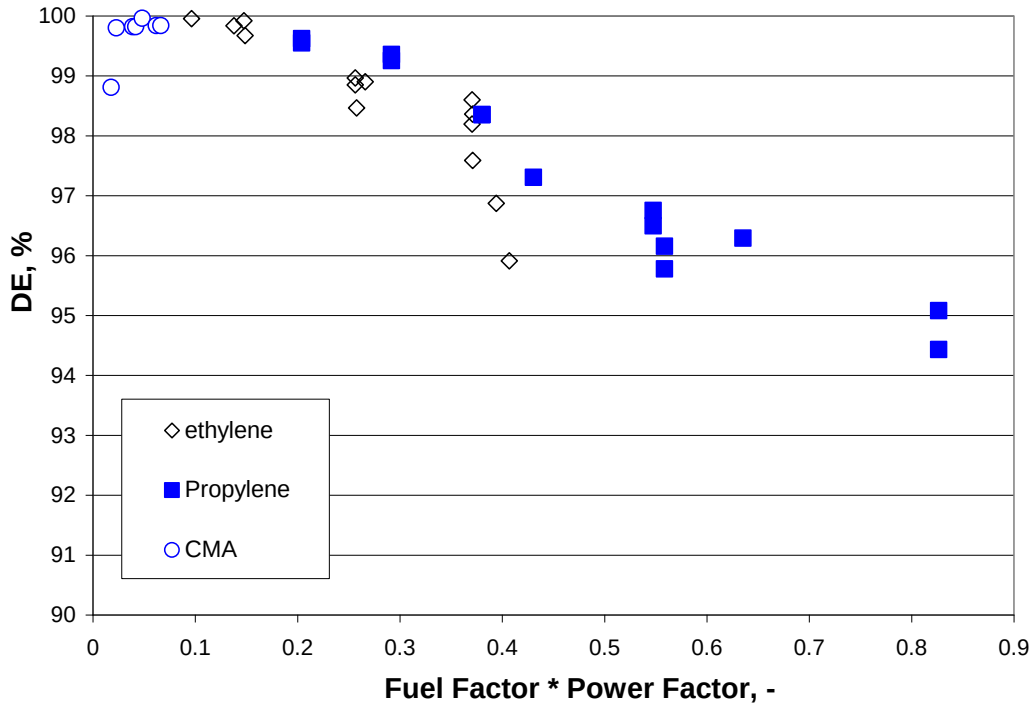

Figure 46 - Destruction Efficiency results for steam-assisted flaring of ethylene and propylene, including the CMA data. All data are restricted to RSVF < 0.8. The Fuel Factor is given in equation 4-4.

The previous standard study for the effect of steam-assist rate was the CMA study (McDaniel, 1983). That study showed little degradation of DE up to SFR of 3.5 while flaring raw propylene. Those tests were conducted with a fixed steam flow rate and increasing the fuel flow rate and low wind speed. Our tests are primarily with a fixed fuel rate and increasing the steam flow rate and wind speeds at and above the average.

Fixed steam flow rate produces a fixed air entrainment and penetration depth for the steam/air jet into the flare gas volume. In the CMA tests, the flare gas volume is shrinking as the SFR is increased. Our tests have fixed flare gas rate and increasing steam flow rate. The increasing steam flow rate gives an increase in air entrainment and jet penetration into the fixed flare gas volume. While these two different methods of varying the steaming will give the same range of SFR, it is possible that the effect of steaming on the flare performance is different in the two cases.

However, there is another possibility to explain the difference between our results and the CMA results (McDaniel, 1983). The CMA study used an 8" flare and a different design

of steam ring. The steam effect may be sensitive to the design of the steam ring (number of nozzles, position of nozzles) for smaller flare diameters. This could imply that the minimum scalable flare for steam-assisted flare studies is larger than the 3" pipe used here. Also, the commercial 8" flare tip, with commercial pilot burners, may be more resistant to the effect of wind than our 3" pilot-scale flare tip.

Finally, possibly the most significant difference is the inclusion of the effect of fairly strong wind in these tests. The wind speeds used in our wind tunnel ranged from 3.5 m/s to 9.5 m/s. These winds speeds are greater than the median for most locations, meaning that wind speeds are less than our range more than half the time. The CMA data are a reasonable extrapolation of our results to low Power Factor conditions (low wind speed or high exit velocity). We have shown that keeping the Power Factor low enough, the DE can be kept above 98%. This threshold Power Factor is somewhere around 2 for propylene, around 3 for ethylene.

4.5 Conclusion

The steam-assisted flaring of natural gas, ethylene and propylene was carried out. There are significant differences in the findings compared to the benchmark CMA study (McDaniel, 1983) and the explanation of the differences is not readily available.

The main findings of this chapter are:

- Wind has a strong negative impact on the performance of steam-assisted flares.
- The effect of the wind increases with increased SFR, particularly if SFR > 1.0.
- Our results are correlated with the Power Factor, producing separate curves for separate SFR values for each flare gas tested.
- An alternative parameter to the SFR, the Reduced Steam Volume Fraction (RSVF, equation 4-3), was derived. It is successful in collapsing the results for natural gas, ethylene and propylene, the gases tested here. It appears that a maximum value of 0.8 for the RSVF is needed for good operation of the steam-assisted flare.

- The data with RSVF < 0.8 correlate well with the Power Factor for each fuel gas. A simple Fuel Factor (equation 4-4) based on a mixing argument was derived that successfully collapses the data for ethylene and propylene onto a single curve for the product of the Fuel Factor and the Power Factor. The natural gas data are not well correlated.
- With RSVF < 0.8, the maximum Power Factor to have DE > 98% is around 2 for propylene and around 3 for ethylene.
- The CMA data for flaring propylene fits as an extrapolation of our results to low Power Factor conditions (low wind speed or high exit velocity). However, it may be that the pilot-scale flare tip used in our tests was too small and that larger commercial flare tips are more resistant to the effect of wind.

5.0 DILUTION TESTING

5.1 Introduction

An important part of the flaring regulations and operation is the control of the heat content of the flare gas. The minimum energy content for the flare gas is generally taken as 7.5 MJ/m^3 (200 BTU/scf) for unassisted flares and 11.2 MJ/m^3 (300 BTU/scf) for steam- and air-assisted flares (EPA 40CFR 60). These thresholds arose from an interpretation of the landmark studies by Pohl and co-workers [Pohl et al, 1986].

Subsequently, questions were raised about the adequacy of the energy content. DuPont had an exemption to the regulation for the cases of hydrogen-containing flare gases. Gogolek and Hayden showed that mixtures of natural gas with nitrogen or carbon dioxide with the same energy content have different conversion efficiency when flared in the wake-stabilized mode [Gogolek and Hayden, 2003].

The aim of the tests reported in this chapter is to investigate the effect of nitrogen and carbon dioxide dilution with the model flare gases (natural gas, ethylene and propylene). Nitrogen can be found in flare gas at refineries and chemical plants. Carbon dioxide is generally not found in the flare gas of refineries, but can be found in the flare gas at chemical plants and at some upstream oil processing facilities.

5.2 Test Plan

The following is the procedure for the tests:

- Set the initial fuel rate at 10 kg/h.
- Set the initial diluent rate to give a 50%-vol hydrocarbon/inert mixture.
- Increase the diluent rate in 10 kg/h increments until flare extinction or until maximum inert gas flow rate is achieved.
- If maximum inert gas flow rate is achieved, then decrease the hydrocarbon flow rate in 1 kg/h increments until extinction.

The exit velocity from the pipe increases at the same time as the inert gas supply rate increases. The wind speed was kept low, at 2.5 m/s. As for all the other tests, the flare tip was the 3" FRR.

5.3 Results and Discussion

The results for conversion inefficiency and destruction efficiency for these tests plotted against the energy content are presented in Figures 47 and 48. There is a clear difference in the performance for nitrogen dilution and carbon dioxide dilution – carbon dioxide shows a higher reduction in performance. Table 7 gives the maximum dilution for flammable operation for these tests, with the exit velocity of the flare gas mixture. Here is also tabulated the estimated energy content threshold for 98% DE. Note that with nitrogen dilution the threshold is around 3.9 MJ/m^3, almost half of the minimum level promulgated by the U.S. EPA (EPA 40CFR 60). For dilution with carbon dioxide, the threshold is much higher than the recommended level, even above the level of 11.2 MJ/m^3 set for assisted flares. Keep in mind that these tests are for unassisted flares. Destruction efficiency for N_2 dilution is >99% for NG and ethylene when heat content exceeds 5 MJ/m3. Refineries and petrochemical plant flares have N_2 rather than CO_2 in the flare gases.

Table 7 - Maximum dilution for flammable operation, with energy content and exit velocity.

Mixture	LHV	Fraction inert (Volume basis)	Exit Velocity	Estimated 98% DE Threshold
	MJ/m^3	%	m/s	MJ/m^3
NG/N_2	3.8	89.7	17.1	3.8
NG/CO_2	10.9	70.4	6.2	11.8
Ethylene/N_2	3.7	93.4	16.7	3.9
Ethylene/CO_2	9.1	83.7	7.2	12.0

Propylene/CO_2	16.2	80.1	3.9	20.0

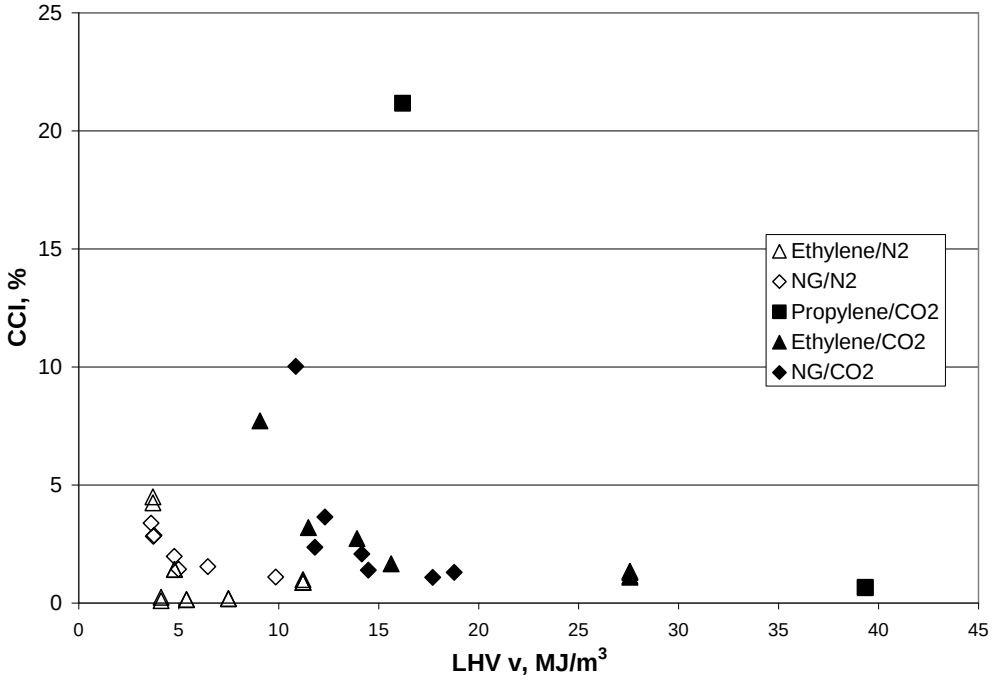

Figure 47 - Conversion inefficiency versus heat content of flare gas.

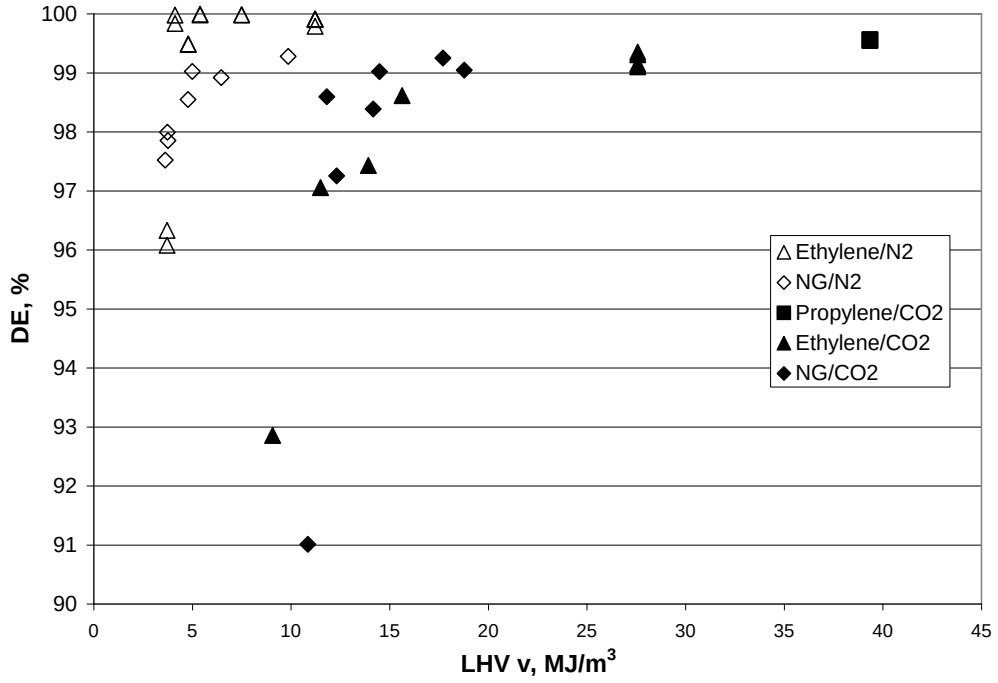

Figure 48 - Destruction efficiency versus heat content, volume basis.

In Figure 49 we have plotted the destruction efficiency against the energy content on a mass basis. This was done because carbon dioxide is much heavier than nitrogen and perhaps the mass basis would have given a better representation of the data, bringing the different mixtures together. This did not turn out to be the case.

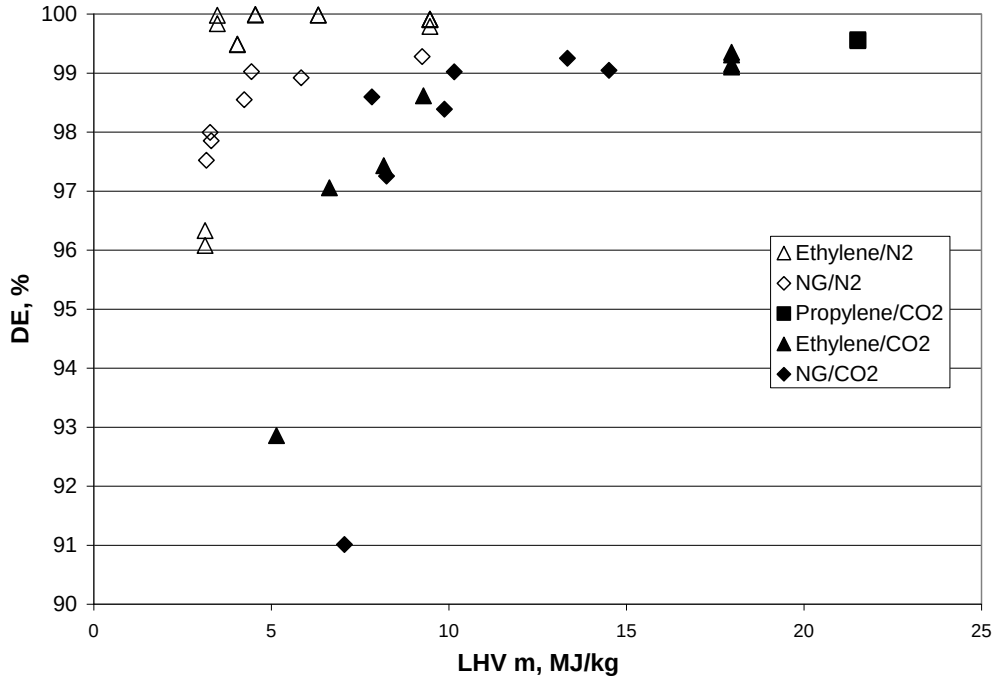

Figure 49 - Destruction efficiency versus heat content, mass basis.

In the chapter on the steam-assisted flaring, we derived a reduced volume fraction of steam to collapse the efficiency data for the different fuels. The same derivation can be applied to theses inert gases using the appropriate *I** values. Table 8 contains the critical volume fractions for the inert gas mixtures for this calculation.

Table 8 - Critical volume fraction for gas mixtures with nitrogen and carbon dioxide.

	I*	λ	Critical volume fraction
Nitrogen with			
Methane	39	9.55	0.871
Ethylene	45	14.32	0.926
Propylene	40	21.48	0.937
Carbon Dioxide with			

Methane	29	9.55	0.812
Ethylene	40	14.32	0.911
Propylene	28	21.48	0.897

The calculated Reduced Volume Fraction Inert, RVFI, is used in Figure 50. This parameter is not successful in collapsing all the data together. There are still some conclusions to be drawn. The effect of dilution with N_2 is much weaker. For RVFI < 1 the destruction efficiency is greater than 99%. This has significance for refineries and petrochemical plants where the inert gas is usually nitrogen.

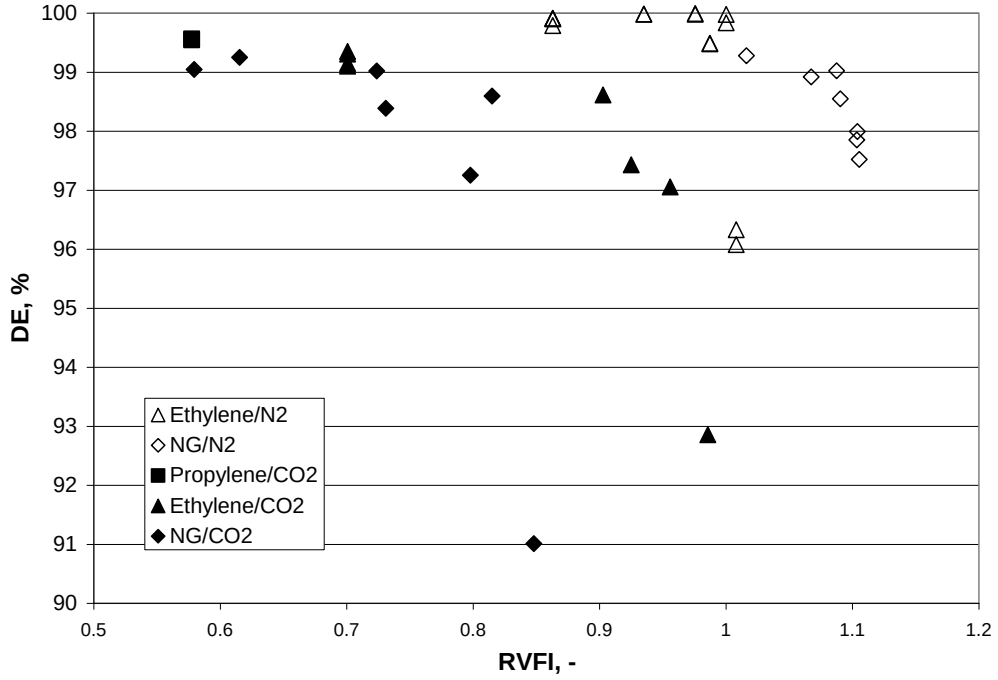

Figure 50 - Destruction efficiency for diluted flare gases versus Reduced Volume Fraction of inert.

5.4 Conclusion

Tests of dilution of the flare gas with nitrogen or carbon dioxide confirmed the significant difference between the two inert gases. Energy content does not adequately represent the effect of dilution. While nitrogen dilution has very little effect on combustion performance until very close to the extinction limit, carbon dioxide has a much stronger

deleterious effect. The estimated energy content to give 98% DE for the mixtures tested here are given in Table 7. Note that the threshold energy content with carbon dioxide dilution is higher than the requirement for assisted flares. The corresponding threshold for nitrogen dilution is much lower, almost half the requirement for unassisted flares.

Neither the energy content on a mass basis or the Reduced Volume Fraction Inert that was used to correlate the destruction efficiency of steam-assisted flares could be used to correlate the destruction efficiency measured when the inert gases nitrogen and carbon dioxide were used to dilute the flare gas. Clearly there is need for a new parameter to handle the effects of dilution with different inert gases on flare performance.

6.0 TRACE EMISSIONS

6.1 Introduction

In the preceding chapters we have discussed the conversion inefficiency, which is the failure to convert to carbon dioxide, and the destruction efficiency, which is the success in the destruction of the flared hydrocarbon. There remains the discussion of the other species that can be formed in a combustion system and emitted. First among these is carbon monoxide, the primary product of interrupted oxidation of hydrocarbons. In our first chapter with the natural gas baselines and scale-up, we showed that the contribution of methane (fuel) to the inefficiency was in the range from 60% to 80%. This means the carbon monoxide contribution was from 20% to 40%.

Nitrogen oxides, nitric oxide and nitrogen dioxide, are formed in the flame region through the fixing of atmospheric nitrogen at high temperature when there is no fuel-bound nitrogen present. The emissions of these compounds are not related to the conversion of a compound in the flare gas, but need to be related to the flaring process. This can be accomplished through the use of an Emission Factor (EF), which gives the mass emission of the species of interest relative to the energy content of the flare gas. The units for the emission factor are g/MJ or mg/MJ. This normalizes the emissions by the flaring process. Reporting simple stack concentrations biases the results by the dilution of the wind tunnel air flow, which is an artefact of the experimental set-up and has no significance for the flaring process.

The emissions of primary concern to the IFC are the HRVOCs and BTEX. HRVOCs are the highly reactive volatile organic compounds. These are reactive in the atmospheric, particularly urban air-sheds, and contribute to the formation of ozone. BTEX are the simple aromatic compounds benzene, toluene, ethylbenzene and xylenes. These are of concern as toxic or carcinogenic compounds. We had two analysis systems for these groups of organic compounds, described in an earlier report (Caravaggio and Caverly, 2008). These systems have a very low detection limit, 20 ppbv for the HRVOCs and 10 ppbv for the BTEX. The detection limit establishes lower limits for the emission factors for these trace compounds. The emission factor for a species Σ is given by

$$EF_{\Sigma} = \frac{x_{\Sigma}\left(M_{\Sigma}/M_{air}\right)\dot{m}_a}{LHV_m \dot{m}_f} \tag{6-1}$$

The emission factor depends on the air flow rate and the fuel flow rate, as well as the detection limit of the analysis system, and the ratio of the molecular mass of the species of interest to that of air. For example, the emission factor at the detection limit of ethylene, 20 ppbv, ranges from 0.2 mg/MJ to 2 mg/MJ.

6.2 Carbon Monoxide

Carbon monoxide is a product of incomplete or interrupted combustion. It is the other major product in the flare exhaust gas, after carbon dioxide (complete combustion) and the fuel hydrocarbon (no combustion). The emission of carbon monoxide is best calculated as a conversion of the fuel-carbon. Figure 51 gives the conversion of fuel-carbon to carbon monoxide relative to the conversion inefficiency. Note that the conversion to carbon monoxide reaches a maximum of 10% at inefficiency of 30%, with the steam-assisted trials. This indicates that the inefficiency with over-steaming is primarily due to fuel-stripping.

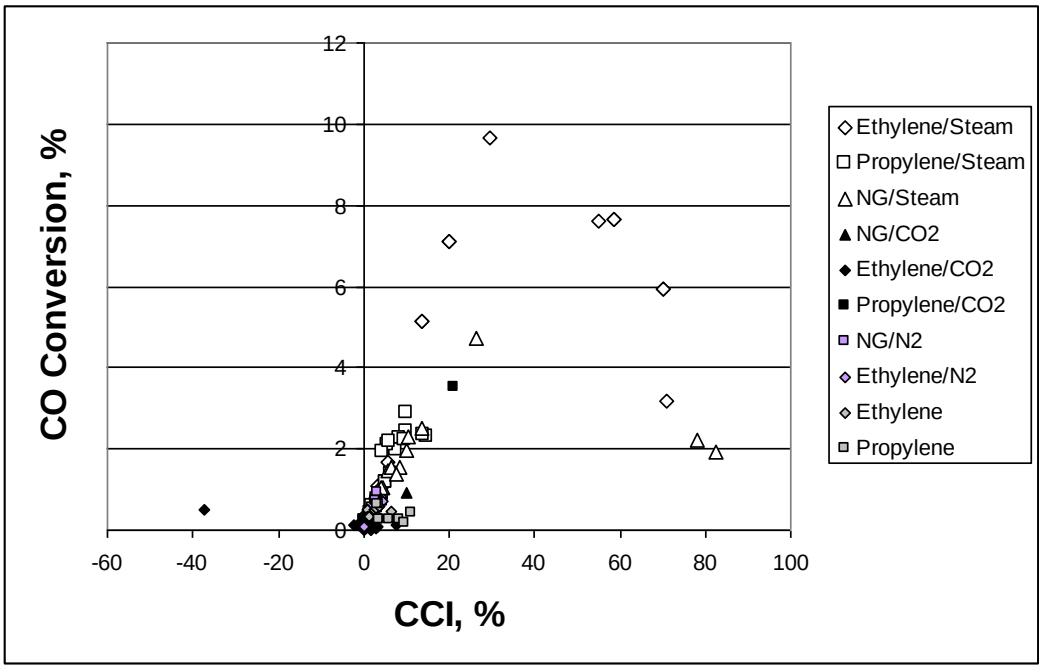

Figure 51- Conversion of fuel-carbon to carbon monoxide for all tests.

The conversion to carbon monoxide as a function of the conversion inefficiency for the natural gas baseline tests (Chapter 2) was shown to be in the range from 20% to 40%. A rough correlation with the power factor was obtained for those tests. Figure 52 shows the correlation of conversion to carbon monoxide with conversion inefficiency. Three sets of data are removed from that figure. The two simple fuel tests were removed, with ethylene and propylene, because those trials had significant generation of particulate carbon which is a very different chemical mechanism. The ethylene/carbon dioxide tests are also removed, because they displayed significant deviation from the others. No explanation is readily available for that difference.

The remaining runs, including steam-assist and dilution with nitrogen and carbon dioxide, show that carbon monoxide contributes around 25% of the inefficiency. This is in full agreement with the baseline results for natural gas for 3", 4" and 6" pipe sizes.

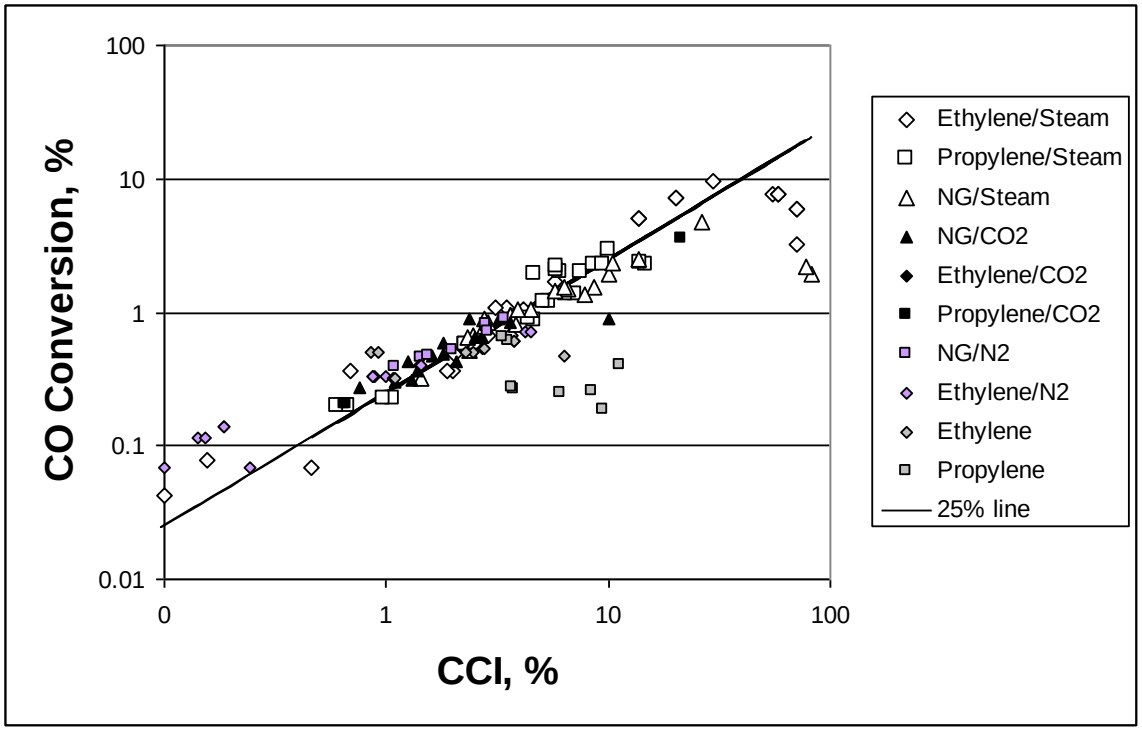

Figure 52 - Log-log plot of the conversion to CO against the conversion inefficiency. The solid line indicates 25% of the inefficiency is due to carbon monoxide.

6.3 Nitrogen Oxides

Unless there are nitrogenous species in the flare gas, the dominant mechanism for generation of nitrogen oxides (NO_x) is thermal fixing of atmospheric nitrogen through the Zeldovich mechanism. Thus NO_x emissions are related to the peak flame temperature. Peak flame temperature is a function of several variables, physical and operational. These variable are in addition to the variables used in these flare tests. However, the testing did not include these variables, were flame temperatures measured.

The emission factor for NO_x is plotted against conversion inefficiency in Figure 53. The general trend is for the emission factor to decrease with increased inefficiency. The range of emission factor is from 0.004 g/MJ to 0.04 g/MJ ($9.3x10^{-15}$ lb/MBTU and $9.3x10^{-14}$ lb/MBTU) which agrees with the range reported by Pohl and Soelberg (1986) for hydrocarbon flare gases.

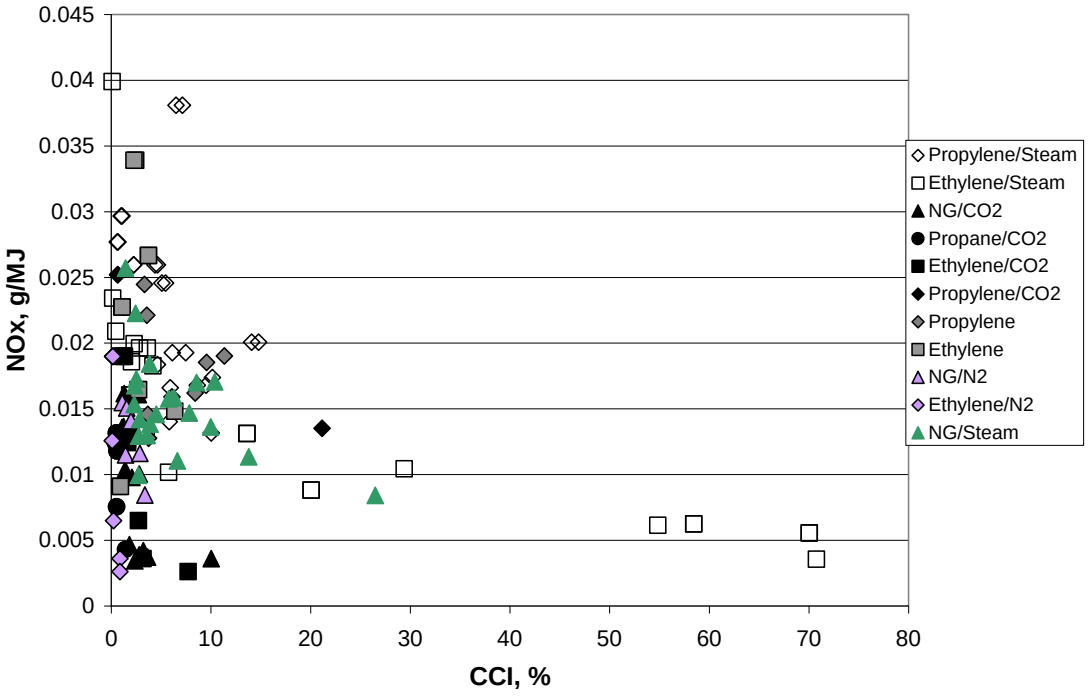

Figure 53 - Emission factor for NO_x plotted against conversion inefficiency for all tests.

The emission factors for NO_x for steam-assisted trials only are presented in Figure 54. The decrease in emission factor with increase SFR is as expected, since the increased steam flow rate will lower the flame temperature. However, the spread of the emission factors for unassisted trials covers the range of the steam-assisted trials, so it may not be reasonable to draw too many conclusions from this figure.

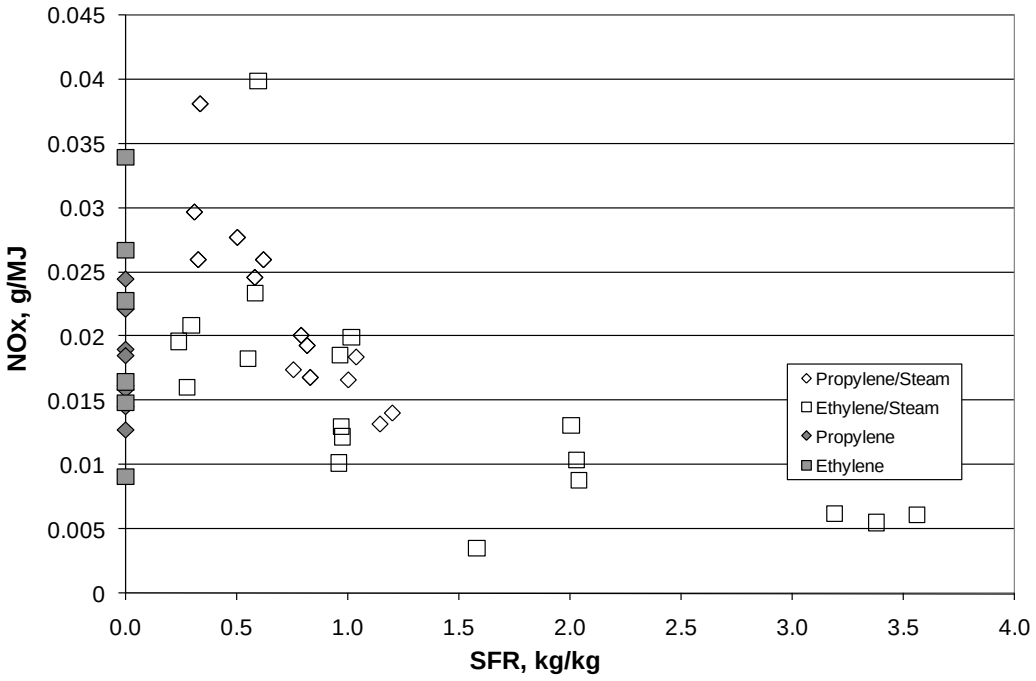

Figure 54 - Emission factor for NO_x for steam-assisted trials.

6.4 Hydrocarbons

The two groups of hydrocarbon emissions are the HRVOCs and the BTEX. There were no measureable emissions of BTEX in any of the tests. The detection limit for the BTEX analysis system is 10 ppbv. The HRVOCs measured were ethylene, propylene, the butenes, and 1,3-butadiene. The flare gases tested included ethylene and propylene, simply, steam-assisted, or diluted with nitrogen or carbon dioxide. The fuel stripping mechanism will be responsible for the emission of those compounds when they are present in the flare gas and these results are presented as the destruction efficiency results in previous chapters. This section deals with the HRVOC emissions.

Ethylene was measured in tests with natural gas and propylene. 1-butene was measured in the steam-assisted flaring of propylene. None of the other HRVOCs were detected in these tests.

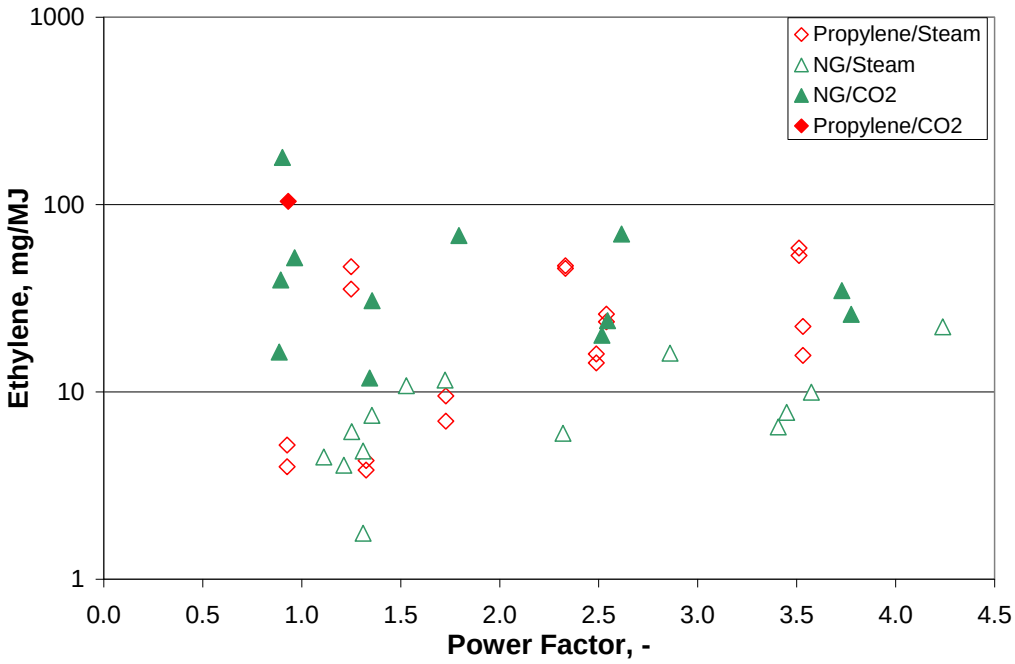

Figure 55 - Emission factors for ethylene plotted against Power Factor for tests with natural gas and propylene.

The emission factors for ethylene are in the range from 5 mg/MJ to 100 mg/MJ ($1.2x10^{-14}$ lb/MBTU to $2.3x10^{-13}$ lb/MBTU) for natural gas and propylene. There is little discernable difference in the emission factors for the two gases being flared. Figure 55 plots the emission factors against the Power Factor, with no evident correlation.

Figure 56 plots the emission factors for ethylene against the steam-to-fuel mass ratio (SFR) for the steam-assisted flaring of natural gas and propylene. There may be an increase of emission factor with SFR.

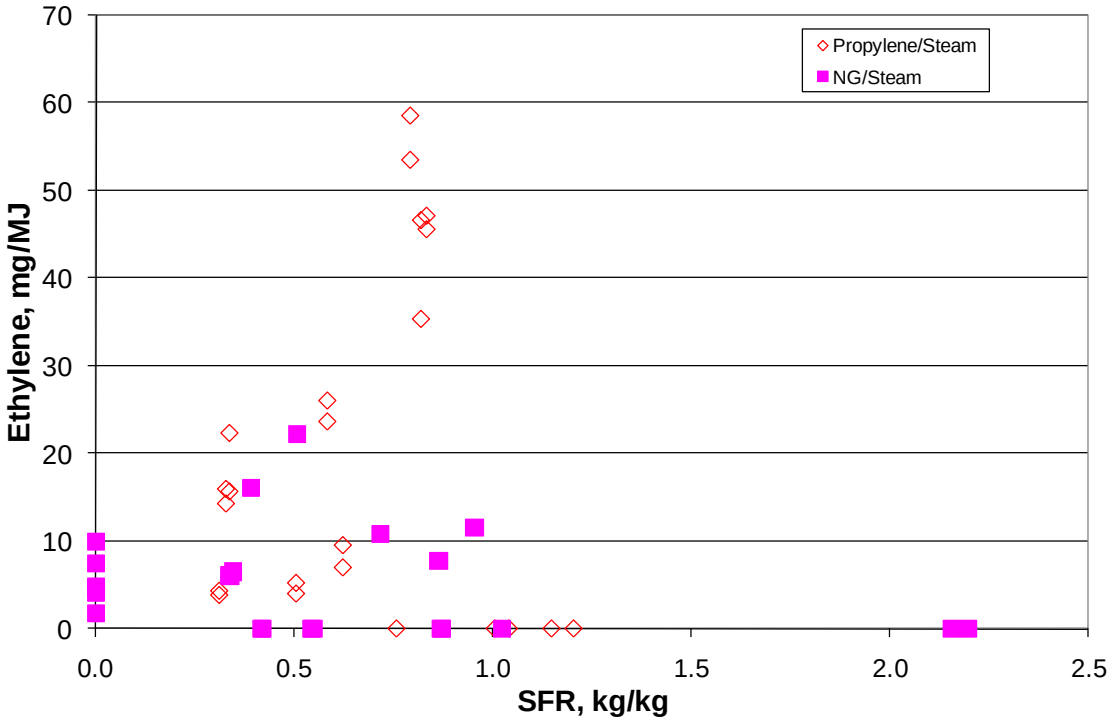

Figure 56 - Emission factors for ethylene plotted against SFR for steam-assisted flaring of natural gas and propylene.

Figure 57 presents the emission factor for ethylene from flaring tests for natural gas, propane, and propylene diluted with carbon dioxide. These are in the same range as for the steam-assisted tests. There does appear to be a correlation with energy content of the flare gas mixture that the emission factor for ethylene decreases with increasing energy content of the mixture.

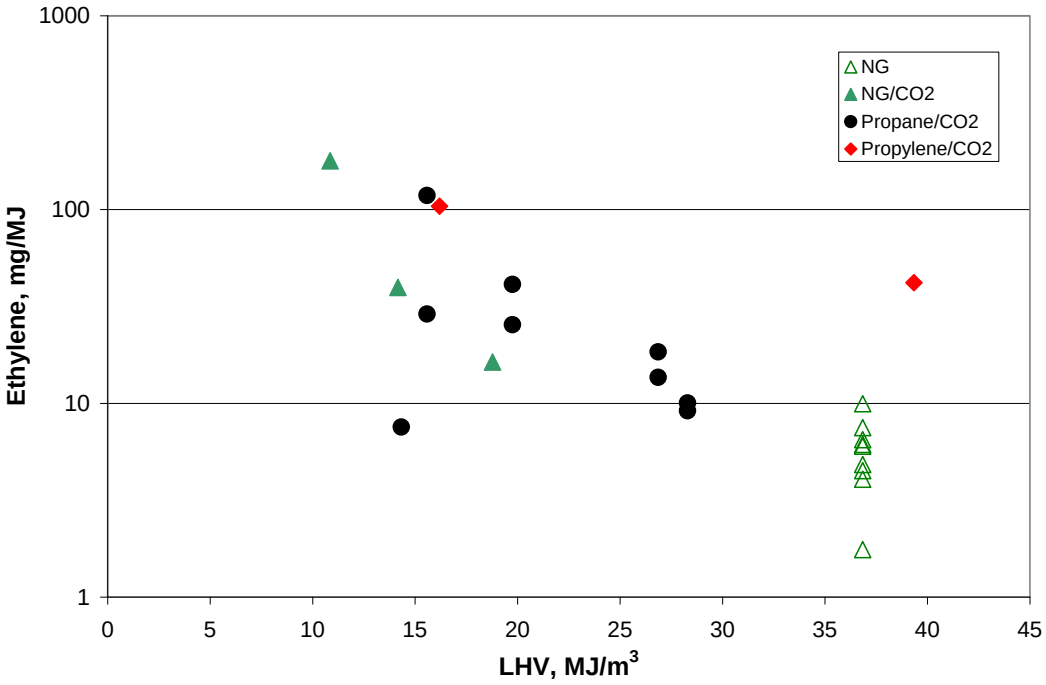

Figure 57 - Emission factor for ethylene for tests wtih dilution of natural gas, propane and propylene with carbon dixoide.

The only other HRVOC detected was 1-butene, and only for the steam-assisted flaring of propylene. Figure 58 presents the emission factor for 1-butene plotted against the SFR for the steam-assisted flaring of propylene. These emission factors are an order of magnitude smaller than those for ethylene.

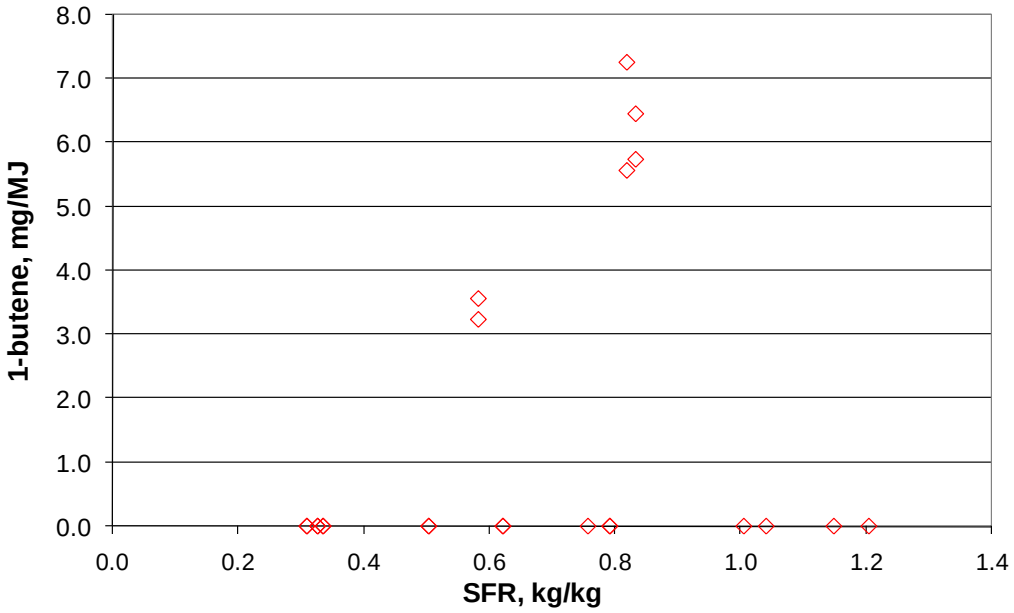

Figure 58 - Emission factor for 1-butene against SFR for steam-assisted flaring of propylene.

The emission factors for 1-butene are plotted against the emission factors for ethylene for the steam-assisted flaring of propylene. Included in the figure are the emission factors at the detection limits of the HRVOC analysis system (20 ppbv). This shows that for the detectable levels of 1-butene, these are 0.14 of the emission factor of ethylene. For the two trials with high levels of ethylene emission factors of between 50 and 60 mg/MJ ($1.2x10^{-13}$ lb/MBTU and $1.4x10^{-13}$ lb/MBTU) propylene flared, the expected emissions of 1-butene are at the detection limit of the HRVOC measurement system.

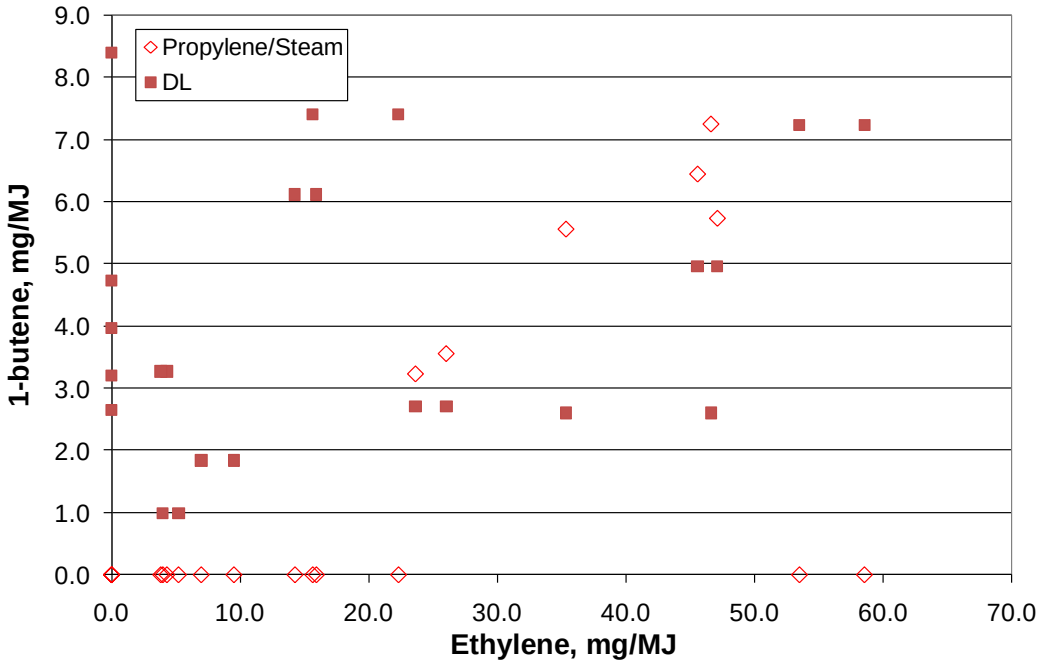

Figure 59 - Emission factor for 1-butene plotted against the emission factor for ethylene for the steam-assisted flaring of propylene. The solid square symbols are the emission factors at the detection limit for these trials.

6.5 Conclusion

The trace emissions from flaring systems are carbon monoxide, nitrogen oxides (NO_x), and hydrocarbons.

The emissions of carbon monoxide are best expressed as a percentage of the conversion inefficiency. The inefficiency due to carbon, in non-sooting systems, is 25% of the total. This is in agreement with the baseline data for natural gas with different diameter flare tips.

The range of emission factor for NO_x is from 0.004 g/MJ to 0.04 g/MJ ($9.3x10^{-15}$ lb/MBTU and $9.3x10^{-14}$ lb/MBTU), which agrees with the range reported by Pohl and Soelberg (1986) for hydrocarbon flare gases without nitrogenous species.

There were no measureable emissions of BTEX in any of the tests at the detection limit of 10 ppbv. Ethylene was measured in tests with natural gas and propylene. 1-butene was

measured in the steam-assisted flaring of propylene. None of the other HRVOCs were detected in these tests.

The emission factors for ethylene are in the range from 5 mg/MJ to 100 mg/MJ ($1.2x10^{-14}$ lb/MBTU to $2.3x10^{-13}$ lb/MBTU) for natural gas and propylene. There is little discernable difference between the two gases.

1-butene was measured in the steam-assisted flaring of propylene. The emission factor for 1-butene is 0.14 of the emission factor for ethylene.

7.0 CONCLUSION

Over 400 test runs were performed in the Flare Test Facility under the auspices of the IFC, covering the conditions of unassisted, steam-assisted, and diluted flaring of natural gas, propylene and ethylene. The results of these tests have provided the information for some of the six gaps in the flaring knowledge base listed in the Introduction. There remain significant gaps. Before getting to the six points, there is one important result that needs to be highlighted.

The question of scale-up of the pilot-scale results in the wind dominated wake-stabilized regime was addressed. Testing was done on pipes of 1", 2", 3", 4" and 6" diameter flaring natural gas. The "Three Inch Rule", which states that flaring results with pipes smaller than 3 inches do not scale-up to larger flare pipe sizes, was established for the wake-stabilized regime. The "Three Inch Rule" was already established in the literature for the jetting regime [Gogolek et al. 2009]. The results for CCI and DE for natural gas with flare pipes larger than 3 inches were correlated with the Power Factor (equations 2-2 and 2-4). The Power Factor is

$$PF = \left(\frac{\rho_a U_w^3 D_p^2}{\dot{m}_f LHV_m} \right)^{1/3} = \left(\frac{\rho_a U_w^3 D_p^2}{\rho_f A_p U_f LHV_m} \right)^{1/3} \tag{7-1}$$

This dimensionless parameter is used to correlate the results for unassisted and steam-assisted flaring of ethylene and propylene.

It was also shown that the Flame Retention Ring (FRR) has an effect on the efficiency of the flare. The 3" pipe with FRR has lower efficiency than the 6" pipe with FRR for a given Power Factor.

7.1 Experimental studies of the flare efficiency in the transition between jetting and wake-stabilized regimes.

These tests were described in Chapter 2. The transition from jetting to wake-stabilized was investigated on a 3" pipe firing natural gas. The transition is accomplished either by reducing the flare gas rate or by increasing the wind speed. It was found that reducing the flare gas rate has little effect on the efficiency of the flare, while increasing the wind

speed decreased the efficiency. The change in efficiency was continuous and almost linear with wind speed, so that there is no sharp change in efficiency with the establishment of the wake-stabilized operation.

7.2 Experimental studies of the effect of wind on steam-assisted flares.

Testing was performed on the 3" flare tip with FRR (Flame Retention Ring) with steam-assist for natural gas, ethylene and propylene, with cross-wind from 3.5 m/s to 9.5 m/s. Previous work, particularly the CMA study [McDaniel 1983], was done with little or no wind. Steam-assisted flares are more sensitive to the effect of cross-wind than the unassisted flare for all three gases tested. Ethylene is the least affected by the addition of steam, natural gas the most affected. For a given level of Steam to Fuel Ratio (SFR), the effects of varying wind speed and fuel rate is correlated with the Power Factor. The CMA results for flaring propylene are the extrapolation of our results to low values of Power Factor (see Figure 42).

The Reduced Steam Volume Fraction (RSVF) was derived as the ratio of the steam volume fraction to the theoretical maximum steam dilution for continued flammability. This parameter was used to bring together all the steam-assist tests and is put forward as a replacement for the SFR for controlling the steam-assist rate. The maximum RSVF should be 1; the 'over-steaming' tests in the CMA study had RSVF slightly larger than 1. Our data indicate that with wind present the maximum RSVF should be 0.8. This translates into maximum SFR = 1.8 for ethylene and maximum SFR = 1.2 for propylene.

With that limit, the data show further that there is a maximum Power Factor to ensure 98% DE – 3 for ethylene and 2 for propylene. This translates into a minimum exit velocity for the flare gas for a given wind speed. Figure 60 shows the curves for the minimum exit velocity for wind speed up to 30 m/s. It is clear that most operating flares will usually be operating with exit velocities above this boundary.

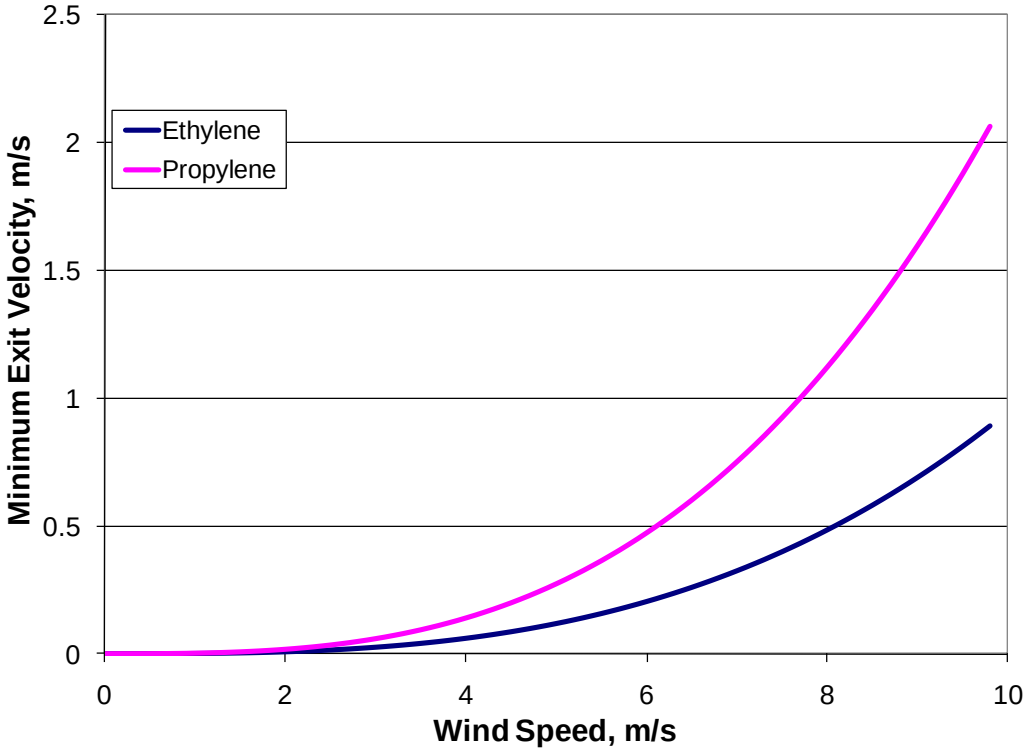

Figure 60 - Minimum exit velocities for steam-assisted flaring of ethylene and propylene based on RSVF<0.8 and maximum Power Factor of 2 for propylene and 3 for ethylene.

7.3 Experimental studies on the limiting hydrogen concentration for steam-assisted flares and wind blown flares.

No work was done on this gap.

7.4 Experimental measurements of HRVOC and NO_x measurements for flares with and without steam-assist.

Measurements were taken of the various trace emissions, described in detail in Chapter 7. The trace emissions from flaring systems are carbon monoxide, nitrogen oxides (NO_x), and hydrocarbons. There are several quite notable findings:

1. Carbon monoxide is 25% of the CCI (carbon conversion inefficiency), for assisted and unassisted flaring of natural gas, ethylene and propylene.
2. There was no measureable emission of BTEX compounds, or of the HRVOCs 2-butenes, 1-3 butadiene, or of propylene except when it was the flare gas.

3. Ethylene was measured during the flaring of natural gas and propylene, although at very low levels. The emission factors for ethylene are in the range from 5 mg/MJ to 100 mg/MJ ($1.2x10^{-14}$ lb/MBTU to $2.3x10^{-13}$ lb/MBTU) for natural gas and propylene. There is little discernable difference between the two gases.
4. 1-butene was measured from the steam-assisted flaring of propylene and the emission factor is 0.14 times the emission factor for ethylene for those tests.
5. The range of emission factor for NO_x is from 0.004 g/MJ to 0.04 g/MJ, which agrees with the range reported by Pohl and Soelberg (1986) for hydrocarbon flare gases without nitrogenous species.

7.5 Correlation of fuel properties to correlate the flare efficiency with flare gas composition, particularly accounting for the special case of hydrogen, and the inert gases nitrogen and carbon dioxide.

There was only limited success in correlating the flare efficiency results with fuel properties. The Fuel Factor (equation 4-4) does bring together the DE data for steam-assisted flaring of ethylene and propylene (see Figure 46). If the conjecture that this fuel factor does not work for natural gas is because of reaction rate limitations in the combustion of that gas, then it should have general applicability. Natural gas is the least reactive of the hydrocarbons. We were not successful in finding a factor that can handle the difference between the inert species nitrogen and carbon dioxide.

7.6 Correlation of flare efficiency with steam-assist rate that includes the flare gas composition, perhaps unifying steam with the handling of nitrogen and carbon dioxide dilution.

The Reduced Steam Volume Fraction (RSVF) is put forward as a parameter for correlating the effect of steam-assist on flaring (see Figure 43). The concept behind this factor is that there is a maximum dilution with steam that a combustible gas can endure and remain flammable. This maximum dilution is used to normalize the steam volume fraction (if the steam was uniformly mixed with the flare gas). RSVF of 1 is the

theoretical maximum steam that can be added. Our data shows that RSVF = 0.8 is a practical maximum for flaring in the presence of wind.

We attempted to use the same reasoning to produce a similar factor (Reduced Volume Fraction Inert, RVFI) correlating the dilution with nitrogen and carbon dioxide. It showed that the dilution with nitrogen can proceed to the theoretical maximum (RVFI = 1) with DE > 98%. This means that the restriction on minimum energy content to 7.5 MJ/m^3 (200 BTU/scf) for unassisted flares is too high when the inert gas is nitrogen. Dilution with carbon dioxide has a much stronger effect. Our results show that the minimum energy content restriction is too low and does not guarantee 98% DE when the inert gas is carbon dioxide.

7.7 Gaps Remaining or Identified

A great deal of progress was made in closing the gaps in understanding the dependence of flare efficiency on the operating parameters of wind speed, flare gas rate and composition, and steam-assist rate. However, several gaps remain.

1. The effect of hydrogen: Hydrogen is the most flammable gas and the addition of even small amounts to a gas increases the flammable range, flame speed, and other combustion properties. We did not perform any testing with hydrogen in our flare gas.
2. Scale-up of steam-assisted flare results: Our testing was with a simple pilot-scale flare tip. It may be that this tip is most vulnerable to the effects of cross-wind than a commercial flare tip, with robust pilot burners. Measurements on larger scale flares are needed for full confidence in the value of the results reported here.
3. Fuel factor that reconciles the different fuel gases and inert gases is needed. Some progress has been made and the data reported here can be used to test hypotheses. Data from the flaring of gas mixtures are needed.

8.0 REFERENCES

Caravaggio, G. and A. Caverly, [2008] “Online Analysis of Flaring Emissions”, report to IFC.

Gogolek, P., A. Caverly, J. Pohl, R. Schwartz, J, Seebold [2009]

a) “Emissions from Elevated Flares – A Survey of the Literature”, report to IFC.

b) “Flare Test Facility – Equipment and Calculations”, report to IFC.

Gogolek, P.E.G., and Hayden, A.C.S. [2003] "Performance of flare flames in a crosswind with nitrogen dilution." Journal of Canadian Petroleum Technology **43** pp. 43-47.

McDaniel, M. [1983] "Flare Efficiency Study." CMA.

Pohl, J.H., and Soelberg, N.R. [1986] "Evaluation of the Efficiency of Industrial Flares: H2S Gas Mixtures and Pilot Assisted Flares".

9.0 APPENDIX

Imperial Unit Figures

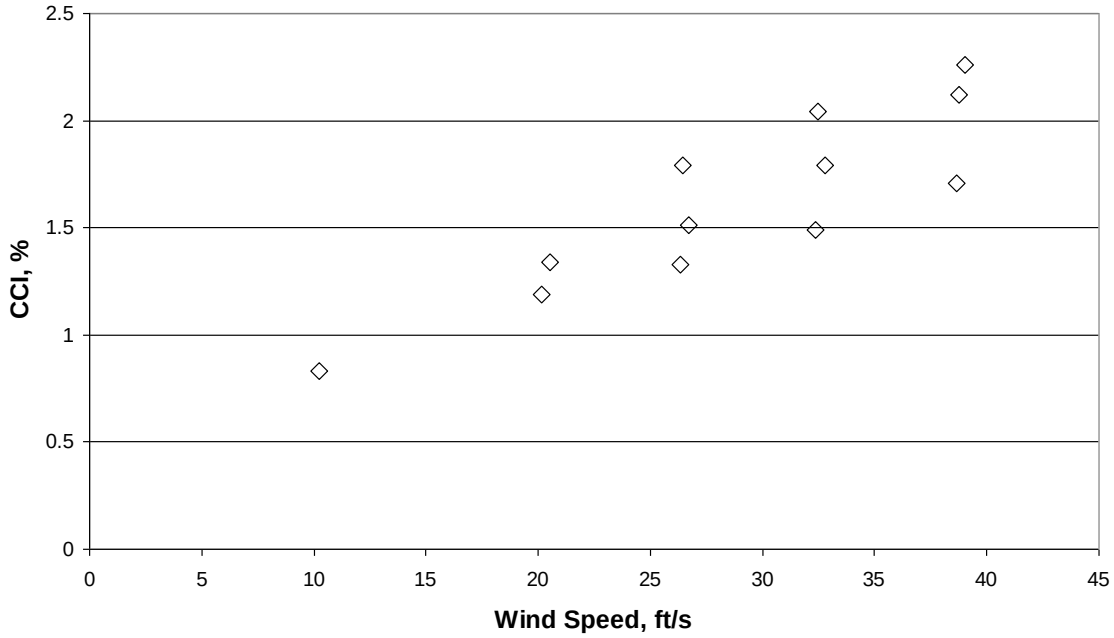

Figure 61 - Baseline testing results for 1" basic pipe firing natural gas.

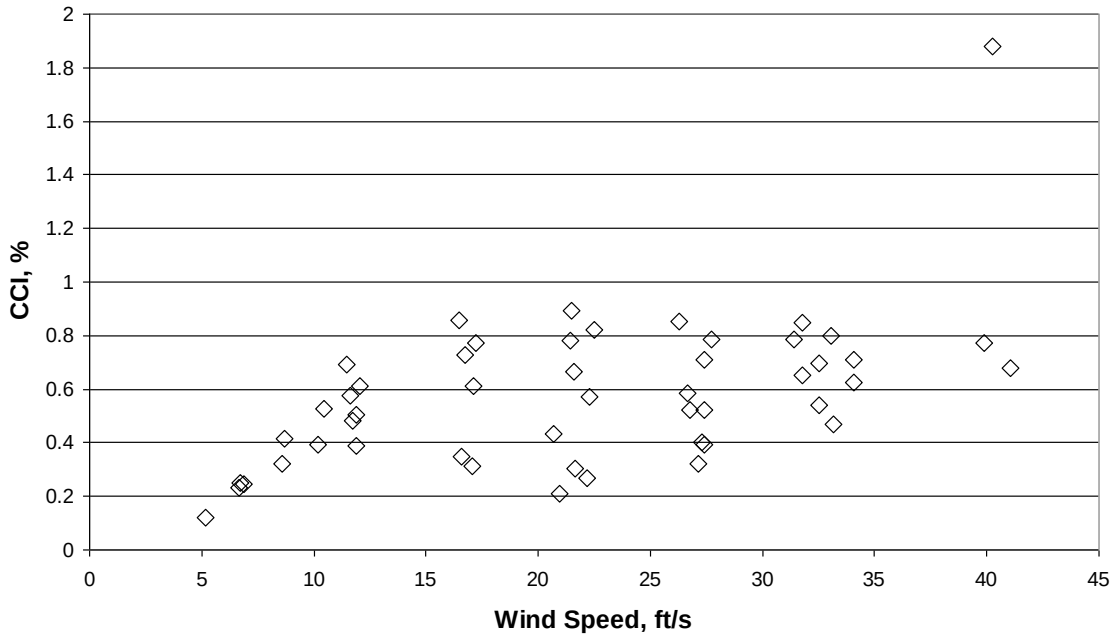

Figure 62 - Baseline testing results for 2" basic pipe firing natural gas.

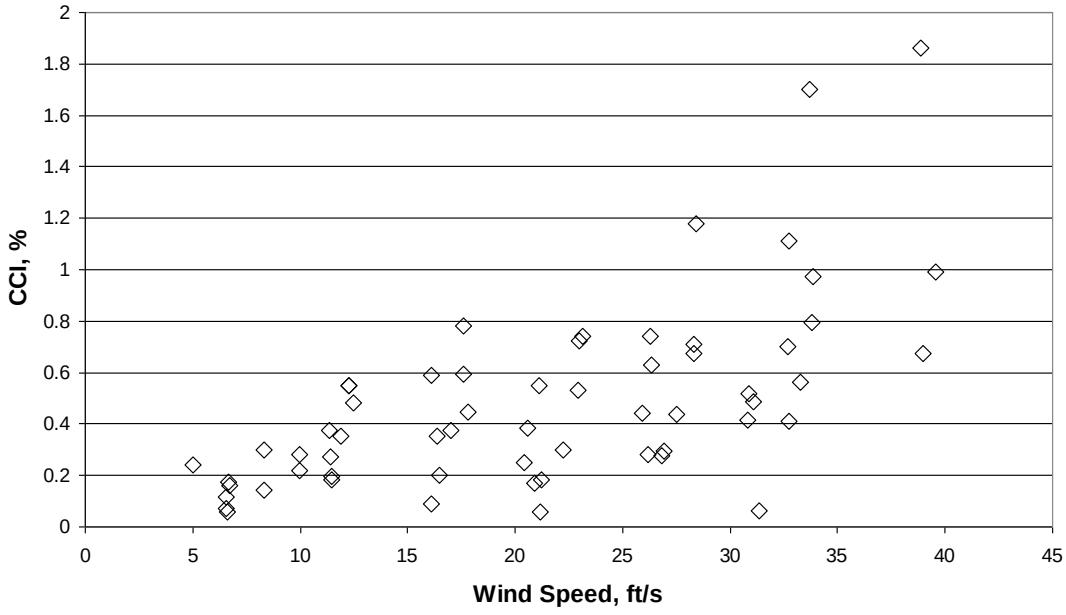

Figure 63 - Baseline testing results for 3" basic pipe firing natural gas.

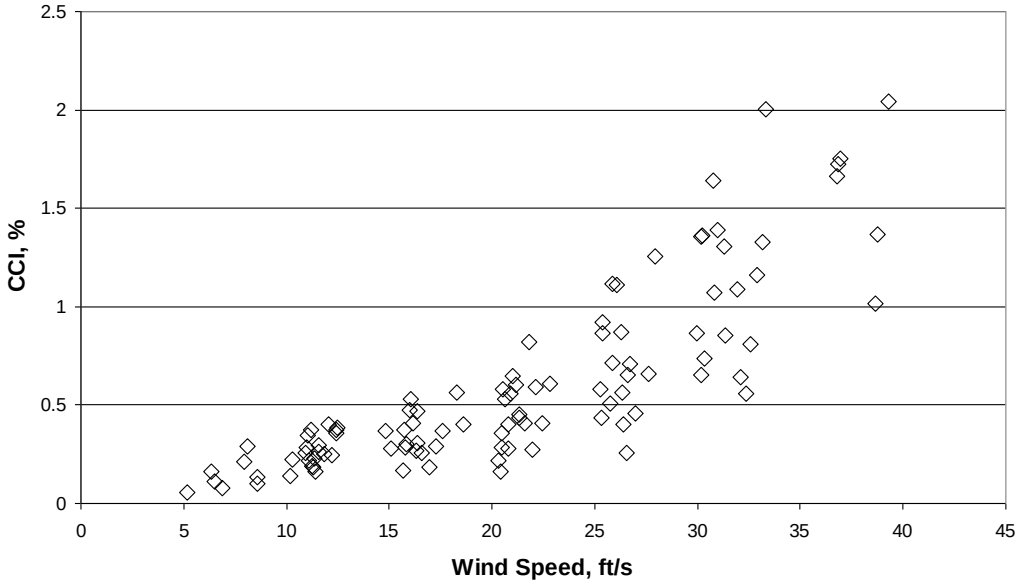

Figure 64 - Baseline testing results for 4" basic pipe firing natural gas.

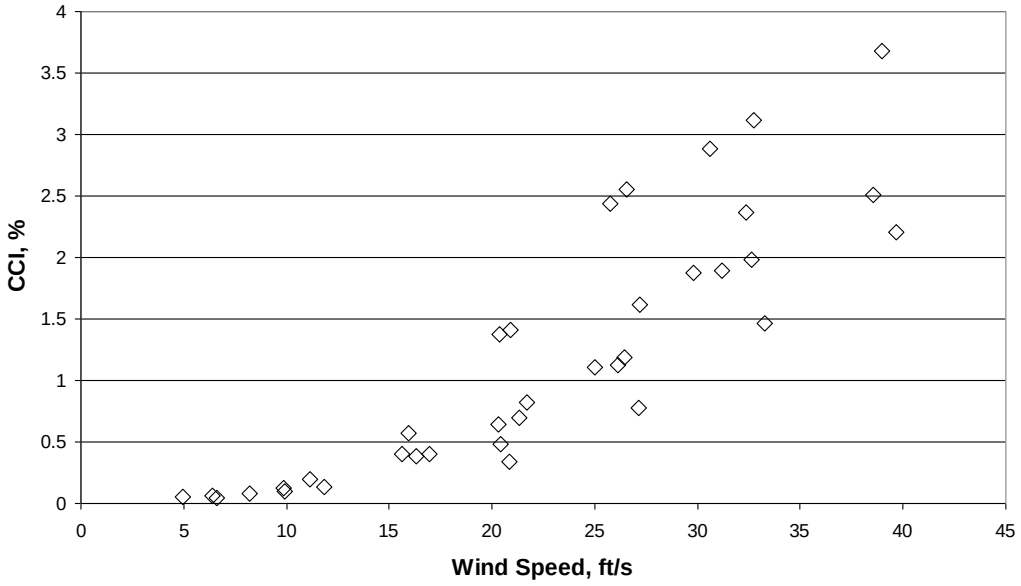

Figure 65 - Baseline testing results for 6" basic pipe firing natural gas.

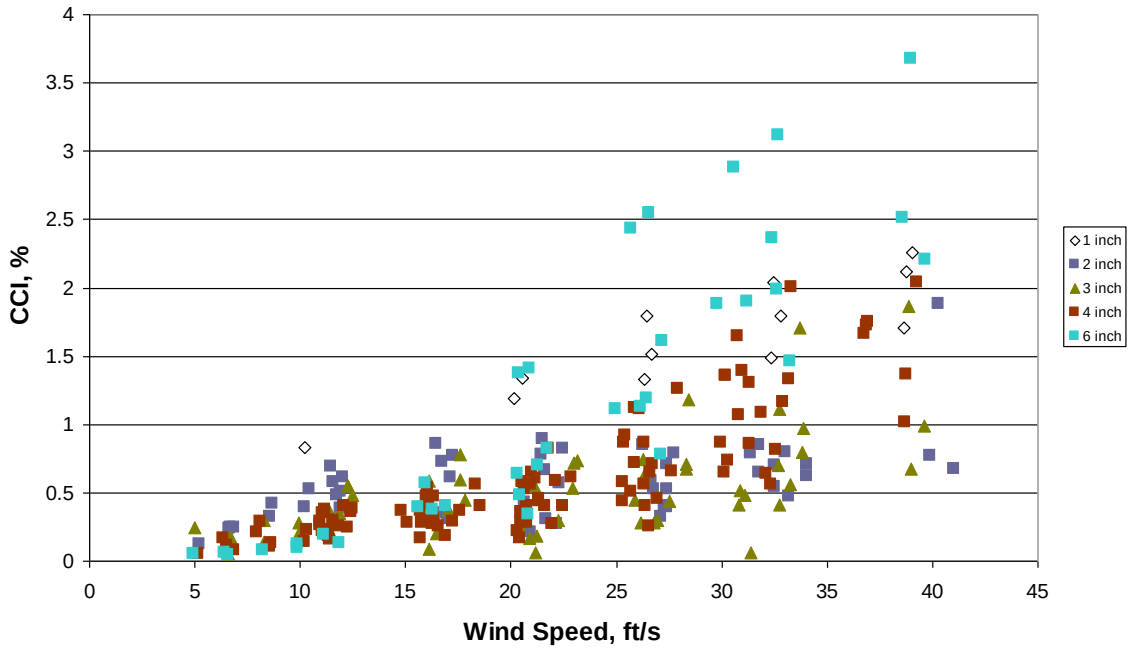

Figure 66 - Results of all baseline tests firing natural gas.

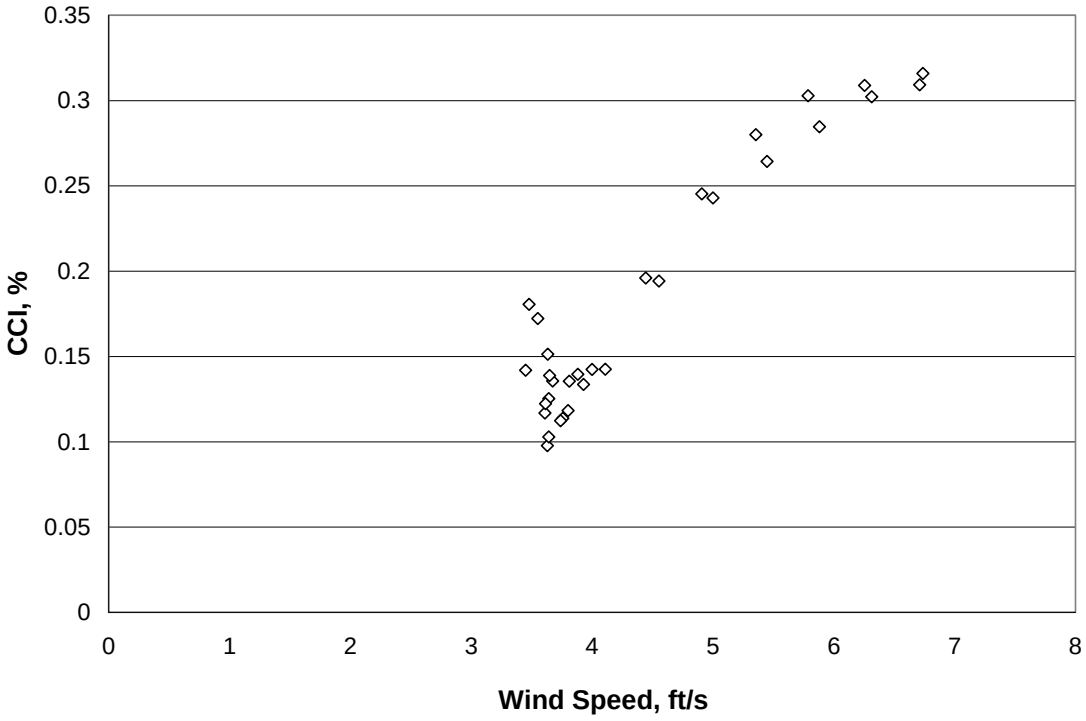

Figure 67 - Results for 3" pipe for transition testing versus wind speed. The change in fuel rate at 4 km/h has much smaller effect than the increase of wind speed.

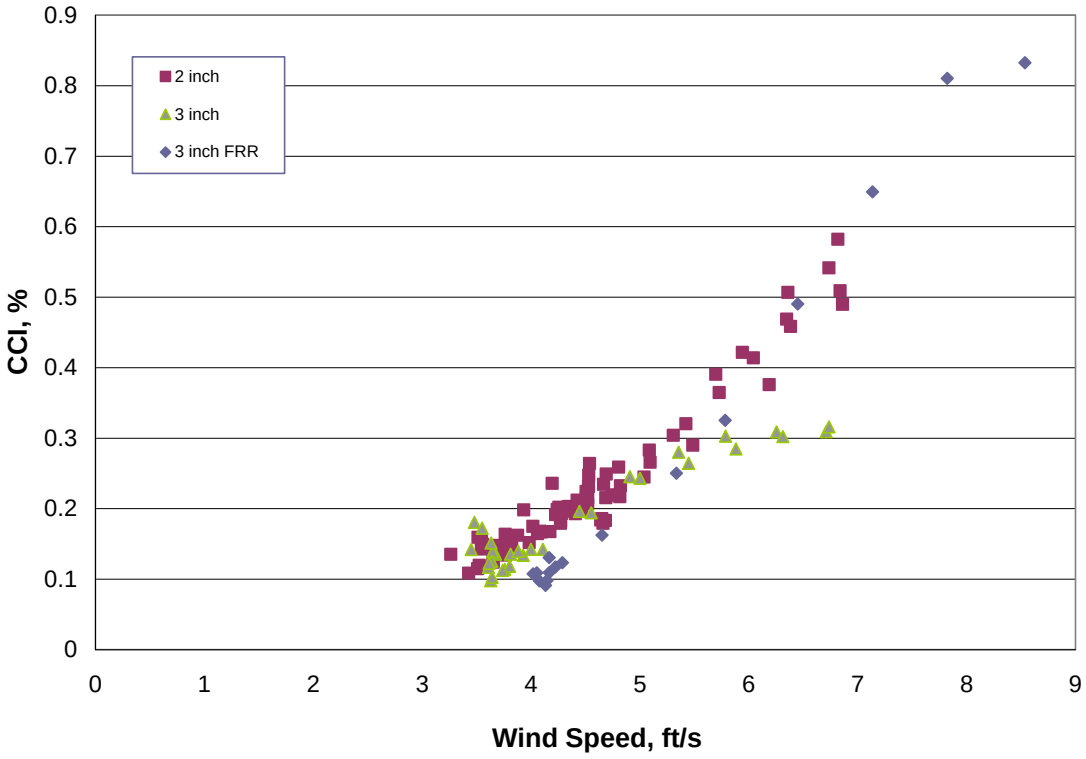

Figure 68 - All transition test results versus wind speed.

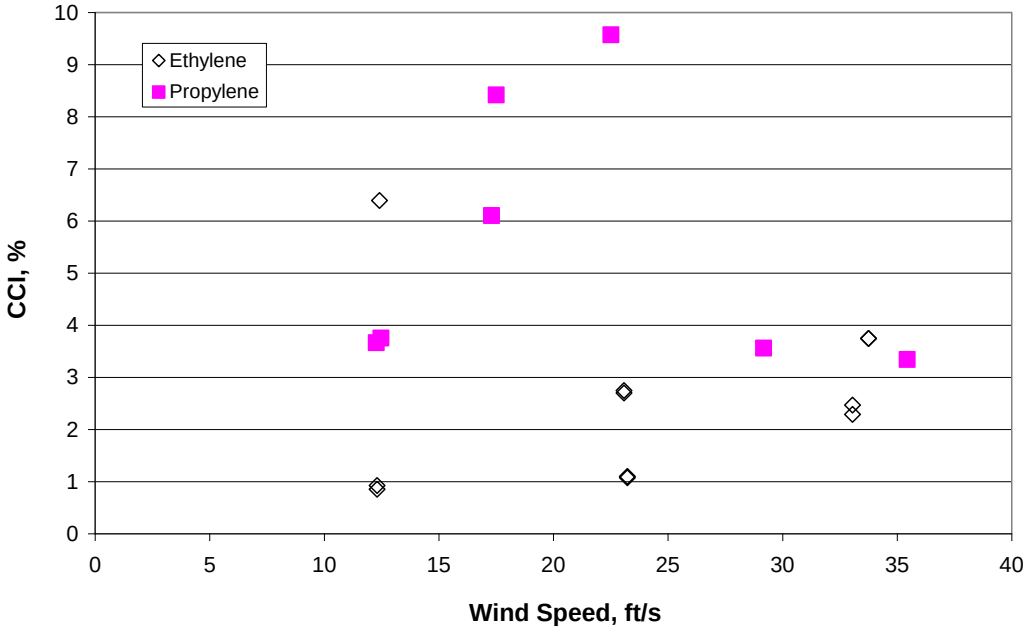

Figure 69 - Conversion inefficiency for unassisted flaring of ethylene and propylene in 3" FRR tip.

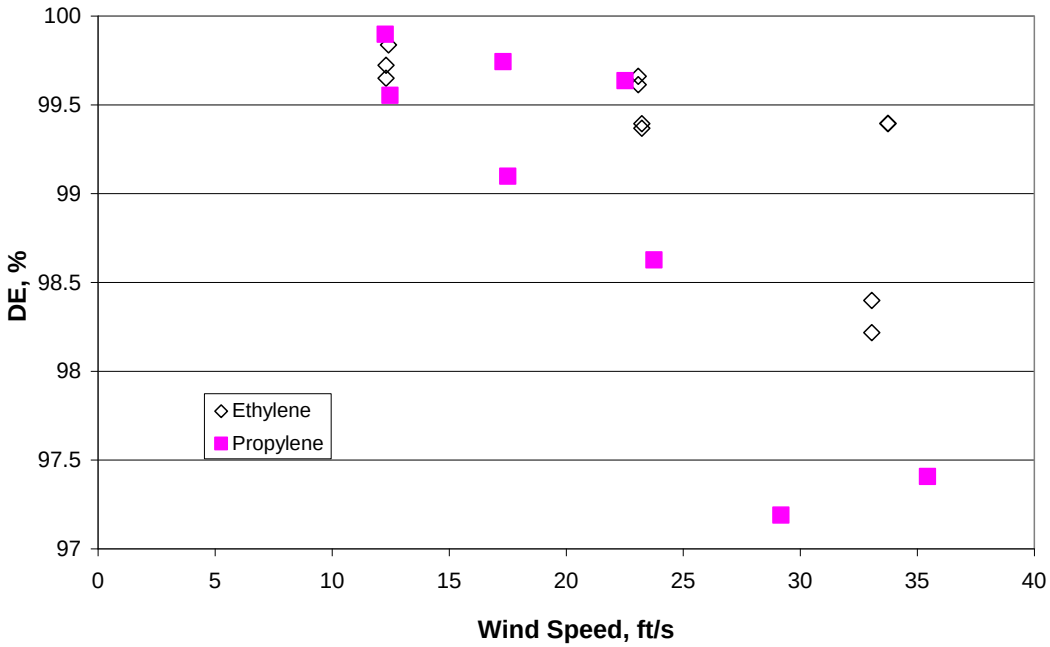

Figure 70 - Destruction efficiency for unassisted flaring of ethylene and propylene in 3" FRR tip.

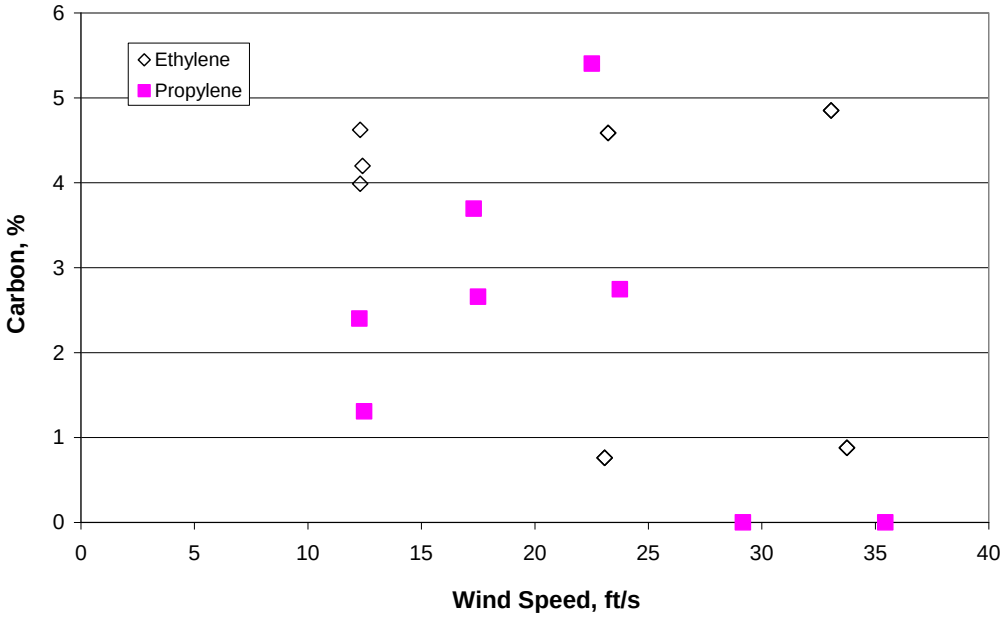

Figure 71 - Solid carbon emission as a percentage of the total carbon for unassisted flaring of ethylene and propylene in 3" FRR flare tip.